Proceedings of the Mini-Workshop

Dressing Hadrons

Bled, Slovenia, July 4 – 11, 2010

Edited by

Bojan Golli

Mitja Rosina

Simon Širca

University of Ljubljana and Jožef Stefan Institute

The Mini-Workshop *Dressing hadrons*

List of participants

Luis Alvarez Ruso, Coimbra, `alvarez@teor.fis.uc.pt`
Eef Van Beveren, Coimbra, `eef@teor.fis.uc.pt`
Pedro Bicudo, Lisboa, `pedro.bicudo@gmail.com`
Marko Bračko, Ljubljana, `marko.bracko@ijs.si`
Ki-Seok Choi, Graz, `ki.choi@uni-graz.at`
Veljko Dmitrašinović, Belgrade, `dmitrasin@yahoo.com`
Bojan Golli, Ljubljana, `bojan.golli@ijs.si`
Maria Gomez Rocha, Graz, `maria.gomez-rocha@uni-graz.at`
Regina Kleinhappel, Graz, `regina.kleinhappel@gmx.at`
Norma Mankoč Borštnik, Ljubljana, `Norma.Mankoc@fmf.uni-lj.si`
Saša Prelovšek, Ljubljana, `Sasa.Prelovsek@ijs.si`
Mitja Rosina, Ljubljana, `mitja.rosina@ijs.si`
Wolfgang Schweiger, Graz, `wolfgang.schweiger@uni-graz.at`
Ica Stancu, Liege, `fstancu@ulg.ac.be`
Simon Širca, Ljubljana, `simon.sirca@fmf.uni-lj.si`
Sachiko Takeuchi, Tokio, `s.takeuchi@jcsw.ac.jp`

Contents

Preface

It is a solemn day when a new book appears, whether it is poetry, history, or a modest Book of Proceedings. The collection of our presentations and discussions made us feel again how entangled our activities are and that physics is an efficient interaction between physicists, not only an effective interaction between particles. We may make reminiscences of the inspiring environment of Lake Bled with its hills and mountains, like perhaps quarks enjoy their mesonic and quark-antiquark environment.

We could sort our topics in three groups: baryonic resonances, heavy mesons and tetraquarks, and search for new symmetries.

Progress was made in understanding the peculiar Roper resonance, as well as the Roper-like resonances in the high-lying Δ^* by using pion electroproduction. Coupled-channel calculations indicate significant pion cloud contributions in all processes. Suitable experimental conditions for a double-polarisation experiment $p(\vec{e}, e'\pi^0)\vec{p}$ were discussed. At higher resonances, the axial charge is decreasing rapidly when parity doublets become almost degenerate. A better description of the decay widths is obtained by coupling of qqq and $qqq\pi$ channels (pion dressing by using an optical potential). Resonances in the $[70,1^-]$ multiplet were classified and new ones predicted; the $1/N_c$ hierarchy reduces the number of free parameters and improves the predictive power.

It remains an open question which excited mesons can be described as $q\bar{q}$ systems and which possess additional $q\bar{q}$ pairs, as well as whether the dominant configurations are diquark-diantiquarks, dimesons or compact four-particle clusters. Caveats were heard that resonant states may not appear as peaks; near threshold or in presence of other channels they may appear as dips! The X(3872) resonance exhibits interesting isospin violation effects. Various Lattice QCD methods were discussed to distinguish resonances from two mesons: for example, the Y(4260) behaves as a bound state. New motivations are coming from experiments at Belle (states with surprisingly low masses or peculiar branching ratios).

The classical three-body problem is still suggesting a search for new dynamical symmetries. On the other hand, studies beyond the standard model suggest new candidates for dark matter with a hadron-like strucutre; using SO(1,13) symmetry, eight families are predicted, the fifth family offering a stable superheavy "neutron".

We have opened as many new problems as we have resolved old ones, so the interest in our Mini-Workshop will not wane. We hope to see you again at Bled.

Ljubljana, November 2010

M. Rosina
B. Golli
S. Širca

Workshops organized at Bled

Also published in this series

On the nature of the Roper resonance

L. Alvarez-Ruso

Centro de Física Computacional, Departamento de Física, Universidade de Coimbra, Portugal

Abstract. The lightest N^* state, $N(1440)$ P_{11}, also known as Roper resonance, has puzzled physicists for decades. A large variety of theoretical models aimed to understand its properties have been proposed. Some of them are briefly reviewed here, together with the hadronic processes where the Roper resonance is revealed or plays an important role.

1 Roper resonance properties

In the 1950ies, Fermi and coworkers started to measure pion-nucleon cross sections and to analyze the data in terms of partial waves, leading the way to the discovery of a large number of baryon resonances. In 1963, in a partial-wave analysis performed at the Lawrence Livermore National Laboratory, L. D. Roper found a P_{11} resonance at $\sqrt{s} \approx 1.43$ GeV (≈ 600 MeV pion laboratory kinetic energy) [1]. The result was surprizing as there were no hints for such a state and the P_{11} scattering length is rather large and negative. In words of Roper: *I spent a much time trying to eliminate the* P_{11} *resonance* [2].

The Particle Data Group estimates for the main $N^*(1440)$ properties are listed in Table 1. Considerable uncertainties are apparent, specially in the full Breit-Wigner width and the branching ratios to the strong-decay channels. Indeed, different values are obtained with different models, most of them built in terms of Breit-Wigner resonances plus background, meson-exchange or K-matrix formalisms. For example, the recent K-matrix multichannel analysis of Ref. [4], which combines single and double-pion production data induced by pions and photons finds a $\Gamma_{\pi N}/\Gamma_{tot} \approx 61$ %, in agreement with the PDG, but a smaller $\Gamma_{\pi\Delta}/\Gamma_{tot} \approx 18$ % and a considerably larger $\Gamma_{\sigma N}/\Gamma_{tot} \approx 21$ % (to be compared to the $N^* \rightarrow N(\pi\pi)_{S-wave}^{I=0}$ 5-10 % PDG estimate).

Pole positions and residues allow for a parameterization of resonances in a well-defined way, free of assumptions for the background and energy dependence of the resonance part [5]. Actually, many different studies find for the Roper resonance two almost degenerate poles close to the $\pi\Delta$ threshold on two different Riemann sheets of the $\pi\Delta$ channel [6,5,7,8]. The pole positions are stable against larger variations of parameters in meson-exchange mechanisms, with averaged values of $(ReM^*, -ImM^*) = (1363^{+9}_{-6}, 79^{+3}_{-5})$ MeV and $(1373^{+12}_{-10}, 114^{+14}_{-9})$ MeV [8]. The second pole is a replica or shadow of the first one without strong physical implications rather than a new structure [5]. In spite of this agreement, the dynamical origin of the Roper poles is not clear: while in the JLMS model of Ref. [7], they

N(1440) P$_{11}$	I(J^P) = 1/2(1/2$^+$)
Breit-Wigner mass = 1420 to 1470 ($\approx$ 1440) MeV	
Breit-Wigner full width = 200 to 450 ($\approx$ 300) MeV	
Re(pole position) = 1350 to 1380 ($\approx$ 1365) MeV	
2Im(pole position) = 160 to 220 ($\approx$ 190) MeV	
Decay modes	Fraction (Γ_i/Γ_{tot})
Nπ	0.55 to 0.75
N$\pi\pi$	30 − 40 %
$\quad\Delta\pi$	20 − 30 %
$\quad$Nρ	< 8 %
$\quad$N$(\pi\pi)^{I=0}_{S-wave}$	5 − 10 %
gpγ	0.035 − 0.048 %
nγ	0.009 − 0.032 %

Table 1. Summary of the PDG estimates for the Roper resonance properties [3].

evolve from a single bare state that also gives rise to the N*(1710), no genuine pole term is required in the Jülich model [5].

2   (Some of) the many faces of the Roper resonance

In a simple quark model with a harmonic oscillator potential it is easy to understand why it is unexpected to have a radial excitation of the nucleon as the first N*. The energy spectrum is given by $E_n = \hbar\omega(n + 3/2)$ with $n = n_r + l$. If the lowest state with $n = 0$, $l = 0$ is associated with the nucleon (J$^P = 1/2^+$), then the first excited state with $n = 1$, $l = 1$ is N*(J$^P = 1/2^-$) and only the next one with $n = 2$, $l = 0$ is an N*(J$^P = 1/2^+$) like the Roper. However, the first negative parity state N(1535) S$_{11}$ turns out to be heavier than the N(1440) P$_{11}$. This parity reversal pattern cannot be described by successful quark models based on SU(6) symmetry with residual c olor-spin interactions between quarks (see for instance Fig. 9 of Ref. [9]).

Some authors argue that reverse parity is an indication that at low energies the interactions among constituent quarks could be dominated by flavor-dependent Goldstone boson exchange (GBE) (see Ref. [10] for a review). With this assumption it is possible to obtain a good description of the low-lying baryon spectrum and, in particular, the correct level ordering between the N*(1440) and the N*(1535), as can be seen in Fig. 4 of Ref. [11]. The model has been extended to include the exchange of vector and scalar mesons to account for correlated multiple GBE, although the special nature of pseudoscalar Goldstone bosons does not extend to other mesons. Besides, the special status of mesons in this model makes it difficult to achieve a unified description of both mesons and baryons [9].

Further understanding of the nature of the Roper resonance and the level ordering may be provided by lattice QCD. In a recent study, the first positive and negative parity excited states of the nucleon have been obtained with variational analysis in quenched QCD [12,13]. The $1/2^-$ state is below the $1/2^+$ one for heavy quark masses, but the physical ordering is recovered for pion masses below 380 MeV (see Fig. [13]). Caution should be exercised in the interpretation of this result obtained in quenched QCD and for which the identification of the $1/2^-$ at low quark masses, where finite lattice volume effects become significant, still remains. If confirmed, this level crossing could support the hypothesis that there is a transition from heavy quarks, where SU(6) symmetry with color-spin interactions works well, to light quarks where flavor-spin interactions due to GBE prevail [14].

To circumvent the parity reversal problem, alternative descriptions in which the Roper resonance is not (only) a qqq state have also been proposed. For instance, it could have a large gluonic component q^3G, although the masses of such hybrid states calculated with the flux-tube model are quite large ($M_{hyb} > 1870 \pm 100$ MeV) [15]. In one of its oldest representations, the Roper appears as a collective vibration of the bag surface, a breathing mode. Indeed, with the Skyrme model, where baryons are topological solitons of the meson nonlinear fields, a resonance was found in the breathing mode spectrum with a mass of $M^* = 1420$ MeV [16]. In line with the collective picture, Juliá-Díaz and Riska explored the presence of $(q\bar{q})^n$ components in the Roper resonance [17]. They found that the confining interaction mixes the qqq and $qqq\bar{q}q$ components. The $qqq\bar{q}q$ admixture in the Roper ranges from 3 to 25 % depending on the constituent quark mass while the $qqq(\bar{q}q)^2$ components are negligible. The qqq component could even be totally absent in the $N^*(1440)$ as suggested by the fact that the resonance shape is dynamically generated in the Jülich model from meson-baryon interactions in coupled channels [18,5]. Finally, if the baryons are regarded as many-body systems of quarks and gluons, it is natural to expect that they could be deformed. Such a possibility was investigated in Ref. [19], with a deformed oscillator potential. It was shown that low lying masses fit well to rotational spectra with the Roper as an $n = 2$ rotational state.

3   Hadronic reactions

Although the vast majority of the information about the $N^*(1440)$ has been extracted from the $\pi N \to \pi N$ reaction, there are many other processes where the resonance properties can be studied and/or where the reaction mechanism cannot be understood without taking it into account. Some of these processes are reviewed in this Section.

3.1   Electroproduction of the $N^*(1440)$

Valuable information about nucleon resonances is encoded in the electromagnetic $N \to N^*$ transitions, often presented in terms of helicity amplitudes connecting

states with well defined helicities. In the case of the $N - N^*(1440)$ transition, two such amplitudes should be introduced, $A_{1/2}$ and $S_{1/2}$, defined as

$$A_{1/2}(q^2) = \sqrt{\frac{2\pi\alpha}{k_R}} \langle N^* \downarrow | \epsilon_\mu^{(+)} J^\mu | N \uparrow \rangle, \tag{1}$$

$$S_{1/2}(q^2) = \sqrt{\frac{2\pi\alpha}{k_R}} \frac{|\mathbf{q}|}{\sqrt{-q^2}} \langle N^* \uparrow | \epsilon_\mu^{(0)} J^\mu | N \uparrow \rangle. \tag{2}$$

Here, α is fine-structure constant, $k_R = (M_{N^*}^2 - M_N^2)/(2M_{N^*})$, $q = (\omega, \mathbf{q})$ is the four-momentum transfered to the nucleon and $\epsilon^{(+,0)}$ stand for the transverse and longitudinal polarizations of the virtual photon. The $N - N^*(1440)$ transition electromagnetic current can be parametrized with two form factors

$$J^\mu = \bar{u}_{N^*}(p') \left[F_1(q^2) \left(\not{q} q^\mu - q^2 \gamma^\mu \right) + iF_2(q^2) \sigma^{\mu\nu} q_\nu \right] u(p). \tag{3}$$

This current is very similar to the nucleon one, except for the $\not{q} q^\mu$ part. In the nucleon case, the form factor associated with this operator has to vanish to ensure current conservation, but not for the $N - N^*$ transition because the Roper mass differs from the nucleon one. Introducing electric and magnetic form factors, in analogy to the Sachs form factors of the nucleon and substituting Eq. (3) in the expressions for the helicity amplitudes, one obtains that up to well known factors $A_{1/2} \sim G_M$ and $S_{1/2} \sim G_E$ [20,21].

   The $N - N^*(1440)$ helicity amplitudes have been studied using various models with a wide diversity of results. Some of these are shown in Fig. 1, namely, the prediction from the non-relativistic quark model (NRQM) [22], the hybrid model [22], the light-front relativistic quark model (LF) calculation of Ref. [20], the chiral chromodielectric (ChD) model [23] and the extended vector-meson dominance (EVMD) model of Ref. [24].

   The extensive N^* program at JLab has provided a large amount of precision data on pion electroproduction which, together with the data from previous experiments at MIT/Bates and MAMI/Mainz, has made possible the extraction of the transition helicity amplitudes at $0 < Q^2 < 6$ $(GeV/c)^2$ the for several resonances and, in particular, for the Roper [25,26]. The result from the global MAID07 analysis is also shown in Fig. 1. The comparison with the models reveals that non of them is really satisfactory. This is an indication of the difficulties that quark models encounter in the description of the low $Q^2 < 1$ $(GeV/c)^2$ region. At $Q^2 > 2$ $(GeV/c)^2$, where $A_{1/2}^p$ and $S_{1/2}^p$ are positive and decreasing, good agreement is obtained with relativistic quark model calculations assuming that the Roper is the first radial excitation of the nucleon [26,27]. The discrepancies at low Q^2 are interpreted as due to the missing meson cloud effects. The importance of the pion cloud, particularly at low Q^2, has also been demonstrated in a recent study of electroproduction amplitudes with the simple Cloudy Bag Model [28]. The pion cloud is found to be responsible for the large and negative value of $A_{1/2}^p$ at the photon point, while the quark dynamics becomes progressively relevant as Q^2 increases, causing $A_{1/2}^p$ to change sign.

   It is important to bare in mind that extraction of helicities amplitudes in both the MAID [25] and CLAS [26] analyses imply certain model dependent assumptions about the resonant and non-resonant parts of the pion electroproduction
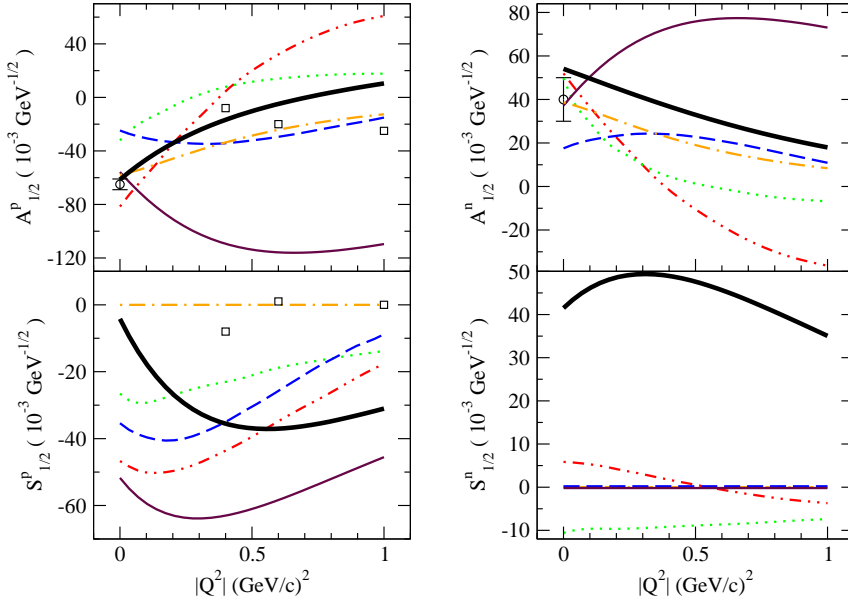
Fig. 1. Transverse ($A_{1/2}$) and longitudinal ($S_{1/2}$) helicity amplitudes for the $N - N^*(1440)$ transition calculated with various models: NRQM (solid line) [22], hybrid model (dash-dotted line) [22], LF (dotted line) [20], ChD (dashed line) [23] and EVMD (dash-double-dotted line) [24]. The result of the global MAID07 analysis [25] is given by the thick solid line.

amplitudes. For this reason, alternative methods are being pursued, like the extraction of transition form factors at the resonance poles using analytic continuation [29].

3.2   Direct observation of the Roper resonance

The excitation of the Roper resonance in πN and γN reactions can only be assessed with partial wave analyses; in the reaction cross section, the N(1440) P_{11} overlaps with the N(1520) D_{13} and the N(1535) S_{11} forming the so called second resonance region. Moreover, all these N^* states might be masked the prominent $\Delta(1232)P_{33}$ excitation since πN and γN interactions mix isospin $1/2$ and $3/2$. However, certain reactions act as filters, making the direct observation of the Roper excitation possible.

An example is the (α, α') reaction of proton target studied at SATURNE with a beam energy of 4.2 GeV [30]. As the projectile has $I = 0$, the $\Delta(1232)$ excitation can occur on the projectile but not on the target. For this reason the Roper excitation appears as small peak on the tail of the dominant $\Delta(1232)$ excitation (see Fig. 2 of Ref. [30]). The theoretical study of Hirenzaki et al. [31] showed that the isoscalar excitation on the proton is the dominant $N^*(1440)$ production mechanism and extracted its strength from data. The fact that the interference with the $\Delta(1232)$ excitation on the α is important allowed to establish also the relative sign of the amplitudes.

An even clearer case of direct N*(1440) observation has been made by the BES Collaboration with the decay $J/\psi \rightarrow \bar{N}N\pi$ [32]. Here, because of isospin conservation, the πN system is in pure isospin 1/2. Several N* were observed in the πN invariant mass distribution, the first of them corresponding to the Roper resonance. Its mass and width, estimated with a simple Breit-Wigner function were found to be $1358 \pm 6 \pm 16$ MeV and $179 \pm 26 \pm 50$ MeV respectively. As a constant width was used in the Breit-Wigner, the extracted mass is close to the pole value.

3.3   Double-pion production reactions

The Roper resonance is a vital ingredient in double-pion production reaction mechanisms. In spite of its small branching ratio, the S-wave character of the $N^*(1440) \rightarrow N(\pi\pi)^{I=0}_{S-wave}$ decay (or $N^*(1440) \rightarrow N\sigma$ as often denoted in the literature) makes it a very important nonvanishing contribution at threshold. This is the case for the $\pi N \rightarrow \pi\pi N$ reaction, as was shown long ago in Ref. [33] and supported by other models. For instance, in Fig. 10 of Ref. [34] the dotted lines denoting the results without $N^*(1440)$ are well below the full model (and the data) in the channels where the $N^*(1440) \rightarrow N(\pi\pi)^{I=0}_{S-wave}$ decay is allowed.

The relevance of the Roper is even more dramatic in $NN \rightarrow NN\pi\pi$, where according to the model of Ref. [35], the isoscalar excitation of the resonance, followed by its decay into $N(\pi\pi)^{I=0}_{S-wave}$ appears to be dominant at laboratory kinetic energies of the incident proton $T_p < 1$ GeV. The other two important reaction mechanisms: $\Delta\Delta$ excitation and $N^*(1440) \rightarrow \Delta\pi$ are negligible at threshold but rise fast to become important above $T_p = 1$ GeV. In recent years, this reaction has been accurately measured at CELSIUS and COSY. At low energies, the main features predicted by the model of Ref. [35] have been confirmed (see for instance Ref. [36]). The situation is more involved at higher energies: an isospin analysis of the data [37] indicates that the contribution from heavier Δ states might be important. Resonances with masses up to 1.72 GeV have been incorporated in the relativistic model of Cao et al. [38], finding large contributions from the $\Delta(1600)$ and $\Delta(1620)$ states. The agreement to data is improved by reducing the $N^*(1440) \rightarrow \Delta\pi$ branching ratio, in line with the findings of Ref. [4].

The $NN \rightarrow NN\pi\pi$ model of Ref. [38] does not include interferences but, in particular, the interference between the $N(\pi\pi)^{I=0}_{S-wave}$ and $\Delta\pi$ decay modes of the Roper has been found to explain some details of the invariant mass and angular distributions for $\pi N \rightarrow \pi\pi N$ (Fig. 12 of Ref. [34]), $NN \rightarrow NN\pi\pi$ (Fig. 4 of Ref. [36]) and specially $np \rightarrow d\pi\pi$. For this later reaction, it has been shown that the shape of the double differential cross sections measured at LAMPF with a neutron beam of $p_n = 1.463$ GeV/c [39] can be explained by the above mentioned interference between the two-pion decay modes of the Roper resonance [40]. As shown in Fig 2, by taking into account the Roper one obtains a good description of the size and energy dependence of the total $np \rightarrow d\pi\pi$ cross section even with a rather simple model as the one of Ref. [40]. The $np \rightarrow d\pi\pi$ reaction close to threshold has been recently investigated in the framework of chiral perturbation theory [41]. The reported results for the total cross section are considerably smaller than those of Fig. 2 even at lower energies.
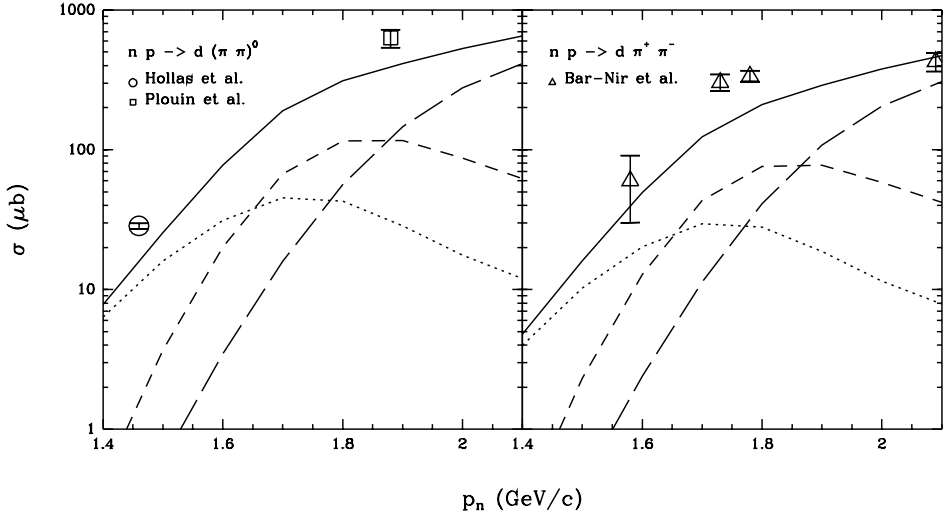
Fig. 2. Total cross section for $np \to d\pi\pi$ as a function of the neutron laboratory momentum (solid line). The dotted line corresponds to the $N^*(1440) \to N(\pi\pi)^{I=0}_{S-wave}$ mechanism, the short-dashed line stands for the $N^*(1440) \to \Delta\pi$ and the long-dashed one for the double-Δ excitation (see Ref. [40] for details). The data are from Refs. [39] (circle), [42] (square) and [43] (triangles).

References

1. L. D. Roper, Phys. Rev. Lett. **12** (1964) 340.
2. http://arts.bev.net/roperldavid/roperres.htm
3. C. Amsler *et al.* [Particle Data Group], Phys. Lett. B **667** (2008) 1.
4. A. V. Sarantsev *et al.*, Phys. Lett. B **659** (2008) 94 [arXiv:0707.3591 [hep-ph]].
5. M. Doring, C. Hanhart, F. Huang, S. Krewald and U. G. Meissner, Nucl. Phys. A **829** (2009) 170 [arXiv:0903.4337 [nucl-th]].
6. R. A. Arndt, J. M. Ford and L. D. Roper, Phys. Rev. D **32** (1985) 1085.
7. N. Suzuki, B. Julia-Diaz, H. Kamano, T. S. Lee, A. Matsuyama and T. Sato, Phys. Rev. Lett. **104** (2010) 042302 [arXiv:0909.1356 [nucl-th]].
8. H. Kamano, S. X. Nakamura, T. S. Lee and T. Sato, Phys. Rev. C **81** (2010) 065207 [arXiv:1001.5083 [nucl-th]].
9. S. Capstick and W. Roberts, Prog. Part. Nucl. Phys. **45** (2000) S241 [arXiv:nucl-th/0008028].
10. L. Y. Glozman and D. O. Riska, Phys. Rept. **268** (1996) 263 [arXiv:hep-ph/9505422].
11. L. Y. Glozman, Nucl. Phys. A **663** (2000) 103 [arXiv:hep-ph/9908423].
12. M. S. Mahbub, A. O. Cais, W. Kamleh, B. G. Lasscock, D. B. Leinweber and A. G. Williams, Phys. Lett. B **679** (2009) 418 [arXiv:0906.5433 [hep-lat]].
13. M. S. Mahbub, W. Kamleh, D. B. Leinweber, A. O. Cais and A. G. Williams, Phys. Lett. B **693** (2010) 351 [arXiv:1007.4871 [hep-lat]].
14. N. Mathur *et al.*, Phys. Lett. B **605** (2005) 137 [arXiv:hep-ph/0306199].
15. S. Capstick and P. R. Page, Phys. Rev. D **60** (1999) 111501 [arXiv:nucl-th/9904041].
16. U. B. Kaulfuss and U. G. Meissner, Phys. Lett. B **154** (1985) 193.
17. B. Julia-Diaz and D. O. Riska, Nucl. Phys. A **780** (2006) 175 [arXiv:nucl-th/0609064].

18. O. Krehl, C. Hanhart, S. Krewald and J. Speth, Phys. Rev. C **62** (2000) 025207 [arXiv:nucl-th/9911080].
19. A. Hosaka, H. Toki and H. Ejiri, Nucl. Phys. A **629** (1998) 160C.
20. F. Cardarelli, E. Pace, G. Salme and S. Simula, Phys. Lett. B **397** (1997) 13 [arXiv:nucl-th/9609047].
21. L. Alvarez-Ruso, M. B. Barbaro, T. W. Donnelly and A. Molinari, Nucl. Phys. A **724** (2003) 157 [arXiv:nucl-th/0303027].
22. Z. p. Li, V. Burkert and Z. j. Li, Phys. Rev. D **46** (1992) 70.
23. P. Alberto, M. Fiolhais, B. Golli and J. Marques, Phys. Lett. B **523** (2001) 273 [arXiv:hep-ph/0103171].
24. F. Cano and P. Gonzalez, Phys. Lett. B **431** (1998) 270 [arXiv:nucl-th/9804071].
25. D. Drechsel, S. S. Kamalov and L. Tiator, Eur. Phys. J. A **34** (2007) 69 [arXiv:0710.0306 [nucl-th]].
26. I. G. Aznauryan *et al.* [CLAS Collaboration], Phys. Rev. C **80** (2009) 055203 [arXiv:0909.2349 [nucl-ex]].
27. G. Ramalho and K. Tsushima, Phys. Rev. D **81** (2010) 074020 [arXiv:1002.3386 [hep-ph]].
28. B. Golli, S. Sirca and M. Fiolhais, Eur. Phys. J. A **42** (2009) 185 [arXiv:0906.2066 [nucl-th]].
29. N. Suzuki, T. Sato and T. S. Lee, arXiv:1006.2196 [nucl-th].
30. H. P. Morsch *et al.*, Phys. Rev. Lett. **69** (1992) 1336.
31. S. Hirenzaki, P. Fernandez de Cordoba and E. Oset, Phys. Rev. C **53** (1996) 277 [arXiv:nucl-th/9511036].
32. M. Ablikim *et al.* [BES Collaboration], Phys. Rev. Lett. **97** (2006) 062001 [arXiv:hep-ex/0405030].
33. E. Oset and M. J. Vicente-Vacas, Nucl. Phys. A **446** (1985) 584.
34. H. Kamano and M. Arima, Phys. Rev. C **73** (2006) 055203 [arXiv:nucl-th/0601057].
35. L. Alvarez-Ruso, E. Oset and E. Hernandez, Nucl. Phys. A **633** (1998) 519 [arXiv:nucl-th/9706046].
36. J. Patzold *et al.*, Phys. Rev. C **67** (2003) 052202 [arXiv:nucl-ex/0301019].
37. T. Skorodko *et al.*, Phys. Lett. B **679** (2009) 30 [arXiv:0906.3087 [nucl-ex]].
38. X. Cao, B. S. Zou and H. S. Xu, Phys. Rev. C **81** (2010) 065201 [arXiv:1004.0140 [nucl-th]].
39. C. L. Hollas, C. R. Newsom, P. J. Riley, B. E. Bonner and G. Glass, Phys. Rev. C **25** (1982) 2614.
40. L. Alvarez-Ruso, Phys. Lett. B **452** (1999) 207 [arXiv:nucl-th/9811058].
41. B. Liu, V. Baru, J. Haidenbauer and C. Hanhart, arXiv:1007.1382 [nucl-th].
42. F. Plouin *et al.*, Nucl. Phys. A **302** (1978) 413.
43. I. Bar-Nir *et al.*, Nucl. Phys. B **54** (1973) 17.

The quark-antiquark spectrum from upside down[*]

E. van Beveren[1] and G. Rupp[2]

[1] Centro de Física Computacional, Departamento de Física, Universidade de Coimbra, P-3004-516 Coimbra, Portugal
[2] Centro de Física das Interacções Fundamentais, Instituto Superior Técnico, Universidade Técnica de Lisboa, Edifício Ciência, P-1049-001 Lisboa, Portugal

Abstract. We argue that the spectra of quark-antiquark systems should better be studied from higher radial excitations and, in particular, from configurations with well-defined quantum numbers, rather than from ground states and lower radial excitations, the most suitable system being charmonium.

In the Resonance-Spectrum Expansion (RSE) [1], which is based on the model of Ref. [2], the meson-meson scattering amplitude is given by an expression of the form (here restricted to the one-channel and one-delta-shell case)

$$T(E) = \left\{ -2\lambda^2 \mu p j_\ell^2 (pr_0) \sum_{n=0}^{\infty} \frac{\left| g_{nL(\ell)} \right|^2}{E - E_{nL(\ell)}} \right\} \Pi(E) \quad , \tag{1}$$

where p is the center-of-mass (CM) linear momentum, $E = E(p)$ is the total invariant two-meson mass, j_ℓ and $h_\ell^{(1)}$ are the spherical Bessel function and Hankel function of the first kind, respectively, μ is the reduced two-meson mass, and r_0 is a parameter with dimension mass^{-1}, which can be interpreted as the average string-breaking distance. The coupling constants g_{NL}, as well as the relation between ℓ and $L = L(\ell)$, were determined in Ref. [3]. The overall coupling constant λ, which can be formulated in a flavor-independent manner, represents the probability of quark-pair creation. The dressed partial-wave RSE propagator for strong interactions is given by

$$\Pi_\ell(E) = \left\{ 1 - 2i\lambda^2 \mu p j_\ell (pr_0) h_\ell^{(1)} (pr_0) \sum_{n=0}^{\infty} \frac{\left| g_{NL} \right|^2}{E - E_{NL}} \right\}^{-1} \quad . \tag{2}$$

In Ref. [4] we have studied an intriguing property of the propagator (2), namely that it vanishes for $E \rightarrow E_{NL}$. Here, we will concentrate on the fact that the scattering amplitude (1) is independent of the way quark confinement is introduced, as only the confinement spectrum E_{NL} appears in expressions (1) and (2).

[*] Talk delivered by E. van Beveren

Hence, whatever one's preferred mechanism for confinement, the scattering amplitude only depends on the resulting spectrum. As a consequence, one merely has to deduce from experiment a suitable set of values of E_{NL} and then try to guess the corresponding dynamics for confinement.

However, in the recent past we have found that analysing experimental data is far from trivial. For instance, the expressions (1) and (2) may also lead to dynamically generated resonances, like the light scalar-meson nonet [5], or the D_{s0} (2317) [6], which do not stem directly from the confinement spectrum. Furthermore, the mountain-shaped threshold enhancements in plots of events versus invariant mass for particle production can easily be mistaken for resonances [7]. Also, to properly analyse certain hadronic decay modes, one has to turn the resulting data upside down, so as to find the true quarkonium resonances and threshold enhancements [8], instead of erroneously classifying the leftovers as unexpected new resonances [9]. Moreover, in studying resonances from production processes, one has no control over their quantum numbers [10].

Our simple formulas (1) and (2) for meson-meson scattering are certainly not good enough for a detailed description of production processes, but must be adapted in order to account for, at least, the threshold enhancements [11]. However, the precise dynamics of production processes is still far from being fully understood. Nevertheless, for the low-lying part of the spectra we may deduce some properties without too much dependence on a specific confinement spectrum. We found that meson loops, which are properly accounted for in expressions (1) and (2), have most influence on the mass shifts of the ground states. Consequently, upon deducing a confinement spectrum from the lowest-lying states, one is urged to seriously consider the meson loops [2].

Threshold enhancements are more conspicuous for sharp thresholds, i.e., when the involved particles have small widths, rather than for diffuse thresholds, concerning decay products that have considerable widths themselves [12]. The latter phenomenon tends to happen higher up in the spectrum. There, we may expect a smoothened-out pattern of overlapping broad threshold enhancements. Therefore, higher radial excitations of quarkonium resonances can more easily be disentangled from other enhancements. The disadvantage is that any confinement mechanism predicts, for higher excitations, abundantly many states of the $q\bar{q}$ propagator, with a variety of different quantum numbers.

Now, in order to avoid a large number of partly overlapping resonances, one best studies resonances obtained in electron-positron annihilation, which process is dominated by vector quarkonia. But this is not the full solution for cleaning up the data, since in the light-quark sector one has nonstrange and strange $q\bar{q}$ combinations with comparable spectra, which will come out on top of each other, besides possibly significant mixing of isoscalar $n\bar{n}$ ($n = u, d$) and $s\bar{s}$ states. Moreover, decay channels involving kaons are common to both $n\bar{n}$ and $s\bar{s}$ resonances. Actually, the only system with a sufficient number of established states to find evidence (see Table 3 of Ref. [13]) for a regular level splitting of about 380 MeV is given by the radially excited f_2 mesons. A way out is to study a well-isolated system, with just one set of quantum numbers, like vector $c\bar{c}$ states, which can be produced in e^+e^- annihilation. Once the spectrum of vector $c\bar{c}$ is well estab-

lished, one can with some confidence apply its properties to other spectra. Unfortunately, the well-established $J^{PC} = 1^{--}$ $c\bar{c}$ spectrum anno 2010 still consists of J/ψ, $\psi(2S, 3S, 4S)$, and $\psi(1D, 2D)$ only.
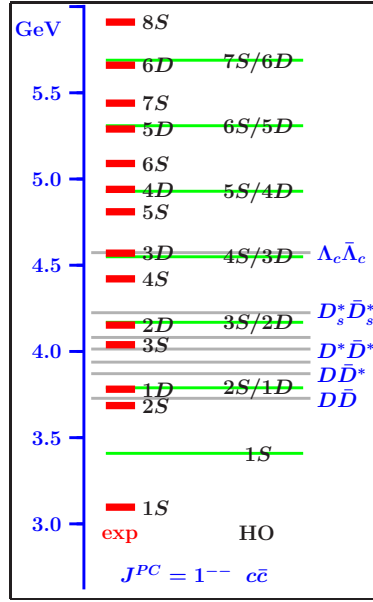
Fig. 1. The higher charmonium vector states (exp) as extracted by us from data: (i) the $\psi(3D)$ [8], in BABAR data [9] on $e^+e^- \to J/\psi\pi^+\pi^-$; (ii) the $\psi(5S)$ and $\psi(4D)$ [17], in data obtained by the Belle Collaboration on $e^+e^- \to \Lambda_c^+\Lambda_c^-$ [18], $D^0D^{*-}\pi^+$ [19], and $D^0D^{*-}\pi^+$ [20], as well as in the missing signal of Ref. [9], and in further BABAR data on $D^*\bar{D}^*$ [16]; (iii) the $\psi(5S)$, $\psi(4D)$, $\psi(6S)$, and $\psi(5D)$ [21], in the data of Ref. [18]; (iv) the $\psi(3D)$, $\psi(5S)$, $\psi(4D)$, $\psi(6S)$, and $\psi(5D)$ [22], in new, preliminary BABAR data [23] on $e^+e^- \to J/\psi\pi^+\pi^-$; (v) the $\psi(7S)$, $\psi(6D)$, and $\psi(8S)$ [15], in data from BABAR on $D^*\bar{D}^*$ [16]. We also indicate the level scheme as predicted by pure HO confinement (HO) (━). Meson and baryon loops shift the D states a few MeV down/up, whereas the S states shift 100–200 MeV downwards. For completeness, we also indicate the levels of the sharp, low-lying meson-meson and baryon-baryon thresholds (━) of the channels $D\bar{D}$, $D\bar{D}^*$, $D_s\bar{D}_s$, $D^*\bar{D}^*$, $D_s\bar{D}_s^*$, $D_s^*\bar{D}_s^*$, and $\Lambda_c^+\Lambda_c^-$.

In the following, we will concentrate on a specific choice for confinement, namely the harmonic oscillator (HO), though not so much the corresponding potential or geometry (anti-De-Sitter [14]), but just the HO spectrum that follows from these approaches. For vector $c\bar{c}$ systems, one has a single $^3S_1$ ground state, and radial excitations, which can be either $^3S_1$ or $^3D_1$. In the HO spectrum, $^3S_1$ states with radial quantum number n and $^3D_1$ states with $n-1$ are degenerate. However, due to the interaction generated by the meson loops, the poles associated with the resonances repel each other in such a way that one is subject to a small mass shift, whereas the other shifts considerably more and downwards. Higher up in the $c\bar{c}$ spectrum, the mass shift of the lower pole, which is dominantly $^3S_1$, becomes of the order of 150–200 MeV, whereas the higher pole, mostly

$^3D_1$, acquires a central resonance position that is only a few to at most about 50 MeV away from the HO spectrum [2]. In Ref. [15] we found evidence, in data obtained by the BABAR Collaboration [16], for further charmonium states, viz. $\psi(5S, 6S, 7S, 8S)$ and $\psi(3D, 4D, 5D, 6D)$, which confirm the above observation. In Fig. 1 we display the resulting spectrum for vector charmonium.

We can conclude from Fig. 1 that our guess of an HO spectrum for vector $c\bar{c}$ states, with a radial level spacing of 380 MeV [24], seems to work well in view of the data. Furthermore, we may observe the advantage of studying the $c\bar{c}$ vector spectrum from above, where the pattern of dominantly S and dominantly D states becomes rather regular.

Summarizing, we have shown that the $c\bar{c}$ confinement spectrum, which underlies scattering and production of multi-meson systems containing open-charm pairs, can best be observed by starting from higher radial excitations of vector charmonium in electron-positron annihilation. Moreover, we have shown that a constant radial level splitting of about 380 MeV is consistent with light and heavy meson spectra.

References

1. E. van Beveren and G. Rupp, Int. J. Theor. Phys. Group Theor. Nonlin. Opt. **11**, 179 (2006).
2. E. van Beveren, C. Dullemond, and G. Rupp, Phys. Rev. D **21**, 772 (1980) [Erratum-ibid. D **22**, 787 (1980)].
3. E. van Beveren, Z. Phys. C **21**, 291 (1984).
4. E. van Beveren and G. Rupp, in Proceedings *Bled Workshops in Physics*, Vol. 9, no. 1, pp 26-29 (2008).
5. E. van Beveren, T. A. Rijken, K. Metzger, C. Dullemond, G. Rupp and J. E. Ribeiro, Z. Phys. C **30**, 615 (1986).
6. E. van Beveren and G. Rupp, Phys. Rev. Lett. **91**, 012003 (2003).
7. E. van Beveren and G. Rupp, Phys. Rev. D **80**, 074001 (2009).
8. E. van Beveren, G. Rupp and J. Segovia, Phys. Rev. Lett. **105**, 102001 (2010).
9. B. Aubert *et al.* [BABAR Collaboration], Phys. Rev. Lett. **95**, 142001 (2005).
10. B. Aubert [BaBar Collaboration], Phys. Rev. D **80**, 092003 (2009).
11. E. van Beveren and G. Rupp, Ann. Phys. **323**, 1215 (2008).
12. S. Coito, G. Rupp and E. van Beveren, arXiv:1008.5100.
13. E. van Beveren and G. Rupp, Eur. Phys. J. A **31**, 468 (2007).
14. C. Dullemond, T. A. Rijken and E. van Beveren, Nuovo Cim. A **80**, 401 (1984).
15. E. van Beveren and G. Rupp, arXiv:1004.4368.
16. B. Aubert [The BABAR Collaboration], Phys. Rev. D **79**, 092001 (2009).
17. E. van Beveren and G. Rupp, arXiv:1005.3490.

18. G. Pakhlova *et al.* [Belle Collaboration], Phys. Rev. Lett. **101**, 172001 (2008).
19. G. Pakhlova *et al.* [Belle Collaboration], Phys. Rev. D **80**, 091101 (2009).
20. G. Pakhlova *et al.* [Belle Collaboration], Phys. Rev. Lett. **100**, 062001 (2008).
21. E. van Beveren, X. Liu, R. Coimbra, and G. Rupp, Europhys. Lett. **85**, 61002 (2009).
22. E. van Beveren and G. Rupp, arXiv:0904.4351.
23. B. Aubert [BaBar Collaboration], SLAC-PUB-13360, BABAR-CONF-08-004, see also arXiv:0808.1543.
24. E. van Beveren, G. Rupp, T. A. Rijken, and C. Dullemond, Phys. Rev. D **27**, 1527 (1983).

Tetraquark resonances, flip-flop and cherry in a broken glass model[⋆]

P. Bicudo, M. Cardoso, and N. Cardoso

CFTP, Dep. Física, Instituto Superior Técnico,
Av. Rovisco Pais, 1049-001 Lisboa, Portugal

Abstract. We develop a formalism to study tetraquarks using the generalized flip-flop potential, which include the tetraquark potential component. Technically this is a difficult problem, needing the solution of the Schrödinger equation in a multidimensional space. Since the tetraquark may at any time escape to a pair of mesons, here we study a simplified two-variable toy model and explore the analogy with a cherry in a glass, but a broken one where the cherry may escape from. We also compute the decay width in this two-variable picture, solving the Schrödinger equation for the outgoing spherical wave.

1 Introduction, tetraquarks with flux tubes

Our main motivation is to contribute to understand whether exotic hadrons exit or not. Although there is no QCD theorem ruling out exotics, they are so hard to find, that many friends even state that either exotics dont exist, or that at least they should be very broad resonances. Nevertheless candidates for different continue to exotics exit [1]! Here we specialize in tetraquarks, the less difficult multiquarks to compute beyond the baryons and hybrids. Notice that there are many possible sorts of tetraquarks:
— the borromean 3-hadron molecule
— the Heavy-Heavy-antilight-antilight
— the hybrid-like tetraquark
— the Jaffe-Wilczek diquark-antidiquark with a generalized Fermat string

1.1 The borromean 3-hadron molecule

In an exotic channel, quark exchange leads to repulsion, while quark-antiquark annihilation is necessary for attraction. A possible way out is adding another meson, allowing for annihilation, to bind the three body system. This has already led to the computation of decay widths, which turned out to be wide [2,3].

1.2 The Heavy-Heavy-antilight-antilight

The heavy quarks are easy to bind since the kinetic energy $p^2/(2m)$ is smaller, thus their Coulomb short distance potential could perhaps provide sufficient binding, while the light antiquarks would form a cloud around them [4].

[⋆] Talk delivered by P. Bicudo

1.3 The hybrid-like tetraquark

Possibly a quark and antiquark may be in a colour octet, and then the tetraquark is equivalent to a quark-gluon-antiquark hybrid. Recently we computed in Lattice QCD the color fields for the static hybrid quark-gluon-antiquark system, and studied microscopically the Casimir scaling [5].

Notice that our lattice simulation shows that flux tubes prefer to divide into fundamental flux tubes, or flux tubes carrying a colour triplet flux, as we show in Fig. 1.
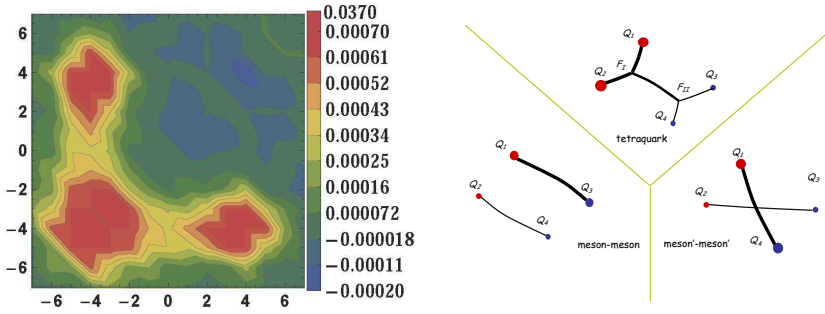
Fig. 1. (left) In a hybrid, flux tubes divide into two fundamental flux tunes, one connecting the octet with the quark and another connecting the octet to the antiquark. In the baryon and in the three-gluon glueball, static quenched Lattice QCD simulations also show confinement via fundamental flux tubes. (right) Triple flip-flop Potential potential. To the list of potentials to minimize including usually only two different meson pair potentials, we join another potential, the tetraquark potential.

1.4 The Jaffe-Wilczek diquark-antidiquark with a generalized Fermat string

Since there is no evidence for long distance polarization forces, or Van der Waals forces, in hadron-hadron interactions, the two-body confinement potentials cannot be right for multiquarks [6]! A solution to this problem consists in considering the flip-flop potential, where confining flux tubes or strings take the geometry minimizing the energy of the system. Quark Confinement And Hadronic Interactions [7].

Again the flux tubes in the tetraquark are expected to divide and link into fundamental flux tubes, and a possible configuration is in a H-like or butterfly-like flux tube. This tetraquark can be classified as a Jaffe-Wilczek one since the quarks are combined in a diquark-like antitriplet and the antiquarks are combined in a antidiquark-like triplet [8].

The technical difficulty in that framework is to compute the decay widths since this tetraquark is open for the decay into a pair of mesons. Moreover it is expected that the absence of a potential barrier above threshold may again produce a very large decay width to any open channel, although Marek and Lipkin suggested that multiquarks with angular excitations may gain a centrifugal barrier, leading to narrower decay widths [9].

Here we continue a previous work, where we assumed confined (harmonic oscillator-like) wavefunctions for the confined objects, one tetraquark and two different pairs of final mesons, and computed their hamiltonian. We utilized the Resonating Group Method and were surprised by finding very small decay widths [10].

1.5   Our approach to study the tetraquark with a generalized Fermat string

We thus return to basics and decide to have no overlaps. We want to solve the Schrödinger equation for the four particles, and from the Schrödinger solutions also compute the decay widths. Our starting point is the extended triple flip-flop potential [11], obtained minimizing the three lengths depicted in Fig. 1. Recently, we devised a numerical algorithm to compute the Fermat points of the tetraquark and the tetraquark potential [12].

Solving the Schrödinger equation is then a well defined problem which should be solvable, placing our system in a large 12 dimensional box. However this is a very difficult problem. Even assuming s-vaves, we would get 3 variables, some confined and some in the continuum (similar to problems in extra compactified dimensions or to lattice QCD) so we decide to work in a toy model, where the number of variables is simplified. We thus simplify the triple flipflop potential, with a single inter-meson variable, using the approximation on the diquark and anti-diquark Jacobi coordinates,

$$\rho_{13} = \rho_{24} \tag{1}$$

of having a single internal variable ρ in the mesons. We get a flipflop potential where ρ is open to continuum and r is confined, minimizing only two potentials,

$$V_{MM}(r, \rho) = \sigma(2r) , \tag{2}$$
$$V_T(r, \rho) = \sigma(r + \sqrt{3}\rho) . \tag{3}$$

Our problem is similar to the classical student's problem of a Cherry in a glass. However this is not a simple student's problem since the glass is broken and the cherry may escape from the glass! The flip-flop and broken glass potentials are depicted in Fig. 2. Here we report on our answer [13] to the question, *in the quantum case, are there resonances, and what is their decay width?*

2   Finite difference method

Since there is a single scale in the potential and a single scale in the kinetic energy, we can rescale the energy and the coordinates, to get a dimensionless equation,

$$H\Phi(r, \rho) = [-\Delta_r/2 - \Delta_\rho/2 + \min(r + \sqrt{3}\rho, 2r)]\Phi(r, \rho) = E\Phi(r, \rho) , \tag{4}$$

that we first solve with the finite difference method. Thus, our results and figures are dimensionless. This case is adequate to study equal mass quarks, where
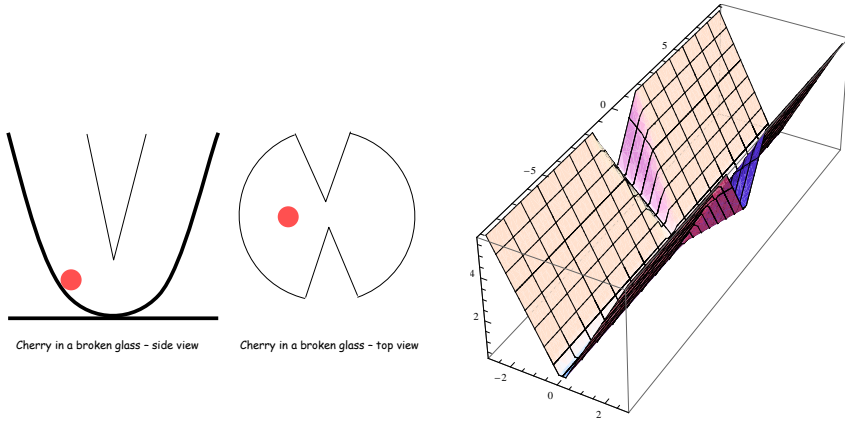
Fig. 2. (left) Cherry in a broken glass. Our simplified two-variable toy model is analogous to the classical mechanics textbook problem of a cherry in a glass, but a broken one where the cherry may escape from. Here we solve this model in quantum mechanics, addressing the decay widths of a system compact in one variable and open in the other. (right) Plot of our simplified flip-flop potential, as a function of the two radial variables r (compact) and ρ (open).

the mesons and the tetraquark have no constant energy shifts. For instance that would be ok for the light tetraquark and meson-meson system

$$uu\bar{d}\bar{d}_{(S=2)} \leftrightarrow \rho^+ \, \rho^+ \, , \tag{5}$$

or the heavy quark system

$$cc\bar{c}\bar{c}_{(S=2)} \leftrightarrow J/\psi \, J/\psi \, . \tag{6}$$

We discretize the space in anisotropic lattices and solve the finite difference Schrödinger equation, in up to 6000×6000 sparse matrices (equivalent to 40 points in the confined direction $\times$ 150 points in the radial continuum direction). We first look for localized states, selecting among the 6000 eigenvalues the ones more concentrated close to the origin at $\rho = 0$.

To measure the momenta k_i and the phase shifts δ_i, we simply fit the large ρ region of the non-vanishing ψ_i, where i indexes the factorized Airy wavefunction in r, the expression

$$\psi_i \to A_i \frac{\sin(k_i\rho + \delta_i)}{\rho} \, . \tag{7}$$

As can be seen in Fig. 4, the momenta k_i obey the relation

$$k_i(E) = \sqrt{2(E - \epsilon_i)}, \tag{8}$$

where ϵ_i is the threshold energy of the respective channel.

However, the phase shifts we get are not only discrete but rather irregular above threshold. In the next Section 3 we compute the phase shifts with an improved method.
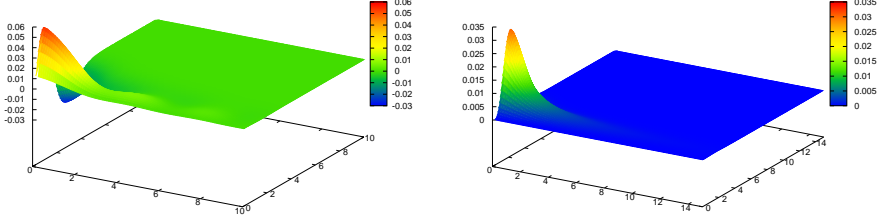
Fig. 3. (left) Semi-localized state, or resonance for $l_r = 1$.(right) Bound state for $l_r = 3$.
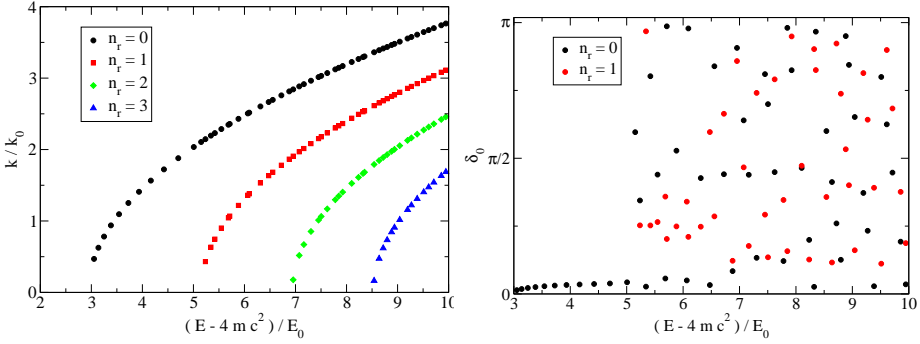
Fig. 4. (left) Momenta of the various components as a function of the energy. (right) "Phase shifts" obtained from the finite differences (by projecting the eigenstates in the meson-meson eigenstates). As can be seen the behaviour is irregular when we have more than one channel, this is due to the different contributions of multiple channels, for each eigenstate calculated in the finite difference scheme.

3 Outgoing spherical wave method

Because the finite difference method is not entirely satisfactory for the computation of the phase shifts δ, we move to another method, consisting in in studying the outgoing spherical waves. Since the finite difference method shows clearly bands for the different internal energies of the mesons, we integrate the confined coordinate r with eigenvalues of the meson equation, i.e. with Airy functions, and thus we are left with a system of ordinary differential equations in the coordinate ρ .

3.1 Projecting onto the ρ coordinate

We can reduce our problem in the dimensions ρ, r to a one-dimensional problem in ρ but with of coupled channels. We just have to expand the two-dimensional

wavefunction as

$$\Phi(\mathbf{r}, \boldsymbol{\rho}) = \sum_i \psi_i(\boldsymbol{\rho})\phi_i(\mathbf{r}) , \qquad (9)$$

where the ϕ_i are the eigenfunctions of the r confined hamiltonian. The one-dimensional potentials V_{ij} are given by

$$V_{ij}(\rho) = \int d^3\mathbf{r} \quad \phi_i^*(r)(V_{FF}(r, \rho) - V_{MM}(r))\phi_j(r) \qquad (10)$$

where we subtract V_{MM} from the potential, since $\hat{H}_{MM}$ is already accounted for in its eigenvalues and eigenfunctions, used for instance in Eq. (9).
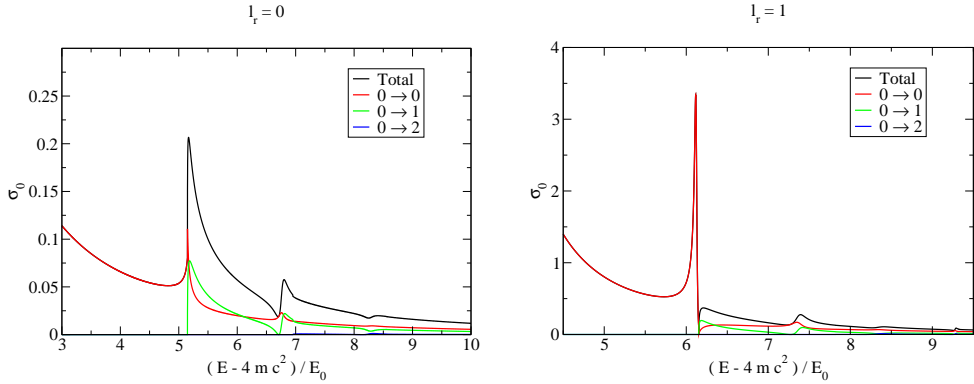
Fig. 5. (left) S-wave scattering cross sections from the channel with $l_r = 0$ and $n_r = 0$. (right) S-wave scattering cross sections from the channel with $l_r = 1$ and $n_r = 0$.

3.2 Phase shifts

We now compute the phase shifts, in order to search for resonances in our simplified flip-flop model. Solving the outgoing spherical Eq. for this system we can compute the partial cross sections and the total cross section for the partial wave l — either directly or by using the optical theorem — and determine the phase shifts as well.

Note that our flip-flop potential has the same scales of the simple Schrödinger equation for a linear potential, which has a single dimension

$$E_0 = \left(\frac{\hbar^2\sigma^2}{m}\right)^{1/3} , \qquad (11)$$

the only energy scale we can construct with $\hbar$, σ and m, the three relevant constants in the non-relativistic region. Thus the number of non-relativistic bound-states or resonances is independent both of the quark mass m and of the string constant σ.

3.3 The centrifugal barrier effect

Note that we have two distinct angular momenta, which are both conserved, $\mathbf{L}_r = \mathbf{r} \times \mathbf{p}_r$ and $\mathbf{L}_\rho = \rho \times \mathbf{p}_\rho$. So, each assimptotic state is indexed by its angular momentum l_r and its radial number n_r, and the scattering partial waves are indexed by l_ρ. Thus the system can be diagonalized not only in the scattering angular momenta $\mathbf{L}_\rho$ but also on the confined angular momenta $\mathbf{L}_r$. We can describe the scattering process with four quantum numbers: The scattering angular momentum l_ρ, the confined angular momentum l_r and the initial and final states radial number in the confined coordinate r, n_i and n_j.
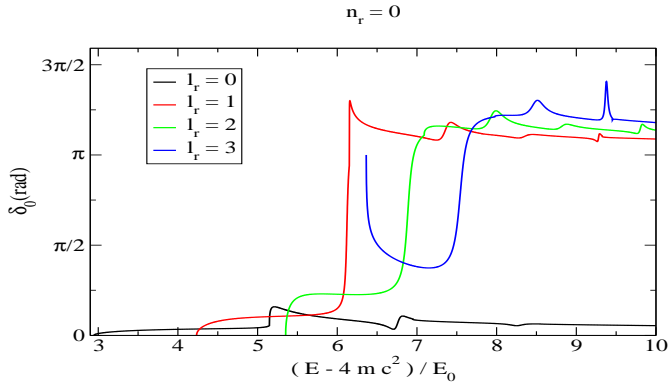
Fig. 6. Comparison of the phase shifts for $l_r = 0, 1, 2$ and 3, with $n_r = 0$.

On Fig. 5 we show the $l_\rho = 0$ partial cross sections for the scattering from the channel with $l_r = 0$ and for $l_r = 1$, with $n_r = 0$. Interestingly, the bumps in the cross section seem to occur prior to the opening of a new channel.

In Fig. 6 we compare the phase shifts for different values of l_r, namely for $l_r = 0, 1, 2$ and 3. For $l_r = 0$, we don't observe a resonance, since the phase shift doesn't even cross $\pi/2$. However, for the $l_r = 1$ and $l_r = 2$ cases, the phase shifts clearly cross the $\pi/2$ line, and a resonance is formed. This behaviour is somewhat expected, since a centrifugal barrier in r would, in the case of a true tetraquark, maintain the two diquarks separated, favouring the formation of a bound state. The tendency of greater stability for greater orbital angular momenta seems to be further confirmed by the $l_r = 3$, where besides the resonance, a true bound state seems to be formed, as can be seen by the different qualitative behaviour of the phase shifts for this case. This bound state formation confirms our observation of a localized states in Section 2, with the finite difference simulation.

Finally we can compute the decay width utilizing the phase shift derivative, $\Gamma/2 = (d\delta/dE)^{-1}$ computed when the phase shift δ crosses $\pi/2$, and get the results of Table 1. For instance, for light quarks where $m \simeq \sqrt{(\sigma)} \simeq 400$ MeV this results in a $l_r = 1$ decay width close to 15 MeV.

Table 1. Decay widths as a function of l_r.

l_r	$(E - 4mc^2)/E_0$	Γ / E_0
1	6.116	0.037
2	6.855	0.131
3	7.462	0.352

4   Conclusion and outlook to tetraquarks

We study pentaquarks in the Jaffe-Wilczek model, with a H/butterfly string, but include the open channels of decays to meson-meson pairs. We consider an extended flip-flop model, where we add the tetraquark string to the two-meson strings. We first apply the RGM method assuming that the mesons have gaussian wavefunctions, and we obtain very narrow widths.

We then utilize an approximate toy-model, simplifying the number of Jacobi variables. The model is similar to the model of a Cherry in a Broken Glass. This allows the solution of the Schrödinger equation with finite differences in a box, where we look for localised states, and try to compute phase shifts.

To compute clearly the phase shifts we then solve the Schrödinger equation for the outgoing spherical waves. We compute de decay widths from the phase shifts, and we find relatively narrow decay widths. When the produced mesons are unstable, the total decay width of the tetraquark is then dominated by the final decays of the produced mesons.

References

1. M. Alekseev *et al.* [COMPASS Collaboration], Phys. Rev. Lett. **104**, 241803 (2010) [arXiv:0910.5842 [hep-ex]].
2. P. Bicudo and G. M. Marques, Phys. Rev. D **69**, 011503 (2004) [arXiv:hep-ph/0308073].
3. F. J. Llanes-Estrada, E. Oset and V. Mateu, Phys. Rev. C **69**, 055203 (2004) [arXiv:nucl-th/0311020].
4. B. Silvestre-Brac and C. Semay, Z. Phys. C **57**, 273 (1993).
5. M. Cardoso, N. Cardoso and P. Bicudo, Phys. Rev. D **81**, 034504 (2010) [arXiv:0912.3181 [hep-lat]].
6. M. B. Gavela, A. Le Yaouanc, L. Oliver, O. Pene, J. C. Raynal and S. Sood, Phys. Lett. B **82** (1979) 431.
7. F. Lenz, J. T. Londergan, E. J. Moniz, R. Rosenfelder, M. Stingl and K. Yazaki, Annals Phys. **170**, 65 (1986).
8. R. Jaffe and F. Wilczek, Eur. Phys. J. C **33**, S38 (2004) [arXiv:hep-ph/0401034]; R. Jaffe and F. Wilczek, Phys. World **17**, 25 (2004).
9. M. Karliner and H. J. Lipkin, Phys. Lett. B **575**, 249 (2003) [arXiv:hep-ph/0402260].

10. M. Cardoso and P. Bicudo, arXiv:0805.2260 [hep-ph].
11. J. Vijande, A. Valcarce, J. M. Richard and N. Barnea, Few Body Syst. **45**, 99 (2009) [arXiv:0902.1657 [hep-ph]]; J. Vijande, A. Valcarce and J. M. Richard, Phys. Rev. D **76**, 114013 (2007) [arXiv:0707.3996 [hep-ph]].
12. P. Bicudo and M. Cardoso, Phys. Lett. B **674**, 98 (2009) [arXiv:0812.0777 [physics.comp-ph]].
13. P. Bicudo and M. Cardoso, arXiv:1010.0281 [hep-ph].

Baryon axial charges[*]

Ki-Seok Choi, W. Plessas, and R. F. Wagenbrunn

Theoretical Physics, Institute of Physics, University of Graz, Universitätsplatz 5, A-8010 Graz, Austria

In the Standard Model of elementary-particle physics the axial charges g_A of baryons are decisive quantities for the comprehension of both the electroweak and strong interactions. In the first instance they govern weak processes, such as the β decay. Furthermore, they also relate to the strong interaction, what is most clearly seen through the Goldberger-Treiman relation. In case of the nucleon N, for example, it reads $g_A = f_\pi g_{\pi NN}/M_N$. Therefore, given the π decay constant f_π and the nucleon mass M_N, the πNN coupling constant $g_{\pi NN}$ just turns out to be proportional to g_A. By this relation one can thus estimate the role of π degrees of freedom in low-energy hadronic physics: Whenever g_A becomes sizable, the π coupling should also become appreciably strong and vice versa. In other words, g_A can also be viewed as an indicator for the phenomenon of spontaneous breaking of chiral symmetry of low-energy quantum chromodynamics (QCD). Consequently, any reasonable model for hadronic physics should yield the g_A of correct sizes.

More recently, the axial charges not only of the baryon ground states but also of the N resonances have come into the focus of interest. In particular, it has been suggested that the sizes of g_A should become small for almost degenerate parity-partner N resonances; these can be interpreted as chiral doublets, indicating the onset of chiral-symmetry restoration with higher excitation energies [1,2]. Unfortunately, the g_A values of the N resonances are unknown from phenomenology and will be hard to measure in experiment. However, the problem can be explored with the use of lattice QCD. Corresponding first results have already become available, but only for two of the N resonances, namely, N(1535) and N(1650) [3]. Both of these resonances have the same spin $J = \frac{1}{2}$ and parity $P = -1$. Since there is not yet any lattice-QCD result for positive-parity states, the above issue relating to parity-doubling remains unresolved from this side.

In addition, the axial charges of octet and decuplet ground states N, Σ, Ξ, Δ, Σ*, and Ξ* are also important to learn about the role of $SU(3)_F$ flavor-symmetry breaking. Under the assumption of $SU(3)_F$ symmetry, the axial charges of the N, Σ, and Ξ ground states are connected by the following simple relations:

$$g_A^N = F + D, \quad g_A^\Sigma = \sqrt{2}F, \quad g_A^\Xi = F - D. \tag{1}$$

---

[*] Talk delivered by Ki-Seok Choi

Violation of these relations indicates the amount of $SU(3)_F$ symmetry breaking.

Recently, we have performed a comprehensive study of the axial charges of octet and decuplet ground states N, Σ, Ξ, Δ, Σ^*, and Ξ^* as well as their resonances along RCQMs [4,5]. Specifically, we have employed the RCQMs whose quark-quark hyperfine interactions derive from one-gluon-exchange and Goldstone-boson-exchange dynamics; for the latter we have considered both the version with only the spin-spin interaction from pseudoscalar exchange as well as the extended version (EGBE) that includes all force components (i.e. central, tensor, spin-spin, and spin-orbit) from pseudoscalar, scalar, and vector exchanges [6]. In this contribution we refer only to results of this version. The calculations have been performed in the framework of Poincaré-invariant quantum mechanics. In order to keep the numerical computations manageable, we had to restrict the axial current operator to the so-called spectator model (SM) [7]. It means that the weak-interaction gauge boson couples only to one of the constituent quarks in the baryon. This approximation has turned out to be very reasonable already in previous studies of the axial and induced pseudoscalar as well as electromagnetic form factors of the nucleon.

Table 1. Axial charges g_A^B of octet and decuplet ground states as predicted by the EGBE RCQM [5] in comparison to experiment [8] and lattice-QCD results from Lin and Orginos (LO) [9] and Erkol, Oka, and Takahashi (EOT) [10] as well as results from chiral perturbation theory by Jiang and Tiburzi (JT) [11,12]; also given is the nonrelativistic limit (NR) from the EGBE RCQM.

	Exp	EGBE	LO	EOT	JT	NR
N	1.2695±0.0029	1.15	1.18±0.10	1.314±0.024	1.18	1.65
Σ	$\cdots$	0.65	0.636±0.068[†]	0.686±0.021[†]	0.73	0.93
Ξ	$\cdots$	-0.21	-0.277±0.034	-0.299±0.014[‡]	-0.23[‡]	-0.32
Δ	$\cdots$	-4.48	$\cdots$	$\cdots$	~-4.5	-6.00
Σ^*	$\cdots$	-1.06	$\cdots$	$\cdots$	$\cdots$	-1.41
Ξ^*	$\cdots$	-0.75	$\cdots$	$\cdots$	$\cdots$	-1.00

[†] Because of another definition of g_A^Σ this numerical value is different by a $\sqrt{2}$ from the one quoted in the original paper.
[‡] Because of another definition of g_A^Ξ this value has a sign opposite to the one in the original paper.

In Table 1 we present the predictions of the EGBE RCQM for the axial charges g_A^B of the octet and decuplet ground states B = N, Σ, Ξ, Δ, Σ^*, and Ξ^*. Except for the N there are no direct experimental data for g_A^B. The EGBE RCQM prediction for g_A^N come close to the experimental value, with only slightly falling below it. This is also the trend of most modern lattice-QCD calculations; only the result by Erkol et al. seems to represent a notable exception. In addition, our result compares well with the g_A^N prediction obtained from chiral perturbation theory by Jiang and Tiburzi. In the last column of Table 1 we quote also the nonrelativistic

limit of the prediction by the EGBE RCQM. It deviates grossly from the relativistic result, indicating that a nonrelativistic treatment of axial charges is unreliable.

For the g_A^B of the other octet and decuplet ground states, the EGBE RCQM again yields results very similar to the other approaches. For the octet states Σ and Ξ the figures compare well with the lattice-QCD as well as chiral-perturbation-theory results. For the decuplet states we can only compare the result for g_A^Δ to the one by Jiang and Tiburzi, what shows again a striking similarity. Evidently, all the results from the nonrelativistic limit of the EGBE RCQM fall short; as in the case of the N, the corresponding values are always bigger (in absolute value) than all of the other results.

In Table 2 we have collected the predictions of the EGBE RCQM for g_A of all ground and resonance states of N, Σ, Ξ, Δ, Σ^*, and Ξ^*. They are classified as belonging to the flavor octets and decuplets specified by total angular momentum and parity, J^P, where in addition their total orbital angular momenta L and total spins S (in the rest frame) are given. Except for N(1535) and N(1650), which are known from a lattice-QCD calculation [3] to be of the same sizes as our results, these are first relativistic predictions for axial charges of baryon resonances.

Table 2. Axial charges of octet (upper part) as well as decuplet (lower part) baryon ground states and resonances as predicted by the EGBE RCQM. The flavor-multiplet assignments follow ref. [13].

$(LS)\,J^P$	State	g_A	State	g_A	State	g_A
$(0\frac{1}{2})\,\frac{1}{2}^+$	N(939)	1.15	Σ(1193)	0.65	Ξ(1318)	-0.21
$(0\frac{1}{2})\,\frac{1}{2}^+$	N(1440)	1.16	Σ(1660)	0.69	Ξ(1690)	-0.23
$(0\frac{1}{2})\,\frac{1}{2}^+$	N(1710)	0.35	Σ(1880)	0.38		
$(1\frac{1}{2})\,\frac{1}{2}^-$	N(1535)	0.02	Σ(1560)	-0.15		
$(1\frac{3}{2})\,\frac{1}{2}^-$	N(1650)	0.51	Σ(1620)	0.62		
$(2\frac{1}{2})\,\frac{3}{2}^+$	N(1720)	0.35				
$(1\frac{1}{2})\,\frac{3}{2}^-$	N(1520)	-0.64	Σ(1670)	-0.92	Ξ(1820)	-0.38
$(1\frac{3}{2})\,\frac{3}{2}^-$	N(1700)	-0.10	Σ(1940)	-0.45		
$(2\frac{1}{2})\,\frac{5}{2}^+$	N(1680)	0.84				
$(1\frac{3}{2})\,\frac{5}{2}^-$	N(1675)	0.89	Σ(1775)	1.06		
$(0\frac{3}{2})\,\frac{3}{2}^+$	Δ(1232)	-4.48	Σ^*(1385)	-1.06	Ξ^*(1535)	-0.75
$(0\frac{3}{2})\,\frac{3}{2}^+$	Δ(1600)	-4.41	Σ^*(1690)	-1.05		
$(1\frac{1}{2})\,\frac{1}{2}^-$	Δ(1620)	-0.76	Σ^*(1750)	-0.08		
$(1\frac{1}{2})\,\frac{3}{2}^-$	Δ(1700)	-1.68				

We find it noticeable that the axial charges of members of two particular flavor multiplets are all relatively small, namely the ones of the $J^P = \frac{1}{2}^-$ octet with N(1535) and decuplet with Δ(1620). Interestingly, they are both the first $\frac{1}{2}^-$ excitations above the corresponding positive-parity ground states, the N(939) and the Δ(1232).

Our results in Table 2 cannot tell anything regarding the issue of chiral-symmetry restoration higher in the baryon excitation spectra. The more it will be interesting to have in the near future calculations of resonance axial charges from lattice QCD and other approaches. They will hopefully confirm or disprove the pattern of results as produced by the RCQMs.

References

1. L. Y. Glozman, Phys. Rept. **444**, 1 (2007).
2. L. Y. Glozman and A. V. Nefediev, Nucl. Phys. A **807**, 38 (2008).
3. T. T. Takahashi and T. Kunihiro, Phys. Rev. D **78**, 011503 (2008).
4. K. S. Choi, W. Plessas, and R. F. Wagenbrunn, Phys. Rev. C **81**, 028201 (2010).
5. K. S. Choi, W. Plessas, and R. F. Wagenbrunn, Phys. Rev. D **82**, 014007 (2010).
6. K. Glantschnig, R. Kainhofer, W. Plessas, B. Sengl, and R. F. Wagenbrunn, Eur. Phys. J. A **23**, 507 (2005).
7. T. Melde, L. Canton, W. Plessas, and R. F. Wagenbrunn, Eur. Phys. J. A **25**, 97 (2005).
8. C. Amsler *et al.* [Particle Data Group], Phys. Lett. B **667**, 1 (2008).
9. H. W. Lin and K. Orginos, Phys. Rev. D **79**, 034507 (2009).
10. G. Erkol, M. Oka, and T. T. Takahashi, Phys. Lett. B **686**, 36 (2010).
11. F. J. Jiang and B. C. Tiburzi, Phys. Rev. D **78**, 017504 (2008).
12. F. J. Jiang and B. C. Tiburzi, Phys. Rev. D **80**, 077501 (2009).
13. T. Melde, W. Plessas, and B. Sengl, Phys. Rev. D **77**, 114002 (2008).

Some classical motions of three quarks tethered to the Torricelli string⋆

V. Dmitrašinović[a], M. Šuvakov[b], and K. Nagata[c]

[a] Vinča Institute for Nuclear Sciences, Belgrade University, Physics lab 010, P.O.Box 522, 11001 Beograd, Serbia; Permanent address after October 1st 2010: Institute of Physics, Belgrade University, Pregrevica 118, Zemun, P.O.Box 57, 11080 Beograd, Serbia
[b] Institute of Physics, Belgrade University, Pregrevica 118, Zemun, P.O.Box 57, 11080 Beograd, Serbia
[c] Research Institute for Information Science and Education, Hiroshima University, Higashi-Hiroshima 739-8521, Japan

In this talk we report some soon to be published results [1] of our studies of figure-eight orbits of three-bodies in three potentials: 1) the Newtonian gravity, i.e., the pairwise sum of $-1/r$ two-body potentials; 2) the pairwise sum of linearly rising r two-body potentials (a.k.a. the Δ string potential); 3) the Y-junction string potential [2] that contains both a genuine three-body part, as well as two-body contributions (this is the first time that the figure-eight has been found in these string potentials, to our knowledge). These three potentials share two common features, *viz.* they are attractive and symmetric under permutations of any two, or three particles. We were led to do this study after recognizing the existence of a dynamical symmetry underlying the remarkable regularity in the Y- and Δ string energy spectra [3].

We have found that a set of variables that consists of the "hyper-radius" $R = \sqrt{\rho^2 + \lambda^2}$, the "rescaled area of the triangle" $\frac{\sqrt{3}}{2R^2}|\boldsymbol{\rho} \times \boldsymbol{\lambda}|$) and the ("braiding") hyper-angle $\phi = \arctan\left(\frac{2\boldsymbol{\rho}\cdot\boldsymbol{\lambda}}{\lambda^2-\rho^2}\right)$ makes this permutation symmetry manifest; we use them to plot the motion of the numerically calculated figure-eight orbit. According to Ref. [4], H. Hopf was the first one to introduce these variables, Ref. [5]. As there are three independent three-body variables, and there are two independent permutation-symmetric three-body variables, R and the area the third variable cannot be permutation-symmetric. Moreover, it must be a continuous variable and not be restricted only to a discrete set of points, as is natural for permutations. We identify here the third independent variable as $\phi = \arctan\left(\frac{2\boldsymbol{\rho}\cdot\boldsymbol{\lambda}}{\lambda^2-\rho^2}\right)$ and show that it grows/descends (almost) linearly with the time t spent on the figure-eight trajectory and reaches $\pm 2\pi$ after one period T. Thus, on the figure-eight orbit ϕ is, for most practical purposes, interchangeable with the time variable t. The hyper-angle ϕ is the continuous braiding variable that interpolates smoothly be-

---

⋆ Talk delivered by V. Dmitrašinović

tween permutations and thus plays a fundamental role in the braiding symmetry of the figure-eight orbits [6,8].

Then we constructed the hyper-angular momentum $G_3 = \frac{1}{2}(\mathbf{p}_\rho \cdot \boldsymbol{\lambda} - \mathbf{p}_\lambda \cdot \boldsymbol{\rho})$ conjugate to ϕ, the two forming an (approximate) pair of action-angle variables for this periodic motion. Here we calculate numerically and plot the temporal variation of ϕ, as well as the hyper-angular momentum $G_3(t)$, the hyper-radius R and r. We show that the hyper-radius $R(t)$ oscillates about its average value $\overline{R}$ with the same angular frequency 3ϕ and phase, as the new ("reduced area") variable $r(t)$. Thus, we show that $\phi(t)$ is, for most practical purposes, interchangeable with the time variable t, in agreement with the tacit assumption(s) made in Refs. [7], [4], though the degree of linearity of this relationship depends on the precise functional form of the three-body potential.

As stated above, ϕ is not exactly proportional to time t, but contains some non-linearities that depend on the specifics of the three-body potential; consequently the hyper-angular momentum G_3 is not an exact constant of this motion, but oscillates about the average value $\overline{G}_3$, with the same basic frequency 3ϕ. Thus, the time-averaged hyper-angular momentum $\overline{G}_3$ is the action variable conjugate to the linearized hyper-angle ϕ'.

We used these variables to characterize two new planar periodic, but nonchoreographic three-body motions with vanishing total angular momentum. One of these orbits corresponds to a modification of the figure-eight orbit with $\phi(t)$ that also grows more or less linearly in time, but has a more complicated periodicity pattern defined by the zeros of the area of the triangle formed by the three particles (also known as "eclipses", "conjunctions" or "syzygies"). Another new orbit has $\phi(t)$ that grows in time up to a point, then stops and "swings back". We show that this motion, and the other two, can be understood in view of the analogy between the three-body hyper-angular ("shape space") Hamiltonian on one hand and a variable-length pendulum in an azimuthally periodic in-homogeneous gravitational field, on the other.

References

1. M. Šuvakov, V. Dmitrašinović, "Approximate action-angle variables for the figure-eight and new periodic three-body orbits", submitted to Phys. Rev. **E**, (2010).
2. V. Dmitrašinović, T. Sato and M. Šuvakov, Eur. Phys. J. C **62**, 383 (2009)
3. V. Dmitrašinović, T. Sato and M. Šuvakov, Phys. Rev. D **80**, 054501 (2009).
4. A. Chenciner, R. Montgomery, Ann. Math. **152**, 881 (2000).
5. H. Hopf, Math. Annalen **104**, 637 (1931).
6. C. Moore, Phys. Rev. Lett. **70**, 3675 (1993).
7. T. Fujiwara, H. Fukuda and H. Ozaki, J. Phys. **A 36**, 2791 (2003).
8. G.C. Rota, Mathematical Snapshots, Killian Faculty Achievement Award Lecture (1997).

Heavy-light form factors: the Isgur-Wise function in point-form relativistic quantum mechanics[*]

M. G. Rocha and W. Schweiger

Institut für Physik, Universität Graz, A-8010 Graz, Austria

Though the point-form of relativistic quantum dynamics is the least explored of the three common forms of relativistic dynamics, it has several properties that makes it well suited for applications to hadronic physics. Its main characteristics are that interaction terms (if present) enter all four components of the 4-momentum operator, whereas the generators of Lorentz transformations stay free of interactions. As a particular example we are going to present the calculation of electroweak form factors of heavy-light mesons within a constituent-quark model. Since the dependence of matrix elements on the heavy-quark mass is rather obvious in point-form relativistic quantum mechanics, it is comparably easy to study the heavy-quark symmetry and its breaking due to finite masses of the heavy quarks.

Starting point of our investigations are the physical processes from which such electroweak form factors are extracted, i.e. elastic electron-meson scattering and the weak decay of heavy-light mesons. We use a coupled-channel framework in which the dynamics of the intemediate gauge bosons – either photon or W-boson – is fully taken into account. Poincaré invariance is ensured by employing the Bakamjian-Thomas construction [1]. Its point-form version amounts to the assumption that the (interacting) 4-momentum operator $\hat{P}^\mu$ can be factorized into an interacting mass operator and a free 4-velocity operator

$$\hat{P}^\mu = \hat{M}\hat{V}^\mu_{\text{free}}.$$ (1)

It is therefore only necessary to study an eigenvalue problem for the mass operator.

In case of elastic electron-meson scattering a mass eigenstate $\hat{M}|\psi\rangle = m|\psi\rangle$ is written as a direct sum of a quark-antiquark-electron component $|\psi_{Q\bar{q}e}\rangle$ and a quark-antiquark-electron-photon component $|\psi_{Q\bar{q}e\gamma}\rangle$. Here we have already assumed that the quark carries the heavy flavor. The mass eigenvalue equation to be solved has the form

$$\begin{pmatrix} \hat{M}_{Q\bar{q}e} & \hat{K} \\ \hat{K}^\dagger & \hat{M}_{Q\bar{q}e\gamma} \end{pmatrix} \begin{pmatrix} |\psi_{Q\bar{q}e}\rangle \\ |\psi_{Q\bar{q}e\gamma}\rangle \end{pmatrix} = m \begin{pmatrix} |\psi_{Q\bar{q}e}\rangle \\ |\psi_{Q\bar{q}e\gamma}\rangle \end{pmatrix},$$ (2)

---

[*] Talk delivered by M. G. Rocha

where $M_{Q\bar{q}e}$ and $M_{Q\bar{q}e\gamma}$ consist of a kinetic term and an instantaneous confining potential between quark and antiquark, and $\hat{K}$ is a vertex operator which accounts for the emission and absorption of a photon by the electron or (anti)quark. It is determined by the interaction Lagrangean density of QED [2].

For the calculation of the electromagnetic meson currents and form factors it is most convenient to apply a Feshbach reduction to the mass eigenvalue problem

$$(\hat{M}_{Q\bar{q}e} - m)|\psi_{Q\bar{q}e}\rangle = \underbrace{\hat{K}^{\dagger}(\hat{M}_{Q\bar{q}e\gamma} - m)^{-1}\hat{K}}_{\hat{V}_{\text{opt}}(m)}|\psi_{Q\bar{q}e}\rangle \tag{3}$$

and study the optical potential $\hat{V}_{\text{opt}}(m)$. The electromagnetic meson current

$$J^{\mu}(\mathbf{k}'_{M};\mathbf{k}_{M})$$

can then be extracted from the invariant 1-γ-exchange amplitude which is essentially given by on-shell matrix elements of the optical potential. These have the structure

$$\mathcal{M}_{1\gamma}(\mathbf{k}'_{e}, \mu'_{e}; \mathbf{k}_{e}, \mu_{e}) \propto \langle V'; \mathbf{k}'_{e}, \mu'_{e}; \mathbf{k}'_{M}|\hat{V}_{\text{opt}}(m)|V; \mathbf{k}_{e}, \mu_{e}; \mathbf{k}_{M}\rangle_{\text{on-shell}}$$

$$\propto V^{0}\delta^{3}(\mathbf{V} - \mathbf{V}')\frac{j_{\mu}(\mathbf{k}'_{e}, \mu'_{e}; \mathbf{k}_{e}, \mu_{e})J^{\mu}(\mathbf{k}'_{M};\mathbf{k}_{M})}{(k'_{e} - k_{e})^{2}}. \tag{4}$$

$|V; \mathbf{k}_{e}^{(\prime)}, \mu_{e}^{(\prime)}; \mathbf{k}_{M}^{(\prime)}\rangle$ are, so called, "velocity states" that specify the state of a system by the overall velocity and the center-of-mass momenta and canonical spins of its components [3]. In our case $\mathbf{k}_{M}^{(\prime)}$ is the momentum of the confined q-$\bar{q}$ subsystem with the quantum numbers of the heavy-light meson. "On-shell" means that $m = k_{e}^{0} + k_{M}^{0} = k_{e}'^{0} + k_{M}'^{0}$ and $k_{e}^{0} = k_{e}'^{0}$, $k_{M}^{0} = k_{M}'^{0}$. A detailed derivation of Eq. (4) and the explicit expression for the meson current $J^{\mu}(\mathbf{k}'_{M};\mathbf{k}_{M})$ can be found in Ref. [4].

If we are dealing with a pseudoscalar meson its electromagnetic current should be of the form $J^{\mu}(\mathbf{k}'_{M};\mathbf{k}_{M}) = (k'_{M} + k_{M})^{\mu}F(Q^{2})$, which allows us to identify the electromagnetic form factor of the meson uniquely. It is, however, known that the Bakamjian-Thomas construction, that we are using, provides wrong cluster properties [5]. As a consequence, the hadronic current $J^{\mu}(\mathbf{k}'_{M};\mathbf{k}_{M})$ which we extract from Eq. (4) exhibits a slight dependence on the electron momenta k_{e} and k'_{e} [1]. Fortunately this dependence vanishes rather quickly with increasing invariant mass m of the electron-meson system and thus also in the heavy-quark limit ($m_{Q} = m_{M} \to \infty$, $m_{\bar{q}}/m_{Q} \to 0$). This limit has to be taken in such a way that $v' \cdot v = 1 + Q^{2}/2m_{M}^{2}$ stays constant. The function of $(v' \cdot v)$ that is obtained from $F(Q^{2})$ by taking the heavy-quark limit is the famous Isgur-Wise function [7]. In our case it takes on a rather simple analytical form:

$$\xi_{\text{EM}}(v' \cdot v) = \lim_{m_{Q} \to \infty} F(Q^{2})$$

$$= \sum_{\mu'\mu} \int d^{3}\tilde{k}'_{\bar{q}}\sqrt{\frac{\tilde{\omega}_{\bar{q}}}{\tilde{\omega}'_{\bar{q}}}}\sqrt{\frac{2}{1 + v \cdot v'}}\frac{1}{2}D_{\mu'\mu}^{1/2}\left[R_{W}^{-1}\left(\frac{\tilde{k}_{\bar{q}}}{m_{\bar{q}}}, B(v_{Q\bar{q}})\right)R_{W}\left(\frac{\tilde{k}'_{\bar{q}}}{m_{\bar{q}}}, B(v'_{Q\bar{q}})\right)\right]$$

$$\times \psi_{\text{out}}(\tilde{k}'_{\bar{q}})\psi_{\text{in}}(\tilde{k}_{\bar{q}}). \tag{5}$$

---

[1] See Ref. [6] for a short discussion of this problem.

It is just an integral over incoming and outgoing wave functions, a Wigner-rotation factor and kinematical factors. The tildes in the integral indicate that the corresponding quantities are given in the Q-q̄ rest system. In accordance with heavy-quark symmetry $\xi_{EM}(v' \cdot v)$ does not depend on the heavy-quark mass.

Heavy-quark symmetry allows us also to relate the electromagnetic form factor of a pseudoscalar heavy-light meson to its weak decay form factors for heavy-to-heavy flavor transitions (like, e.g., $\bar{B} \rightarrow D^{(*)}\ell\bar{\nu}$). In the heavy-quark limit the electromagnetic form factor and the weak decay form factors (modulo kinematical factors) should lead to only one Isgur-Wise function [8]. If we apply our coupled channel framework to semileptonic decays of pseudoscalar heavy-light mesons, identify the decay form factors from the optical potential and take the heavy-quark limit we end up with

$$\xi_W(v' \cdot v) = \sum_{\mu'\mu} \int d^3\tilde{k}'_{\bar{u}} \sqrt{\frac{\tilde{\omega}_{\bar{u}}}{\tilde{\omega}'_{\bar{u}}}} \sqrt{\frac{2}{1+v'\cdot v}} \frac{1}{2} D_{\mu'\mu}^{1/2} \left[R_W \left(\frac{\tilde{k}'_{\bar{u}}}{m_{\bar{u}}}, B(v'_{c\bar{u}}) \right) \right]$$
$$\times \psi_{out}(\tilde{k}'_{\bar{u}})\psi_{in}(\tilde{k}_{\bar{u}}) . \tag{6}$$

At first sight $\xi_{EM}(v' \cdot v)$ and $\xi_W(v' \cdot v)$ seem to be different and we are still not able to show their equality analytically. A numerical study, however, reveals that they coincide (see Fig.1). These investigations show that heavy-quark symmetry is recovered in the heavy-quark limit within our relativistic coupled channel approach.
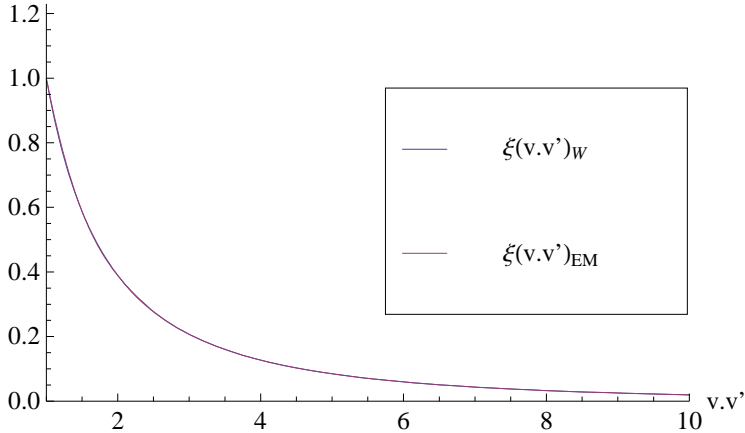
Fig. 1. Isgur-Wise function for a heavy-light meson as obtained from electron-meson scattering (cf. Eq. (5)) and semileptonic decays (cf. Eq. (6)). For the Q-q̄ bound-state wave function we have taken a Gaussian with the same oscillator parameter ($a = 0.55$ GeV) and light-quark mass ($m_{u,d} = 0.25$ GeV) as in Ref. [9].

It is also interesting to study the breaking of heavy-quark symmetry caused by finite values of the heavy-quark mass. This is done in Fig. 2 for the two weak

decay form factors $F_0(v' \cdot v)$ and $F_1(v' \cdot v)$ that show up in the semileptonic $B^- \to D^0 e^- \bar{v}$ decay. If heavy-quark symmetry was perfect RF_1 and $R(1 - q^2/(m_B + m_D)^2)^{-1}F_0$ (with $R = 2\sqrt{m_B m_D}/(m_B + m_D)$) should coincide with the Isgur-Wise function $\xi(v' \cdot v)$ (see Ref.[8]). What we rather observe is that the physical values of the b- and c-quark mass give rise to a considerable breaking of heavy-quark symmetry (left plot). Here we have not even taken into account a (heavy) flavor dependence of the meson wave functions. If both masses were about a factor of 10 larger heavy-quark symmetry would nearly hold (right plot).

A more comprehensive study of heavy-light systems along the lines presented here, including the discussion of (heavy-quark) spin symmetry, can be found in Ref. [4].
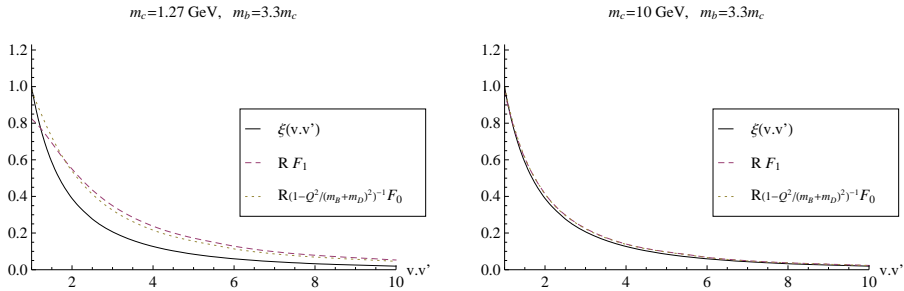
Fig. 2. Weak decay form factors (multiplied with appropriate kinematical factors) for the process $B^- \to D^0 e^- \bar{v}$ for finite m_Q in comparison with the Isgur-Wise function. The wave-function parameterization is the same as in Fig. 1.

References

1. B. Bakamjian and L. H. Thomas, Phys. Rev. **92** (1953) 1300.
2. W. H. Klink, Nucl. Phys. A **716** (2003) 123.
3. W. H. Klink, Phys. Rev. C **58** (1998) 3617.
4. M. Gómez Rocha and W. Schweiger, paper in preparation.
5. B. D. Keister and W. N. Polyzou, Adv. Nucl. Phys. **20** (1991) 225.
6. E. P. Biernat, W. H. Klink and W. Schweiger, arXiv:1008.0244 [nucl-th].
7. N. Isgur and M. B. Wise, Phys. Lett. B **232** (1989) 113; Phys. Lett. B **237** (1990) 527.
8. M. Neubert, Phys. Rept. **245** (1994) 259.
9. H. Y. Cheng, C. Y. Cheung and C. W. Hwang, Phys. Rev. D **55** (1997) 1559

Resonances and decay widths within a relativistic coupled channel approach[*]

R. Kleinhappel and W. Schweiger

Institut für Physik, Universität Graz, A-8010 Graz, Austria

Within constituent-quark models the resonance character of hadron excitations is usually ignored. They rather come out as stable bound states and their bound-state wave function is then used to calculate partial decay widths perturbatively by assuming a particular model for the elementary decay vertex. The fact that the predicted strong decay widths are notoriously too small [1,2] is an indication that a physical hadron resonance is not just a simple bound state of valence (anti)quarks, but it should contain also (anti)quark-meson components.

A good starting point to take such components into account is the chiral constituent quark model (χQCM) [3]. The effective degrees of freedom of the χQCM, that are assumed to emerge from chiral symmetry breaking of QCD, are constituent (anti)quarks and Goldstone bosons which couple directly to the (anti)quarks. In order to take relativity fully into account we work within point-form quantum mechanics [4], which is characterized by the property that the components of the four momentum operator $\hat{P}^\mu$ are the only generators of the Poincaré group which contain interaction terms. A convenient method to add interactions to $\hat{P}^\mu_{\text{free}}$ such that the Poincaré algebra is satisfied is the Bakamijan-Thomas construction [5]. The point-form version of the Bakamjian-Thomas construction amounts to factorize the free 4-momentum operator into a free mass operator $\hat{M}_{\text{free}}$ and a free 4-velocity operator V^μ_{free} and to add a Lorentz-scalar interaction term $\hat{M}_{\text{int}}$ that should also commute with $\hat{V}^\mu_{\text{free}}$ to $\hat{M}_{\text{free}}$. The interacting 4-momentum operator then has the structure

$$\hat{P}^\mu = \hat{P}^\mu_{\text{free}} + \hat{P}^\mu_{\text{int}} = (\hat{M}_{\text{free}} + \hat{M}_{\text{int}})\, \hat{V}^\mu_{\text{free}}\,, \tag{1}$$

and one only needs to study an eigenvalue problem for the mass operator. A very useful basis, which is tailored to this kind of construction, is formed by velocity states [6]. These are usual momentum states in the center-of-momentum of the whole system which are then boosted to the overall four-velocity v^μ. In this basis the usual addition rules of nonrelativistic quantum mechanics can be applied to spin and angular momentum.

In order to allow for the decay of hadron excitations into a lower lying state and a Goldstone boson we formulate the eigenvalue problem for the mass operator as a 2-channel problem. A general mass eigenstate is then a direct sum of

---

[*] Talk delivered by R. Kleinhappel

a valence (anti)quark component and a valence (antiquark) + Goldstone-boson component. The latter can be eliminated by means of a Feshbach reduction and one ends up with a mass-eigenvalue equation for the valence (anti)quark component. In case of a meson, e.g., this equation takes on the form:

$$\left(\hat{M}_{q\bar{q}} + \underbrace{\hat{K}^\dagger (\hat{M}_{q\bar{q}\pi} - m)^{-1} \hat{K}}_{\hat{V}_{\text{opt}}(m)} \right) |\psi_{q\bar{q}}\rangle = m|\psi_{q\bar{q}}\rangle .$$ (2)

The channel mass operator $\hat{M}_{q\bar{q}}$ is assumed to contain already an instantaneous confinement and the optical potential $V_{\text{opt}}(m)$ describes all four possibilities for the (dynamical) exchange of a Goldstone boson between anti(quark) and (anti)-quark, in particular also reabsorption of the Goldstone boson by the emitting (anti)quark. Here we have taken the π as a representative for the Goldstone bosons. The vertex operator $\hat{K}$ is derived from an appropriate field theoretical interaction Lagrangian density [7].
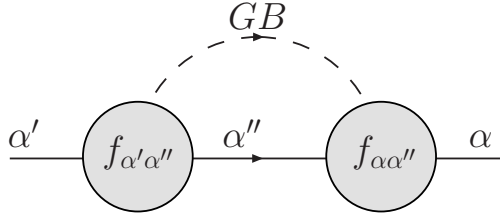
Fig. 1. Graphical representation of the optical potential, $V_{\text{opt}}^{nn'}(m)$ that enters the mass eigenvalue equation (3) on the hadronic level.

In a velocity state representation Eq. (2) becomes an integral equation. In order to make it better amenable to a numerical treatment we expand $|\psi_{q\bar{q}}\rangle$ in terms of (velocity) eigenstates $|v, \alpha\rangle$ of $\hat{M}_{q\bar{q}}$, i.e. the pure confinement problem. α collectively denotes the internal quantum numbers that specify these states. For reasons which will become clear immediately, we call $|v, \alpha\rangle$ a "bare" meson state, whereas $|\psi_{q\bar{q}}\rangle$ is (the q-$\bar{q}$ component of) a "physical" meson state. This expansion leads to an infinite set of coupled algebraic equations for the expansion coefficients A_α:

$$\sum_{\alpha'} \left(m_\alpha \delta_{\alpha\alpha'} + V_{\text{opt}}^{\alpha\alpha'}(m) \right) A_{\alpha'} = mA_\alpha .$$ (3)

The most remarkable feature of this equation is that it is rather a mass-eigenvalue equation for mesons than for quarks. It describes how a physical meson of mass m is composed of bare mesons with masses m_α. The bare mesons are mixed via the optical-potential matrix elements $V_{\text{opt}}^{nn'}(m)$. Even these matrix elements attain a rather simple interpretation in terms of hadronic degrees of freedom. They couple a bare meson state with quantum numbers α' to another bare meson state

with quantum numbers α via a Goldstone-boson loop such that any bare meson state with quantum numbers α'' (that is allowed by conservation laws) can be excited in an intermediate step (see Fig. 1). $f_{\alpha\alpha'}(|\kappa|)$ are (strong) transition form factors that show up at the (bare) meson Goldstone-boson vertices. The eigenvalue problem that one ends up with describes thus bare mesons, i.e. eigenstates of the pure confinement problem, that are mixed and dressed via Goldstone-boson loops. The only places where the quark substructure enters, are the vertex form factors. Here it should be emphasized that due to the instantaneous nature of the confinement potential the dressing happens on the hadron level and not on the quark level, i.e. emission and absorption of the Goldstone boson by the same constituent must not be interpreted as mass renormalization of the (antiquark)quark.

Equation (3) is a nonlinear eigenvalue equation that cannot be solved with standard techniques. In order to study it in some more detail we use a simple toy model in which spin and flavor of the (anti)quark are neglected and a real scalar particle is taken for the Goldstone boson. We use a harmonic oscillator confinement in the square of the mass operator. This model has 5 parameters: the (anti)quark mass m_q, the Goldstone-boson mass m_{GB}, the Goldstone-boson-quark coupling strength g, the oscillator parameter a and a parameter V_0 to shift the mass spectrum. We have taken a standard value of 0.34 GeV for m_q and the pion mass for m_{GB}. To give our toy model some physical meaning the parameters a and V_0 have been fixed in such a way that the the experimental masses of the ω ground state and its first excited state are approximately reproduced. The Goldstone-boson-quark coupling is varied within the range allowed by the Goldberger-Treiman relation, i.e. $0.67 \lesssim g^2/4\pi \lesssim 1.19$ [8]. To simplify things further only radial excitations of bare mesons have been taken into account. The mass eigenvalue problem, Eq. (3), can be solved by an iterative procedure. One first has to restrict the number of bare states, that are taken into account, to a certain number α_{max}. The first step is to insert a start value for m into $\hat{V}_{opt}(m)$ and solve the resulting linear eigenvalue equation. This leads to α_{max} (possibly complex) eigenvalues. From these one has to pick out the right one, reinsert it into $\hat{V}_{opt}(m)$, solve again, etc. Appropriate start values are, e.g., the eigenvalues of the pure confinement problem. Note that the optical potential $V_{opt}^{\alpha\alpha'}(m)$ becomes complex if the mass eigenvalue m is larger than the lowest threshold $m_{th} = m_0 + m_{GB}$, i.e. the mass of the lightest bare meson plus the Goldstone-boson mass. As a consequence also the physical mass eigenvalues m will become complex as soon as their real part is larger than m_{th} and we will get unstable meson excitations. The mass of such an excitation can then be identified with $\mathrm{Re}(m)$, its width Γ with $2\,\mathrm{Im}(m)$.

The results of a first numerical study with our toy model (with $\alpha_{max} = 2$) are shown in Fig. 2. It can be seen that the Goldstone-boson loop provides an attractive force and that the decay width exhibits a maximum as a function of $g^2/4\pi$. As soon as the real part of the mass eigenvalue of the first excited state approaches $m_0 + m_{GB}$, where m_0 is the harmonic oscillator ground-state mass, the decay width vanishes. With a Goldstone-boson-quark coupling of $g^2/4\pi = 1.19$, which is still compatible with the Goldberger-Treiman relation, the 2 lowest lying states are found to have masses of about 0.8 and 1.44 GeV, respectively. The first
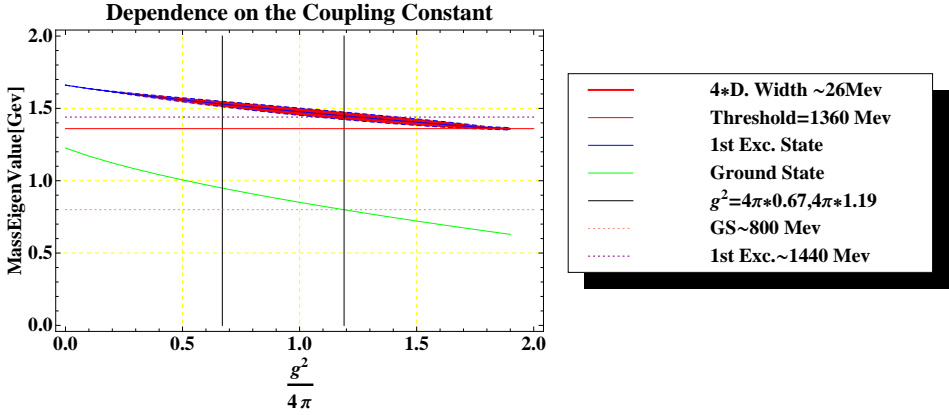
Fig. 2. Predictions of our toy model for the meson masses and widths. Shown are the ground state (green line) and the first excited state (blue line) as functions of the Goldstone-boson-quark coupling. The red band between the dashed blue lines represents four times the decay width of the first excited state.

excited state has a width of 0.026 GeV. An increase of α_{max} changes these values by only a few percent. The iterative procedure converges already after 5 iterations.

These are promising results in view of the simplicity of our toy model and it will be interesting to see whether typical decay widths of 0.1 GeV or more can be achieved within our approach in the more interesting case of baryon resonances for the full chiral constituent-quark model.

References

1. T. Melde, W. Plessas and B. Sengl, Phys. Rev. C **76** (2007) 025204
2. B. Metsch, Eur. Phys. J. A **35** (2008) 275.
3. L. Y. Glozman and D. O. Riska, Phys. Rept. **268** (1996) 263.
4. P. A. M. Dirac, Rev. Mod. Phys. **21** (1949)392.
5. B. Bakamjian and L. H. Thomas, Phys. Rev. **92** (1953)1300.
6. W. H. Klink, Phys. Rev. C **58** (1998) 3617.
7. W. H. Klink, Nucl. Phys. A **716** (2003) 123.
8. L. Ya. Glozman, Z. Papp, W. Plessas, K. Varga, and R. F. Wagenbrunn, Phys. Rev. C **57** (1998) 3406.

Mixed symmetric baryon multiplets in large N_c QCD: two and three flavours[*]

N. Matagne[a] and Fl. Stancu[b]

[a]Service de Physique Nucléaire et Subnucléaire, University of Mons, Place du Parc, B-7000 Mons, Belgium,
[b]Institute of Physics, B5, University of Liège, Sart Tilman, B-4000 Liège 1, Belgium

Abstract. We propose a new method to study mixed symmetric multiplets of baryons in the context of the $1/N_c$ expansion approach. The simplicity of the method allows to better understand the role of various operators acting on spin and flavour degrees of freedom. The method is tested on two and three flavours. It is shown that the spin and flavour operators proportional to the quadratic invariants of $SU_S(2)$ and $SU_F(3)$ respectively are dominant in the mass formula.

1 Introduction

The $1/N_c$ expansion method proposed by 't Hooft [1] is a valuable tool to study nonperturbative dynamics in a perturbative approach, in terms of the parameter $1/N_c$ where N_c is the number of colors. The double line diagrammatic method of 't Hooft implemented by Witten [2] to describe baryons gives convenient power counting rules for Feynman diagrams. According to Witten's intuitive picture, a baryon containing N_c quarks is seen as a bound state in an average self-consistent potential of a Hartree type and the corrections to the Hartree approximation are of order $1/N_c$. These corrections capture the key phenomenological features of the baryon structure.

Ten years after 't Hooft's work, Gervais and Sakita [3] and independently Dashen and Manohar in 1993 [4] discovered that QCD has an exact contracted $SU(2N_f)_c$ symmetry when $N_c \to \infty$, N_f being the number of flavors. For ground state baryons the $SU(2N_f)$ symmetry is broken by corrections proportional to $1/N_c$. Since 1993-1994 the $1/N_c$ expansion provided a systematic method to analyze baryon properties such as ground state masses, magnetic moments, axial currents, etc [5–8].

A few years later the $1/N_c$ expansion method has been extended to excited states also in the spirit of the Hartree approximation [9]. It was shown that for mixed symmetric states the $SU(2N_f)$ breaking occurs at order N_c^0 instead of $1/N_c$ as for the ground and symmetric excited states.

---

[*] Talk delivered by Fl. Stancu

Presently a lattice test of $1/N_c$ baryon masses relations has been performed [10]. The lattice data clearly display both the $1/N_c$ and the SU(3) flavour symmetry breaking hierarchies.

Also, it was shown that the NN potential has an $1/N_c^2$ expansion and the strengths of the leading order central, spin-orbit, tensor and quadratic spin-orbit forces gave a qualitative understanding of the phenomenological meson exchange models [11].

2   The mass formula

Here we are concerned with baryon spectra. The general form of the baryon mass operator is [12]

$$M = \sum_i c_i O_i + \sum_i d_i B_i \tag{1}$$

with the operators O_i having the general form

$$O_i = \frac{1}{N_c^{n-1}} O_\ell^{(k)} \cdot O_{SF}^{(k)}, \tag{2}$$

where $O_\ell^{(k)}$ is a k-rank tensor in O(3) and $O_{SF}^{(k)}$ a k-rank tensor in SU(2), but invariant in SU(N_f). The latter is expressed in terms of SU(N_f) generators S^i, T^a and G^{ia} acting on spin, flavour and spin-flavour respectively. For the ground state one has k = 0. Excited states require $k = 1$ terms, which correspond to the angular momentum component and the k = 2 tensor term

$$L_q^{(2)ij} = \frac{1}{2} \left\{ L_q^i, L_q^j \right\} - \frac{1}{3} \delta_{i,-j} L_q \cdot L_q . \tag{3}$$

The first factor in (2) gives the order $\mathcal{O}(1/N_c)$ of the operator in the series expansion and reflects Witten's power counting rules. The lower index i represents a specific combination of generators, see examples below. The B_i are SU(3) breaking operators. In the linear combination, Eq. (1), c_i and d_i encode the QCD dynamics and are obtained from a fit to the existing data. It is important to find regularities in their behaviour [13] and search for a possible compatibility with quark models [14].

A considerable amount of work has been devoted to ground state baryons summarized in several review papers as, for example, [5–7]. The ground state is described by the symmetric representation [N_c]. For N_c = 3 this becomes [3] or [**56**] in an SU(6) dimensional notation.

In the following we shall concentrate on the description of excited states only and the motivation will be obvious.

3   Excited states

Excited baryons can be divided into SU(6) multiplets, as in the constituent quark model. If an excited baryon belongs to the [**56**]-plet the mass problem can be

treated similarly to the ground state in the flavour-spin degrees of freedom, but one has to take into account the presence of an orbital excitation in the space part of the wave function [15,16]. If the baryon belongs to the mixed symmetric representation [21], or [**70**] in SU(6) notation, the treatment becomes much more complicated.

There is a standard way to study the [**70**]-plets which is related to the Hartree approximation [9]. An excited baryon is described by symmetric core plus an excited quark coupled to this core, see *e.g.* [17–20]. In that case the core can be treated in a way similar to that of the ground state. In this method each $SU(2N_f) \times O(3)$ generator is splitted into two terms

$$S^i = s^i + S_c^i; \quad T^a = t^a + T_c^a; \quad G^{ia} = g^{ia} + G_c^{ia}, \quad \ell^i = \ell_q^i + \ell_c^i, \tag{4}$$

where s^i, t^a, g^{ia} and ℓ_q^i are the excited quark operators and S_c^i, T_c^a, G_c^{ia} and ℓ_c^i the corresponding core operators.

In this procedure the wave function is approximated by the term which corresponds to the normal Young tableau, where the decoupling of the excited quark is straightforward. The other terms needed to construct a symmetric orbital-flavour-spin state are neglected, *i.e.* antisymmetry is ignored. An a posteriori justification is given in Ref. [21].

But the number of linearly independent operators constructed from the generators given in the right-hand side of Eqs. (4) increases tremendously the number of terms in the mass formula so that the number of coefficients to be determined usually becomes much larger than the experimental data available. Consequently, in selecting the most dominant operators one has to make an arbitrary choice, as for example in Ref. [17]. In particular the isospin operator as $t \cdot T^c/N_c$, although important, has been entirely ignored without any reason.

A solution to this problem has been found in Ref. [22], where the separation into a symmetric core and an excited quark is not necessary. The key issue is the knowledge of the matrix elements of the $SU(2N_f)$ generators for mixed symmetric states described by the partition $[N_c-1, 1]$ for arbitrary N_c. These can be obtained by using a generalized Wigner-Eckart theorem [23]. Using $SU(2N_f)$ generators acting on the whole system, the number of operators up to $1/N_c$ order in the mass formula is considerably reduced so that the physics becomes more transparent, as we shall see below.

3.1 The SU(4) case

The SU(4) case has been presented in Ref. [22]. Its algebra is

$$[S^i, S^j] = i\varepsilon^{ijk}S^k, \quad [T^a, T^b] = i\varepsilon^{abc}T^c,$$
$$[G^{ia}, G^{jb}] = \tfrac{i}{4}\delta^{ij}\varepsilon^{abc}T^c + \tfrac{i}{2}\delta^{ab}\varepsilon^{ijk}S^k, \tag{5}$$

with $i, a = 1, 2, 3$. The matrix elements of the SU(4) generators were extracted from Ref. [23], initially proposed for nuclear physics where SU(4) symmetry is nearly exact. The transcription to a system of N_c quarks was straightforward. Instead of 12 operators up to order $\mathcal{O}(1/N_c)$ presented in Ref. [17] we needed only 6

operators for 7 experimentally known three- and four-star nonstrange resonances (no mixing angles). We have introduced the spin and isospin operators on equal footing, as seen from Table 1, and obtained the new result that the isospin term O_4 becomes as dominant in Δ resonances as the spin term O_3 does in N^* resonances, as indicated by the comparable size of the coefficients c_3 and c_4 in Table 1. Column 5 proves that by the removal of O_4 the fit deteriorates considerably.

Table 1. List of operators O_i and coefficients c_i in the $N = 1$ band revisited, 7 resonances of 3 and 4 stars status, no mixing angles.

Operator	Fit 1 (MeV)	Fit 2 (MeV)	Fit 3 (Mev)	Fit 4 (MeV)	Fit 5 (MeV)
$O_1 = N_c \mathbb{1}$	481 ± 5	482 ± 5	484 ± 4	484 ± 4	498 ± 3
$O_2 = \ell^i s^i$	-31 ± 26	-20 ± 23	-12 ± 20	3 ± 15	38 ± 34
$O_3 = \frac{1}{N_c} S^i S^i$	161 ± 16	149 ± 11	163 ± 16	150 ± 11	156 ± 16
$O_4 = \frac{1}{N_c} T^a T^a$	169 ± 36	170 ± 36	141 ± 27	139 ± 27	
$O_5 = \frac{15}{N_c} L^{(2)ij} G^{ia} G^{ja}$	-29 ± 31		-34 ± 30		-34 ± 31
$O_6 = \frac{3}{N_c} L^i T^a G^{ia}$	32 ± 26	35 ± 26			-67 ± 30
χ^2_{dof}	0.43	0.68	0.94	1.04	11.5

3.2   The SU(6) case

Below we present preliminary results for SU(6). The group algebra is

$$[S^i, S^j] = i\varepsilon^{ijk} S^k, \quad [T^a, T^b] = if^{abc} T^c,$$
$$[S^i, G^{ja}] = i\varepsilon^{ijk} G^{ka}, \quad [T^a, G^{jb}] = if^{abc} G^{ic},$$
$$[G^{ia}, G^{jb}] = \tfrac{i}{4}\delta^{ij} f^{abc} T^c + \tfrac{i}{2}\varepsilon^{ijk}\left(\tfrac{1}{3}\delta^{ab} S^k + d^{abc} G^{kc}\right), \qquad (6)$$

with $i = 1,2,3$ and $a = 1,2,...,8$. The analytic work was based on the extension of Ref. [23] from SU(4) to SU(6) in order to obtain matrix elements of all SU(6) generators between symmetric $[N_c]$ states first [24], followed later by matrix elements of all SU(6) generators between mixed symmetric states $[N_c - 1, 1]$ states [25]. The latter work has been recently completed by some new isoscalar factors required by the physical problem [26].

Theoretically the $[\mathbf{70}, 1^-]$ multiplet has 5 octets (N, Λ, Σ, Ξ), 2 decuplets (Δ, Σ, Ξ, Ω) and two flavour singlets $\Lambda_{1/2}$ and $\Lambda_{3/2}$. In the fit we take into account the 17 experimentally known resonances having a 3 or 4 star status and the two known mixing angles between the ^2N_J and ^4N_J ($J = 1/2, 3/2$) states. Table 2 exhibits the

9 operators used in the mass formula, from which the three B_i's break explicitly the SU(3) symmetry. The corresponding fitted coefficients c_i and d_i are indicated under a preliminary fit named Fit 1. We remind that in the symmetric core + excited quark procedure fifteen O_i (flavour invariants) and four B_i operators were included in the fit [27]. However the flavour operator $1/N_c \, t \cdot T^c$ was omitted, without any justification.

Like for nonstrange baryons, one can see that the dominant operators are the spin O_3 and flavour O_4. The latter has the form explained in Ref. [25]. It recovers the matrix elements of $O_4 = 1/N_c \, T^a T^a$ of nonstrange baryons (see Table 1). The operators O_3 and O_4 have similar values for the corresponding coefficients, which proves the importance of the flavour operators in the fit, like for the SU(4) case.

Table 2. Operators and their coefficients in the mass formula obtained from a numerical fit, mixing angles included, $\mathcal{S}$ denotes the strangeness.

Operator	Fit 1 (MeV)
$O_1 = N_c \mathbb{1}$	476.11 ± 4.09
$O_2 = l^i s^i$	63.6 ± 22.6
$O_3 = \frac{1}{N_c} S^i S^i$	165 ± 15
$O_4 = \frac{1}{N_c}(T^a T^a - \frac{1}{12} N_c(N_c + 6))$	181.95 ± 11.6
$O_5 = \frac{3}{N_c} L^i T^a G^{ia}$	-19.4 ± 6
$O_6 = \frac{15}{N_c} L^{(2)ij} G^{ia} G^{ja}$	8.5 ± 0.3
$B_1 = -\mathcal{S}$	163.90 ± 12.04
$B_2 = \frac{1}{N_c} L^i G^{i8} - \frac{1}{2}\sqrt{\frac{3}{2}} O_2$	33.96 ± 31.55
$B_3 = \frac{1}{N_c} S^i G^{i8} - \frac{1}{2\sqrt{3}} O_3$	112.46 ± 62.14
χ^2_{dof}	2.85

In Tables 1 and 2 the operator O_2 contains the one-body part of the spin-orbit term, defined in Ref. [17], while O_5, O_6 and B_2 contain the total orbital angular momentum components L^i, as in Eq. (3). Using the total spin-orbit term it would hardly affect the fit. The contribution of terms containing the angular momentum is generally small, like for nonstrange baryons [22], see Table 1. The SU(3) breaking operator B_1 turns out to be important, as expected.

The $\chi^2_{\text{dof}} = 2.85$ is larger than desired. We found that the basic reason is that it is hard to fit the mass of $\Lambda(1405)$ to be so low. The difficulty is entirely similar to that of quark models, where $\Lambda(1405)$ appears too high. An artificially larger mass of the order of 1500 MeV considerably improves the fit, leading to $\chi^2_{\text{dof}} < 1$. More fits will be presented elsewhere [26].

The difference between our results and those of Ref. [18] can partly be explained as due to the difference in the wave function. In Ref. [18] only the component with $S_c = 0$ is taken into account and this component brings no contribution to the spin term in flavour singlets, so that the mass of $\Lambda(1405)$ remains low. In our case, where we use the exact wave function, both $S_c = 0$ and $S_c = 1$ parts of the wave function contribute to the spin term. This makes the spin term contribution identical for all states of given J irrespective of the flavour, which seems to us natural. Then, in our case, with a non vanishing spin term in flavour singlets as well, the mass formula accomodates a heavier $\Lambda(1405)$ than the experiment, like in quark models (for a review on the controversial nature of $\Lambda(1405)$ see, for example, Ref. [30] where one of the authors S.F. Tuan has predicted together with D.H. Dalitz this resonance in 1959, discovered experimentally two years later.)

4   Conclusion

The $1/N_c$ expansion method provides a powerful theoretical tool to analyze the spin-flavour symmetry of baryons and explains the success of models based on this symmetry. We have shown that the dominant contributions come from the spin and flavour terms in the mass formula both in SU(4) and SU(6). The terms containing angular momentum bring small contributions, which however slightly improve the fit. It is hard to fit the mass of $\Lambda(1405)$, a notorious problem in realistic quark models [28,29]. This suggests again a more complex nature of this resonance, as, for example, a coupling to a $\bar{K}N$ system , which might survive in the large N_c limit [31,32].

References

1. G. 't Hooft, Nucl. Phys. **72** (1974) 461.
2. E. Witten, Nucl. Phys. **B160** (1979) 57.
3. J. L. Gervais and B. Sakita, Phys. Rev. Lett. **52** (1984) 87; Phys. Rev. **D30** (1984) 1795.
4. R. Dashen and A. V. Manohar, Phys. Lett. **B315** (1993) 425; ibid **B315** (1993) 438.
5. R. F. Dashen, E. Jenkins and A. V. Manohar, Phys. Rev. **D51** (1995) 3697.
6. E. Jenkins, Ann. Rev. Nucl. Part. Sci. **48** (1998) 81.
7. E. Jenkins, AIP Conference Proceedings, Vol. 623 (2002) 36, arXiv:hep-ph/0111338.
8. E. E. Jenkins, PoS E **FT09** (2009) 044 [arXiv:0905.1061 [hep-ph]].
9. J. L. Goity, Phys. Lett. **B414** (1997) 140.
10. E. E. Jenkins, A. V. Manohar, J. W. Negele and A. Walker-Loud, Phys. Rev. D **81** (2010) 014502
11. D. B. Kaplan and A. V. Manohar, Phys. Rev. C **56** (1997) 76
12. E. E. Jenkins and R. F. Lebed, Phys. Rev. D **52**, 282 (1995).
13. N. Matagne and F. Stancu, Phys. Lett. **B631** (2005) 7.

14. C. Semay, F. Buisseret, N. Matagne and F. Stancu, Phys. Rev. D **75** (2007) 096001.
15. J. L. Goity, C. Schat and N. N. Scoccola, Phys. Lett. **B564** (2003) 83.
16. N. Matagne and F. Stancu, Phys. Rev. **D71** (2005) 014010.
17. C. E. Carlson, C. D. Carone, J. L. Goity and R. F. Lebed, Phys. Rev. **D59** (1999) 114008.
18. J. L. Goity, C. L. Schat and N. N. Scoccola, Phys. Rev. **D66** (2002) 114014.
19. N. Matagne and F. Stancu, Phys. Rev. **D74** (2006) 034014.
20. N. Matagne and F. Stancu, Nucl. Phys. Proc. Suppl. **174** (2007) 155.
21. D. Pirjol and C. Schat, Phys. Rev. D **78** (2008) 034026.
22. N. Matagne and F. Stancu, Nucl. Phys. A **811** (2008) 291.
23. K. T. Hecht and S. C. Pang, J. Math. Phys. **10** (1969) 1571.
24. N. Matagne and F. Stancu, Phys. Rev. **D73** (2006) 114025.
25. N. Matagne and F. Stancu, Nucl. Phys. A **826** (2009) 161.
26. N. Matagne and F. Stancu, in preparation.
27. C. L. Schat, J. L. Goity and N. N. Scoccola, Phys. Rev. Lett. **88** (2002) 102002; J. L. Goity, C. L. Schat and N. N. Scoccola, Phys. Rev. **D66** (2002) 114014.
28. S. Capstick and N. Isgur, Phys. Rev. D **34** (1986) 2809.
29. L. Y. Glozman, W. Plessas, K. Varga and R. F. Wagenbrunn, Phys. Rev. D **58** (1998) 094030.
30. S. Pakvasa and S. F. Tuan, Phys. Lett. B **459** (1999) 301.
31. C. Garcia-Recio, J. Nieves and L. L. Salcedo, Phys. Rev. D **74** (2006) 036004.
32. T. Hyodo, D. Jido and L. Roca, Phys. Rev. D **77** (2008) 056010.

Isospin symmetry breaking in X(3872)⋆

Sachiko Takeuchi

Japan College of Social Work, Kiyose, Tokyo 204-8555, Japan

Abstract. In this work, we employ a quark model as well as a meson model to investigate the isospin symmetry breaking of X(3872). We find that the quark model, in which the isospin breaking occurs because of the u and d quark mass difference and of the electromagnetic force, can give a shallow bound state where the isospin is mixed but mostly 0. The meson model, where the width of the ρ or ω meson is taken into account, can also give the X(3872) → J/ψρ and J/ψω transition strength with a sharp peak around the $D^0 \overline{D}^{*0}$ threshold. Their strength is comparable in size, which is consistent with the experiment.

1 Introduction

X(3872) is a heavy meson first observed by Belle in 2003 in the B decay, $B^\pm \rightarrow K^\pm J/\psi \, \pi\pi(\pi)$ [1]. It has a mass of (3872.3 ± 0.8) MeV and a width of $(3.0+2.1-1.7)$ MeV [2]. It seems difficult to explain the properties of this particle if one assumes a simple $c\bar{c}$ state. Its rather low mass and small width as well as the momentum distribution of the final π's suggest that X(3872) may be $J^{PC}=1^{++}$ and probably has a large four-quark component, $q\bar{q}c\bar{c}$ [3–5]. Another notable property is that it decays into both J/ψ π^2 and J/ψ π^3 in comparable size [6]:

$$\frac{\mathrm{Br}(X(3872) \rightarrow \pi^+\pi^-\pi^0 J/\psi)}{\mathrm{Br}(X(3872) \rightarrow \pi^+\pi^- J/\psi)} = 1.0 \pm 0.4 \pm 0.3, \tag{1}$$

which means that X(3872) is a mixed state of the isospin 0 and 1.

Table 1. Relevant threshold energy close to X(3872) [2]. All entries are in MeV.

	$m_{X(3872)}$	$m_{D^0} + m_{D^{*0}}$	$m_{J/\psi} + m_\rho$	$m_{J/\psi} + m_\omega$	$m_{D^+} + m_{D^{*-}}$
exp.	3872.3±0.8	3871.8	3872.4	3879.6	3879.9

As seen in Table 1, there are four thresholds which are very close to X(3872). It is natural to consider that X(3872) has large components of those two-meson states. Because of the D^+D^{*-} threshold is by about 8 MeV higher than that of

---

⋆ This work has been done with in collaboration with Dr. Makoto Takizawa and Dr. Kiyotaka Shimizu.

$D^0\overline{D}^{*0}$, the tail of the wave function of X(3872) probably consists mainly of $D^0\overline{D}^{*0}$. This causes the isospin symmetry breaking in X(3872).

The decay into $J/\psi\rho$ or $J/\psi\omega$ requires recoupling of the quarks, thus occurs at the short range. So, it is still nontrivial whether the above threshold difference also affects the short-range part enough to explain the decay ratio shown in eq. (1). To clarify this point, we investigate the situation quantitatively by a quark model as well as by a meson model in the following.

2 Quark model picture

A constituent quark model is an effective model for the low energy hadron physics [7]. There the quarks are treated as dynamical variables whereas the gluon effects are reduced mostly to the single particle energy of quarks or the potential between quarks. The masses of light quarks are considered to increase up around to 300 MeV due to the chiral symmetry breaking.

This picture is more reliable when the concerning quarks are heavy. For example, the summation of $D^{(*)}$ mass and $B_s^{(*)}$ mass is almost the same that of $B^{(*)}$ and $D_s^{(*)}$ (Table 2). This suggests that the bulk effects of the gluon or the sea quark degrees of freedom are effectively included in the single particle energy of the quarks.

Table 2. Mass of (u+s+c+b) systems (in MeV).

	$m_{K^{(*)}} + m_{B_c^{(*)}}$	$m_{D^{(*)}} + m_{B_s^{(*)}}$	$m_{B^{(*)}} + m_{D_s^{(*)}}$
pseudo-scalar mesons	6770	7231	7247
vector mesons	892+?	7420	7437

The difference between the above entries, for example, $(m_D + m_{B_s}) - (m_B + m_{D_s})$, comes from the interaction between quarks. The 0th order terms are considered to be color-Coulomb and the linear confinement terms, which are established in both of the empirical and theoretical ways.

The hadron-hadron interaction arises mostly from the spin-dependent part, which is one of the higher order terms. It is well known that the effective one-gluon exchange gives such a spin-spin term. The interaction is investigated also by the Lattice QCD [8], where the spin-spin term is found to be proportional to $(1/m_1 m_2)$:

$$V_{ss} = \frac{\mathbf{s}_1 \cdot \mathbf{s}_2}{m_1 m_2} V(r) \tag{2}$$

where $V(r)$ is short-ranged ($r < 0.5$ fm) potential.

This spin-spin interaction seems to be modified a little when one of the quarks is the light quark. In Table 3, we listed the observed hyperfine splitting for each

Table 3. Hyperfine splitting of the $q\overline{Q}$ systems (in MeV).

$m_{K^*} - m_K$	$m_{D^*} - m_D$	$m_{D_s^*} - m_{D_s}$	$m_{B^*} - m_B$	$m_{B_s^*} - m_{B_s}$
398	141	144	46	47

$q\overline{Q}$ system[1]. It, however, is still clearly seen that the interaction becomes smaller as the heavy quark is heavier. So the properties of the four-quark systems are governed mainly by the interaction between the light quark-light antiquark pairs.

In Table 4, we show the matrix elements of relevant interactions: the color-magnetic interaction (CMI), the pair-annihilating term of OGE (OGE-a), Ins, and an estimate by a typical parameter set used for a quark model. The most attractive pair is the color-singlet, spin 0, flavor-octet, which exists, *e.g.* in the pion. There is another weak but still attractive pair: the color-octet, spin 1, flavor-octet one. I=0 pairs may also be attractive if OGE-a and Ins are weak, whose size is not well known. Such pairs may be found in the $q\overline{q}c\overline{c}$ systems. We argue that this attraction leads to X(3872) to have a large four-quark configuration.

Table 4. Matrix elements of the interactions between $q\overline{q}$ pairs. The color-magnetic interaction, $-\langle(\lambda \cdot \lambda)(\sigma \cdot \sigma)\rangle$, is denoted as CMI, the pair-annihilating term of OGE (OGE-a), the spin-color part of the instanton induced interaction (Ins), and estimate value by a typical parameter set, E.

color	spin	flavor	CMI	OGE-a	Ins	E(MeV)	States
1	0	1	−16	0	12	84	η
1	0	8	−16	0	−6	−327	π, K
1	1	1	16/3	0	0	63	ω
1	1	8	16/3	0	0	63	ρ
8	0	1	2	0	3/4	41	
8	0	8	2	0	−3/8	15	
8	1	1	−2/3	9/2	9/4	97	
8	1	8	−2/3	0	−9/8	−34	$c\overline{c}q\overline{q}$ with J^{PC}=0^{++},1^{+-},1^{++},2^{++}

3 X(3872) by a quark model

In the quark model, the isospin symmetry breaking occurs due to the u and d quark mass difference and the electromagnetic interaction between quarks. The model hamiltonian and the wave function is taken to be the same as those in ref.[9].

The X(3872) configuration is taken to be $q\overline{q}c\overline{c}$ with a $c\overline{c}$ core. The four quark state is solved by using the resonating group method with a full deformation in

[1] The Table suggests that the SU(3)$_f$ flavor symmetry is good when the one of the quark is heavy, but we do not discuss farther on this topic here.

Table 5. Binding energy and probabilities of each configuration. $(c\bar{c})_1$ [$(c\bar{c})_8$] stands for the $c\bar{c}$ pair is color-singlet [octet].

B.E.	$(c\bar{c})_1(q\bar{q})_1$		$(c\bar{c})_8(q\bar{q})_8$		$c\bar{c}$
	$I = 0$	$I = 1$	$I = 0$	$I = 1$	
5.2 MeV	0.11	0.04	0.44	0.09	0.37

the short distance. So the system can be a molecular state of two mesons with the tetraquark components in the short range region.

It is found that there can be a shallow $J^{PC} = 1^{++}$ bound state which is mostly isospin $I = 0$. The probability of each component is shown in Table 5. By multiplying larger phase space for $J/\psi\rho$ channel, we may have the branching ratio reported in ref.[6].

4   X(3872) by a meson model

In order to investigate the branching ratio directly, we employ the meson model for X(3872). The mesons, D, D^*, ρ and ω are treated as fundamental degrees of freedom in this model. The isospin breaking comes from the mass difference of mesons [10].

The meson-meson interaction is taken to be the gaussian separable type as

$$V_m(p, p') = v_0 \ \exp[-a^2(p^2 + p'^2)/4] \tag{3}$$

with the range $a = 0.4$ fm. As for the coupling between the two-meson channel and the $c\bar{c}$ channel we take

$$V_{m,c\bar{c}}(p) = w_0 \ \exp[-b^2 p^2/4] \tag{4}$$

with also $b = 0.4$ fm. As the first try, we fit v_0 and u_0 to produce an appropriate shape for the peak. This interaction does not break the isospin symmetry.

We solve a four-channel coupled scattering problem, $D^0\overline{D}^{*0}$-$J/\psi\ \rho$-$J/\psi\ \omega$-D^+D^{*-}, with the $c\bar{c}(1P)$ state as a bound state embedded in the continuum [11], and calculate the transition strength of X(3872) to the final α channel with the $D^0\overline{D}^{*0}$ momentum, q:

$$\frac{dW}{dq} = \frac{M_{K-D^0\overline{D}^{*0}}}{\mu_{D^0\overline{D}^{*0}}} \ q \sum_\alpha \mu_\alpha q_\alpha \big|\langle \text{two mesons } q_\alpha | T_{\alpha,c\bar{c}} \ G_0 | c\bar{c}\rangle\big|^2 \tag{5}$$

The probability can be expressed by the $c\bar{c}$ self energy, $\Sigma_c\bar{c}$, as

$$\sum_\alpha \cdots \propto -\Im\langle c\bar{c}|(T_{\alpha,c\bar{c}} \ G_0)^\dagger G_0 \ T_{\alpha,c\bar{c}} \ G_0|c\bar{c}\rangle \tag{6}$$

$$= -\Im\langle c\bar{c}|G_c\bar{c}^* \ \Sigma_c\bar{c} \ G_c\bar{c}|c\bar{c}\rangle \tag{7}$$

In order to include the effects of the ρ and ω meson width, we substitute of the resolvent of the α channel by that with the observed ρ or ω meson width as:

$$-\Im\langle c\bar{c}|G_0 \ T^*_{c\bar{c},\alpha} \ G_0 \ T_{\alpha,c\bar{c}} \ G_0|c\bar{c}\rangle \rightarrow -\Im\langle c\bar{c}|G_0 \ T^*_{c\bar{c},\alpha} \ \tilde{G}_0 \ T_{\alpha,c\bar{c}} \ G_0|c\bar{c}\rangle \tag{8}$$

with $\tilde{G}_0 = (E - K_\alpha + i\Gamma/2)^{-1}$. One of our parameter sets gives the result plotted in Figure 1. A sharp peak appears in the final J/ψ ρ- or J/ψ ω-channel around the $D^0\overline{D}^{*0}$ threshold. Both of the J/ψ ρ and J/ψ ω can be found also below the threshold due to the vector meson width. The size of the decay probability to J/ψ ρ and J/ψ ω are almost the same around the peak, which is consistent with the experiment.
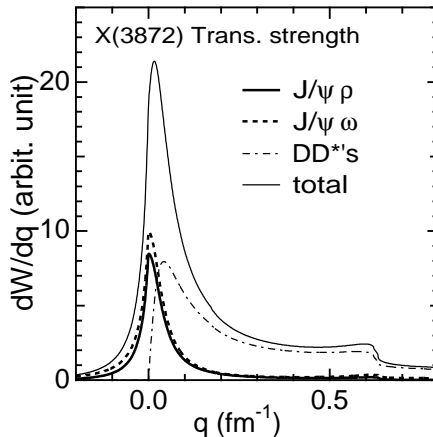
Fig. 1. Transition strength of X(3872) with respect to the $D^0\overline{D}^{*0}$ momentum, q.

We argue that X(3872) can be considered as a meson molecular state with a $c\bar{c}$ core. It is also pointed out that similar heavy mesons above the open charm threshold, $D\overline{D}$, the mass spectrum of charmonia deviates considerably from the quark model prediction [12]. The method we employ here can also be applied to investigate such states.

References

1. S. K. Choi *et al.* [Belle Collaboration], Phys. Rev. Lett. **91** (2003) 262001.
2. C. Amsler *et al.* (Particle Data Group), Phys. Lett. **B667**, 1 (2008). [http://pdg.lbl.gov/].
3. C. Amsler and N. A. Tornqvist, Phys. Rept. **389**, 61 (2004), and references therein.
4. E. S. Swanson, Phys. Rept. **429**, 243 (2006), and references therein.
5. E. Klempt and A. Zaitsev, Phys. Rept. **454**, 1 (2007), and references therein.
6. K. Abe, *et al.*, [Belle Collaboration], arXiv:hep-ex/050537.
7. S. Godfrey and N. Isgur, Phys. Rev. D **32**, 189 (1985).
8. Y. Koma and M. Koma, PoS **LAT2009**, 122 (2009).
9. S. Takeuchi, Bled Workshops in Physics (Bled 2008), Volume 9, pp. 71-77.
10. M. Takizawa and S. Takeuchi, Prog. Theo. Phys. Suppl. **186**, (2010), to be published (NFQCD10 proceedings).
11. S. Takeuchi and K. Shimizu, Phys. Rev. C **79**, 045204 (2009).
12. T. Iijima, Prog. Theo. Phys. Suppl. **186**, (2010), to be published (NFQCD10 proceedings).

News from Belle

M. Bračko[⋆]

University of Maribor, Smetanova ulica 17, SI-2000 Maribor, Slovenia
and J. Stefan Institute, Jamova cesta 39, SI-1000 Ljubljana, Slovenia

Abstract. The Belle experiment at the KEKB asymmetric-energy e^+e^- collider has proven to be an excellent environment for studies in hadron spectroscopy. These studies have led to discoveries of many meson candidates that behave like charmonium states, but due to some of their properties cannot be explained as pure conventional $c\bar{c}$ mesons within the classical quark model. Similar exotic states have been observed also in the $s\bar{s}$ and $b\bar{b}$ systems. In this report, recent Belle results on these newly observed states are reviewed.

1 Introduction

The Belle detector[1] at the asymmetric-energy e^+e^- collider KEKB[2] has accumulated about 1 ab^{-1} of data by the end of its operation in June 2010. The KEKB collider, called a *B-factory*, operated near the $\Upsilon(4S)$ resonance with a peak luminosity that exceeded 2.1×10^{34} cm^{-2}s^{-1}. Large amount of collected experimental data and excellent detector performance enabled searches for new hadronic states as well as studies of their properties. Many interesting spectroscopic results have indeed been obtained at the Belle experiment, and this report covers most recent and interesting ones.

There has been a renewed interest in charmonium spectroscopy since 2002. The attention to this field was drawn by the discovery of the two missing $c\bar{c}$ states below the open-charm threshold, $\eta_c(2S)$ and $h_c(1P)$,[3,4] but even more by observations of a number of new particles [5,6] above the threshold for the open-charm production. Newly observed states – collectively called XYZ– resemble charmonia, but differ from regular $c\bar{c}$ states by some of their properties, or can simply not be identified as charmonia due to lack of available $c\bar{c}$ potential model assignments (see for example Ref. [7]). As a consequence of these properties, XYZ states – although probably containing a $c\bar{c}$ quark pair – could be explained as more complex, exotic type of particles. These include: tightly bound four-quark states called *tetraquarks*; two loosely bound charm mesons forming the so-called *molecular states*; *charmonium hybrids* interpreted as $c\bar{c}$-gluon states with excited gluonic degrees of freedom; or *hadro-charmonium* states, where the traditional charmonium states like J/ψ or η_c are "submerged" in a light hadronic matter. On the other hand, there also exist some alternative models, which try to explain experimental results simply by effects of various open charm thresholds

---

[⋆] Representing the Belle Collaboration.

on the conventional charmonium levels. All these different ideas have been extensively explored in numerous theoretical papers, published recently; the list of these papers is far too long to be quoted in this review. However, it is important to know that many aspects of these spectroscopic questions were also subject of several studies presented by participants of the Bled 2010 workshop [8].

In this review we will present results from some recent Belle analyses of new charmoniun(-like) XYZ states. We will also mention some results, suggesting the existence of similar exotic states in the $s\overline{s}$ and $b\overline{b}$ systems.

2   Charmonium and Charmonium-like States

Experimentaly, many different measurements in charmonium spectroscopy can be performed at a B-factory, since charmonium(-like) particles are produced there by various different mechanisms: via B decays; in e^+e^- annihilation into double $c\overline{c}$; C-even states can be formed in $\gamma\gamma$ processes; and $J^{PC} = 1^{--}$ resonances can be created in e^+e^- annihilation after the photon radiative return.

2.1   The X(3872) news

The story about new charmonium-like states began in 2003, when Belle reported on $B^+ \to K^+ J/\psi\pi^+\pi^-$ analysis,[1] where a new state decaying to $J/\psi\pi^+\pi^-$ was discovered [9]. The new state, called X(3872), was soon confirmed and also intensively studied by the CDF, DØ and *BABAR* collaborations [10–18]. So far it has been established that this narrow state ($\Gamma = (3.0^{+1.9}_{-1.4} \pm 0.9)$ MeV) has a mass of (3872.2 ± 0.8) MeV/c^2, which is very close to the $D^0\overline{D}^{*0}$ threshold [19]. The intensive studies of several X(3872) production and decay modes suggest two possible J^{PC} assignments, 1^{++} and 2^{-+}, and establish the X(3872) as a candidate for a loosely bound $D^0\overline{D}^{*0}$ molecular state. However, results provide substantial evidence that the X(3872) state must contain a significant $c\overline{c}$ component as well.

Just very recently, Belle performed a study of $B \to (c\overline{c}\gamma)K$ using 712 fb^{-1} data sample collected at the $\Upsilon(4S)$ resonance [20]. Pure $D^0\overline{D}^{*0}$ molecular model [21] predicts $\mathcal{B}(X(3872) \to \psi'\gamma)$ to be less than $\mathcal{B}(X(3872) \to J/\psi\gamma)$. Results by the *BABAR* collaboration [18] show that $\mathcal{B}(X(3872) \to \psi'\gamma)$ is almost three times that of $\mathcal{B}(X(3872) \to J/\psi\gamma)$, which is inconsistent with the pure molecular model, and can be interpreted as a large $c\overline{c} - D^0\overline{D}^{*0}$ admixture. We observe X(3872) $\to J/\psi\gamma$ together with an evidence for $\chi_{c2} \to J/\psi\gamma$ in $B^\pm \to J/\psi K^\pm$, while in our search for X(3872) $\to \psi'\gamma$ no significant signal is found (see Table 2). We also observe $B \to \chi_{c1}K$ in both, charged as well as neutral B decays.

The obtained results suggest that the $c\overline{c}$-$D^0\overline{D}^{*0}$ admixture in X(3872) may not be as large as discussed above. This might get us one step closer to resolving the nature of the X(3872) state even without a much larger data sample.

---

[1] In this review, the inclusion of charge-conjugated states is always implied.

Table 1. Summary of newly observed states adapted from Ref. [6]. The naming convention for these new XYZ states indicates the lack of knowledge about their structure and properties at the time of discovery.

State	M [MeV]	Γ [MeV]	J^{PC}	Decay Modes	Production Modes	Observed by
$Y_s(2175)$	2175 ± 8	58 ± 26	1^{--}	$\phi f_0(980)$	e^+e^- (ISR), $J/\psi \to \eta Y_s(2175)$	BABAR, BESII, Belle
$X(3872)$	3871.4 ± 0.6	$3.0^{+2.1}_{-1.7}$	1^{++} or 2^{-+}	$\pi^+\pi^- J/\psi$, $\gamma J/\psi$, $D\bar{D}^*$	$B \to KX(3872)$, $p\bar{p}$	Belle, CDF, DØ, BABAR
$X(3915)$	3914 ± 4	28^{+12}_{-14}	$0/2^{++}$	$\omega J/\psi$	$\gamma\gamma \to X(3915)$	Belle
$Z(3930)$	3929 ± 5	29 ± 10	2^{++}	$D\bar{D}$	$\gamma\gamma \to Z(3940)$	Belle
$X(3940)$	3942 ± 9	37 ± 17	$0^{?+}$	$D\bar{D}^*$ (not $D\bar{D}$, $\omega J/\psi$)	$e^+e^- \to J/\psi X(3940)$	Belle
$Y(3940)$	3943 ± 17	87 ± 34	$?^{?+}$	$\omega J/\psi$ (not $D\bar{D}^*$)	$B \to KY(3940)$	Belle, BABAR
$Y(4008)$	4008^{+82}_{-49}	226^{+97}_{-80}	1^{--}	$\pi^+\pi^- J/\psi$	e^+e^- (ISR)	Belle
$Y(4140)$	4143.0 ± 3.1	$11.7^{+9.1}_{-6.2}$	$?^{?+}$	$\phi J/\psi$	$B^\pm \to K^\pm Y(4140)$	CDF
$X(4160)$	4156 ± 29	139^{+113}_{-65}	$0^{?+}$	$D^*\bar{D}^*$ (not $D\bar{D}$)	$e^+e^- \to J/\psi X(4160)$	Belle
$Y(4260)$	4264 ± 12	83 ± 22	1^{--}	$\pi^+\pi^- J/\psi$	e^+e^- (ISR)	BABAR, CLEO, Belle
$Y(4350)$	4361 ± 13	74 ± 18	1^{--}	$\pi^+\pi^- \psi'$	e^+e^- (ISR)	BABAR, Belle
$X(4630)$	4634^{+9}_{-11}	92^{+41}_{-32}	1^{--}	$\Lambda_c^+ \Lambda_c^-$	e^+e^- (ISR)	Belle
$Y(4660)$	4664 ± 12	48 ± 15	1^{--}	$\pi^+\pi^- \psi'$	e^+e^- (ISR)	Belle
$Z_1^\pm(4050)$	4051^{+24}_{-23}	82^{+51}_{-29}	?	$\pi^\pm \chi_{c1}$	$B \to KZ_1^\pm(4050)$	Belle
$Z_2^\pm(4250)$	4248^{+185}_{-45}	177^{+320}_{-72}	?	$\pi^\pm \chi_{c1}$	$B \to KZ_2^\pm(4250)$	Belle
$Z^\pm(4430)$	4433 ± 5	45^{+35}_{-18}	?	$\pi^\pm \psi'$	$B \to KZ^\pm(4430)$	Belle
$Y_b(10890)$	$10,890 \pm 3$	55 ± 9	1^{--}	$\pi^+\pi^- \Upsilon(1,2,3S)$	$e^+e^- \to Y_b$	Belle

Table 2. Summary of recent B → (c c̄ γ)K results [20]. In all measurements the two consecutive errors indicate statistical and systematic uncertainties, respectively. Significances also include systematic uncertainties.

Decay mode	Signal	Significance (σ)	Branching fraction ($\mathcal{B}$)
$B^{\pm} \to \chi_{c1} K^{\pm}$	2308 ± 52	79	$(4.9 \pm 0.1 \pm 0.3) \cdot 10^{-4}$
$B^{0} \to \chi_{c1} K^{0}$	542 ± 24	37	$(3.78^{+0.17}_{-0.16} \pm 0.3) \cdot 10^{-4}$
$B^{\pm} \to \chi_{c2} K^{\pm}$	$32.8^{+10.9}_{-10.2}$	3.6	$(1.11^{+0.36}_{-0.34} \pm 0.09) \cdot 10^{-5}$
$B^{0} \to \chi_{c2} K^{0}$	$2.8^{+4.7}_{-3.9}$	0.7	$< 2.6 \cdot 10^{-5}$ at 90%C.L.
$B^{\pm} \to (X(3872) \to J/\psi\gamma)K^{\pm}$	$30.0^{+8.2}_{-7.4}$	4.9	$(1.78^{+0.48}_{-0.44} \pm 0.12) \cdot 10^{-6}$
$B^{0} \to (X(3872) \to J/\psi\gamma)K^{0}$	$5.7^{+3.5}_{-2.8}$	2.4	$< 2.4 \cdot 10^{-6}$ at 90%C.L.
$B^{\pm} \to (X(3872) \to \psi'\gamma)K^{\pm}$	$5.0^{+11.9}_{-11.0}$	0.4	$< 3.4 \cdot 10^{-6}$ at 90%C.L.
$B^{0} \to (X(3872) \to \psi'\gamma)K^{0}$	$1.5^{+4.8}_{-3.9}$	0.2	$< 6.6 \cdot 10^{-6}$ at 90%C.L.

2.2   Charged c c̄-like states: $Z^{+}(4430)$; $Z^{+}(4050)$ & $Z^{+}(4250)$

In 2008 an exciting discovery of a new charmonium-like state was reported [22] by Belle in the $B^{+,0} \to K^{0,-}\pi^{+}\psi(2S)$ analysis, performed on a data sample with $657 \cdot 10^{6}$ B$\overline{B}$ pairs. After excluding the Kπ Dalitz regions that correspond to K*(890) and $K_{2}^{*}(1430)$ mesons (*i.e.* K* veto), a strong enhancement is obtained in the $\pi^{+}\psi(2S)$ invariant mass distribution. A fit with an S-wave Breit-Wigner function for the signal and a phase-space-like background function yields a peak mass and width of M = $(4433 \pm 4 \pm 2)$ MeV/c^2 and $\Gamma = (45^{+18+30}_{-13-13})$ MeV, with a 6.5σ statistical significance. The observed resonance, named $Z^{+}(4430)$, is characterised by a product branching fraction of $\mathcal{B}(\overline{B}^{0} \to K^{-}Z^{+}(4430)) \times \mathcal{B}(Z^{+}(4430) \to \pi^{+}\psi(2S)) = (4.1 \pm 1.0 \pm 1.4) \cdot 10^{-5}$. The $Z^{+}(4430)$ is thus seen as the first charmonium-like charged meson with a minimal quark content of c c̄ u $\overline{d}$ – a serious tetraquark candidate.

The signature of this exotic state was also searched for by the *BABAR* collaboration [23]. The performed analysis of the $B^{-,0} \to \psi\pi^{-}K^{0,+}$ ($\psi = J/\psi$ or $\psi(2S)$) decays focuses on a detailed study of the Kπ^{-} system, since its mass and angular-distribution structures strongly influence the Dalitz plots. Using the final *BABAR* data sample of 413 fb^{-1}, no significant evidence for an invariant mass signal peak is obtained for any of the processes investigated, not even in the K* veto region for the $\psi(2S)\pi^{+}$ distribution, where the $Z^{+}(4430)$ was observed by Belle. The most prominent structure in the $\psi(2S)\pi^{-}$ mass distribution for all events is an excess of 2.7σ with a mass and width of M = $(4476 \pm 8((\text{stat.}))$ MeV/c^2 and $\Gamma = 32 \pm 16((\text{stat.}))$ MeV. Using the measured Belle parameters [22] for the $Z^{+}(4430)$, only the upper limit for the product branching fraction is obtained as $\mathcal{B}(\overline{B}^{0} \to K^{-}Z^{+}(4430)) \times \mathcal{B}(Z^{+}(4430) \to \pi^{+}\psi(2S)) < 3.1 \cdot 10^{-5}$ at a 95% confidence level. This result does neither refute nor confirm the existence of the $Z^{+}(4430)$, seen by Belle.

Soon after the *BABAR* group report, the Belle collaboration reanalysed the same data set as used previously in [22]. In order to check for the possible $\psi(2S)\pi^{-}$

mass reflections from the Kπ system, a full Dalitz plot analysis is performed [24], using the same data sample as above and a fit model that takes into account all known Kπ resonances below 1780 MeV/c². Dalitz plot is divided in five $M^2(K\pi)$-regions and the $Z^+(4430)$ signal is clearly seen for the K*-veto-equivalent $M^2(\pi^+\psi(2S))$ distribution. The fit results with 6.4σ peak significance agree with previous Belle measurement, and provide the updated $Z^+(4430)$ parameters: $M = (4443^{+15}_{-12}{}^{+19}_{-13})$ MeV/c², $\Gamma = (109^{+86}_{-43}{}^{+74}_{-56})$ MeV and $\mathcal{B}(\overline{B}^0 \to K^-Z^+(4430)) \times \mathcal{B}(Z^+(4430) \to \pi^+\psi(2S)) = (3.2^{+1.8}_{-0.9}{}^{+5.3}_{-1.6}) \cdot 10^{-5}$.

The observation of the $Z^+(4430)$ state suggests that studies of $B \to K\pi(c\overline{c})$ decays could reveal other similar neutral and charged partners. Belle thus reports also on a Dalitz plot analysis of $\overline{B}^0 \to K^-\pi^+\chi_{c1}$ decays with $657 \cdot 10^6$ $B\overline{B}$ pairs.[25] The fit model for Kπ resonances is the same as in the $Z^+(4430)$ Dalitz analysis, but here it includes also the $K_3^*(1780)$ meson. The fit results suggest that a broad doubly peaked structure in the $\pi^+\chi_{c1}$ invariant mass distribution should be interpreted by two new states, called $Z^+(4050)$ and $Z^+(4250)$. The double-Z^+ hypothesis is favoured when compared to the single-Z^+ (no-Z^+) hypothesis by the statistical significance of 5.7σ (13.2σ), and even with various systematic variations of the fit model, the significance is still at least 5.0σ (8.1σ). The masses, widths and product branching fractions for the two states are: $M(Z^+(4050)) = (4051 \pm 14^{+20}_{-41})$ MeV/c², $\Gamma(Z^+(4050)) = (82^{+21}_{-17}{}^{+47}_{-22})$ MeV, $M(Z^+(4250)) = (4248^{+44}_{-29}{}^{+180}_{-35})$ MeV/c², $\Gamma(Z^+(4250)) = (177^{+54}_{-39}{}^{+316}_{-61})$ MeV; and $\mathcal{B}(\overline{B}^0 \to K^-Z^+(4050)) \times \mathcal{B}(Z^+(4050) \to \pi^+\chi_{c1}) = (3.0^{+1.5}_{-0.8}{}^{+3.7}_{-1.6}) \cdot 10^{-5}$, $\mathcal{B}(\overline{B}^0 \to K^-Z^+(4250)) \times \mathcal{B}(Z^+(4250) \to \pi^+\chi_{c1}) = (4.0^{+2.3}_{-0.9}{}^{+19.7}_{-0.5}) \cdot 10^{-5}$.

3 XYZ counterparts in $b\overline{b}$ and $s\overline{s}$ systems

An interesting question is whether in the $s\overline{s}$ and $b\overline{b}$ systems there exist analogous "XYZ" states, predicted by many of the models proposed to explain the charmonium-like exotic states.

3.1 Y(2175)

A possible candidate in the $s\overline{s}$ system is Y(2175), a 1^{--} state, first observed by BaBar in the ISR process $e^+e^- \to \gamma_{ISR}f_0(980)\phi(1020)$ [26] and later confirmed by BES [27]. At Belle experiment, both $\pi^+\pi^-\phi(1020)$ and $f_0(980)\phi(1020)$ cross sections for the ISR processes $e^+e^- \to \gamma_{ISR}\pi^+\pi^-\phi(1020)$ and $e^+e^- \to \gamma_{ISR}f_0(980)\phi(1020)$ were measured [28]. The mass and width of the high mass peak in the cross section, corresponding to Y(2175), are found to be $M = 2079 \pm 13^{+79}_{-28}$ MeV and $\Gamma = 192 \pm 23^{+25}_{-61}$ MeV, which are consistent with the previous measurements. For First measurements of mass and width are reported for the low mass peak in the $\pi^+\pi^-\phi(1020)$ cross section distribution, corresponding to the $\phi(1680)$, the measured values are: $M = 1689 \pm 7 \pm 10$ MeV and $\Gamma = 211 \pm 14 \pm 19$ MeV. The widths for both, $\phi(1680)$ and Y(2175), are about 200 MeV. This may suggest that the Y(2175) is an excited 1^{--} $s\overline{s}$ state. Since the $f_0(980)$ is expected to have a large $s\overline{s}$ component, $Y(2175) \to f_0(980)\phi(1020)$ can be understood as an open-flavor decay, different from $Y(4260) \to \pi^+\pi^-J/\psi$, which is a

hadronic transition. Studies of $Y(2175)$ in other decay modes are therefore needed to determine if $Y(2175)$ is a conventional $s\bar{s}$ state or an s-quark analogue of the $Y(4260)$.

3.2 $Y_b(10890)$

The Belle experiment used a data sample at the CM energy around the $\Upsilon(5S)$ mass 10.89 GeV, and found large signals for decays into $\pi^+\pi^-\Upsilon(1S)$, $\pi^+\pi^-\Upsilon(2S)$ and $\pi^+\pi^-\Upsilon(3S)$ final states. If these transitions are only from the $\Upsilon(5S)$ resonance, then the corresponding partial widths are between 0.5 and 0.9 MeV. These values are more than two orders of magnitude larged than the corresponding partial widths for $\Upsilon(4S)$, $\Upsilon(3S)$ and $\Upsilon(2S)$ decays to $\pi^+\pi^-\Upsilon(1S)$. This could be explained by $b\bar{b}$ analogue of the $Y(4260)$ state, called $Y_b(10890)$, which overlaps with the $\Upsilon(5S)$. Alternatively, this phenomenon could be explained by the existence of a tetraquark intermediate state, the effect of final state interactions or by a nonperturbative approach for the calculation of the decay widths of dipion transitions of heavy quarkonia.

To distinguish between different possibilities, the Belle experiment performed a measurement of the energy dependence of the cross sections for $e^+e^- \rightarrow \pi^+\pi^-\Upsilon(nS)$ ($n = 1, 2, 3$) at energies around 10.89 GeV [29]. The peak mass and width, obtained by performing a fit with a common Breit-Wigner function to the measured $\pi^+\pi^-\Upsilon(nS)$ cross section distribution, is measured to be $M = 10889.6 \pm 1.8 \pm 1.6$ MeV and $\Gamma = 54.7^{+8.5}_{-7.2} \pm 2.5$ MeV. A fit with the $\Upsilon(5S)$ and $\Upsilon(6S)$ resonance parameters [19], fails to describe the observed $\pi^+\pi^-\Upsilon(nS)$ cross section.

4   Summary and Conclusions

The Belle experiment at the KEKB collider provides an excellent environment for charm and charmonium spectroscopy. As a result, many new particles have already been discovered during the Belle operation, and some of them are mentioned in this report. Some recent Belle results also indicate that analogs to exotic charmonium-like states can be found in $s\bar{s}$ and $b\bar{b}$ systems. As the operation of the experiment heas just finished in June 2010, some interesting results on spectroscopy could still be expected from Belle in the near future.

The Belle experimental results have already raised substantial interest and various interpretations for the nature and properties of newly observed states have been proposed. Perhaps some of the issues about these states might be resolved soon, following also the ideas and studies presented at this workshop.

References

1. A. Abashian *et al.* (Belle Coll.), *Nucl. Instrum. Methods* A **479**, 117 (2002).
2. S. Kurokawa and E. Kikutani, *Nucl. Instrum. Methods* A **499**, 1 (2003), and other papers included in this Volume.

3. S.-K. Choi *et al.* (Belle Collaboration), *Phys. Rev. Lett.* **89**, 102001 (2002).

4. J. L. Rosner *et al.* (Cleo Collaboration), *Phys. Rev. Lett.* **95**, 102003 (2005).

5. For a review of XYZ states see the Eric S. Swanson's contribution to the conference proceedings of Moriond QCD and High Energy Interactions '09, 14-21 March 2009, La Thuile, Italy.

6. S. L. Olsen, *Nucl. Phys.* A **827**, 53 (2009) (arXiv:0901.2371v1 [hep-ex]).

7. T. Barnes, S. Godfrey and E. S. Swanson, *Phys. Rev.* D **72**, 054026 (2005).

8. For approaches and results of these studies see several contributions to these proceedings.

9. S.-K. Choi *et al.* (Belle Collaboration), *Phys. Rev. Lett.* **91**, 262001 (2003).

10. D. Acosta *et al.* (CDF Collaboration), *Phys. Rev. Lett.* **93**, 072001 (2004)
    V. M. Abazov *et al.* (DØ Collaboration), *Phys. Rev. Lett.* **93**, 162002 (2004);
    B. Aubert *et al.* (*BABAR* Collaboration), *Phys. Rev.* D **71**, 071103 (2005).

11. K. Abe *et al.* (Belle Collaboration), arXiv:hep-ex/0505037, arXiv:hep-ex/0505038; submitted to the Lepton-Photon 2005 Conference.

12. G. Gokhroo *et al.* (Belle Collaboration), *Phys. Rev. Lett.* **97**, 162002 (2006).

13. B. Aubert *et al.* (*BABAR* Collaboration), *Phys. Rev.* D **74**, 071101 (2006).

14. I. Adachi *et al.* (Belle Collaboration), arXiv:0809.1224v1 [hep-ex]; contributed to the ICHEP 2008 Conference.

15. N. Zwahlen *et al.* (Belle Collaboration), arXiv:0810.0358v2 [hep-ex]; contributed to the ICHEP 2008 Conference.

16. A. Abulencia *et al.* (CDF), *Phys. Rev. Lett.* **98**, 132002 (2007).

17. B. Aubert *et al.* (*BABAR* Collaboration), *Phys. Rev.* D **77**, 011102 (2008).

18. B. Aubert *et al.* (*BABAR* Collaboration), *Phys. Rev. Lett.* **102**, 132001 (2009).

19. K. Nakamura *et al.* (Particle Data Group), *J. Phys.* G **37**, 075021 (2010).

20. Preliminary results of this analysis were presented at the *Quarkonium Working Group Workshop 2010*, 18th-21st May, 2010, Fermilab, Batavia, Illinois, USA.

21. E. S. Swanson, *Phys. Rep.* **429**, 243 (2006).

22. S.-K. Choi *et al.* (Belle Collaboration), *Phys. Rev. Lett.* **100**, 142001 (2008).

23. B. Aubert *et al.* (*BABAR* Collaboration), *Phys. Rev.* D **79**, 112001 (2009).

24. R. Mizuk *et al.* (Belle Collaboration), *Phys. Rev.* D **80**, 031104 (2009).

25. R. Mizuk *et al.* (Belle Collaboration), *Phys. Rev.* D **78**, 072004 (2008).

26. B. Aubert *et al.* (*BABAR* Collaboration], *Phys. Rev.* D **74**, 091103 (2006).

27. M. Ablikim *et al.* (BES Collaboration), *Phys. Rev. Lett.* **100**, 102003 (2008).

28. C. P. Shen *et al.* [Belle Collaboration], *Phys. Rev.* D **80**, 031101 (2009).

29. K.-F. Chen *et al.* (The Belle collaboration), arXiv:0808.2445 [hep-ex]; to appear in the Phys. Rev. D(RC).

S and D-wave resonances in chiral quark models: coupled channel approach

B. Golli

Faculty of Education, University of Ljubljana, 1000 Ljubljana, Slovenia and Jožef Stefan Institute, 1000 Ljubljana, Slovenia

Abstract. We apply a coupled channel formalism incorporating quasi-bound quark-model states to calculate the S11 and D13 scattering amplitudes. The meson-baryon verteces for πN, ηN, πΔ, ρN and KΛ channels are determined in the Cloudy Bag Model. Using the same values for the model parameters as in the case of the P11 and P33 amplitudes the elastic as well as most of the inelastic amplitudes are reasonably well reproduced.

1 Introduction

This work is a continuation of a joint project on the description of baryon resonances performed by the Coimbra group (Manuel Fiolhais, Luis Alvarez Ruso, Pedro Alberto) and the Ljubljana group (Simon Širca and B. G.)

We have developed a general method to incorporate excited baryons represented as quasi-bound quark-model states into a coupled channel formalism using the K-matrix approach [1]. In our method, the meson-baryon and the photon-baryon verteces are therefore determined by the underlying quark model rather than fitted to the experimental data as is the case in phenomenological approaches. The method can be applied to meson scattering as well as to electro and weak-production of mesons.

In the previous work we have investigated the P33 and P11 amplitude dominated by the low lying positive parity resonances $\Delta(1232)$, $\Delta(1600)$ and $N(1440)$ [1,2]. We have found a good agreement between the model prediction and experiment for the scattering as well as the electro-production amplitudes. We have shown that the pion and the σ-meson considerably contribute in particular to the scattering amplitudes in the energy region just above the two pion threshold and to the electro-excitation amplitudes in the region of low Q^2 transfer. In the present work we investigate the extension of the approach to low lying negative parity resonances. This implies the inclusion of new channels involving the s-wave and the d-wave pions, the η and the ρ mesons, and the K Λ channel.

In the next section we give a short review of the method and in the following sections we discuss in more detail scattering in the S11 and D13 partial waves.

2 A short overview of the K-matrix approach

We consider a class of chiral quark models in which mesons couple linearly to the quark core:

$$H_{\text{meson}} = \int dk \sum_{lmt} \left\{ \omega_k a^\dagger_{lmt}(k) a_{lmt}(k) + \left[V_{lmt}(k) a_{lmt}(k) + V^\dagger_{lmt}(k) a^\dagger_{lmt}(k) \right] \right\},$$

(1)

where $a^\dagger_{lmt}(k)$ is the creation operator for a meson with angular momentum l its third components m and isospin t (absent in the case of s-waves and isoscalar mesons). Here $V_{lmt}(k)$ is a general form of the meson source involving the quark operators and is model dependent. In the following section we give a few examples for $V_{lmt}(k)$ in the Cloudy Bag Model.

   We have shown [1] that in such models the elements of the K matrix in the basis with good total angular momentum J and isospin T take the form:

$$K^{JT}_{M'B'\,MB} = -\pi \mathcal{N}_{M'B'} \langle \Psi^{MB}_{JT} \| V_{M'}(k) \| \widetilde{\Psi}_{B'} \rangle, \qquad \mathcal{N}_{MB} = \sqrt{\frac{\omega_M E_B}{k_M W}}, \quad (2)$$

where ω_M and k_M are the energy and momentum of the incoming (outgoing) meson, E_B is the baryon energy and W is the invariant energy of the meson-baryon system. In addition, the channels are specified by the relative angular momentum of the meson-baryon system and parity. Here $|\Psi^{MB}\rangle$ is the principal value state and assumes the form:

$$|\Psi^{MB}_{JT}\rangle = \mathcal{N}_{MB} \left\{ [a^\dagger(k_M)|\widetilde{\Psi}_B\rangle]^{JT} + \sum_{\mathcal{R}} c^{MB}_{\mathcal{R}} |\Phi_{\mathcal{R}}\rangle \right.$$
$$\left. + \sum_{M'B'} \int \frac{dk\, \chi^{M'B'\,MB}(k, k_M)}{\omega_k + E_{B'}(k) - W} [a^\dagger(k)|\widetilde{\Psi}_{B'}\rangle]^{JT} \right\}. \quad (3)$$

The first term represents the free meson (π, η, ρ, K, ...) and the baryon (N, Δ, Λ,...) and defines the channel, the next term is the sum over *bare* tree-quark states $\Phi_{\mathcal{R}}$ involving different excitations of the quark core, the third term introduces meson clouds around different isobars, $E(k)$ is the energy of the recoiled baryon. In our approach we assume the commonly used picture in which the two pion decay proceeds either through an unstable meson (ρ-meson, σ-meson, ...) or through a baryon resonance ($\Delta(1232)$, $N^*(1440)$ ...). In such a case the state Ψ^{MB} depends on the invariant mass of the subsystem (either $\pi\pi$ or πN) and the sum over $M'B'$ in (3) implies also integration over the invariant mass. The state $\widetilde{\Psi}_B$ is the asymptotic state of the incoming (outgoing) baryon; in the case it corresponds to an unstable baryon it depends on the invariant mass of the πN subsystem, M_B, and is normalized as $\langle \widetilde{\Psi}_B(M'_B) | \widetilde{\Psi}_B(M_B) \rangle = \delta(M'_B - M_B)$, where M_B is the invariant mass M_B of the $N\pi$ subsystem. The meson amplitudes $\chi^{M'B'\,MB}(k, k_M)$ are proportional to the (half) off-shell matrix elements of the K-matrix

$$K_{M'B'\,MB}(k, k_M) = \pi \mathcal{N}_{M'B'} \mathcal{N}_{MB} \chi^{M'B'\,MB}(k, k_M) \quad (4)$$

and obey a Lippmann-Schwinger type of equation:

$$\chi^{M'B'MB}(k, k_M) = -\sum_{\mathcal{R}} c_{\mathcal{R}}^{MB} V_{B'\mathcal{R}}^{M'}(k) + \mathcal{K}^{M'B'MB}(k, k_M)$$

$$+ \sum_{M''B''} \int dk' \frac{\mathcal{K}^{M'B'M''B''}(k, k')\chi^{M''B''MB}(k', k_M)}{\omega_k' + E_{B''}(k') - W}, \quad (5)$$

where

$$\mathcal{K}^{M'B'MB}(k, k') = \sum_{B''} f_{BB'}^{B''} \frac{\widetilde{\mathcal{V}}_{B''B'}^{M'}(k') \widetilde{\mathcal{V}}_{B''B}^{M}(k)}{\omega_k + \omega_k' + E_{B''}(\bar{k}) - W}, \quad (6)$$

$$f_{AB}^{C} = \sqrt{(2J_A + 1)(2J_B + 1)(2T_A + 1)(2T_B + 1)} \, W(1J_A J_B 1; J_C, J) W(1T_A T_B 1; T_C, T).$$

The coefficients $c_{\mathcal{R}}^{MB}$ obey the equation

$$(W - M_{\mathcal{R}}^{(0)})c_{\mathcal{R}}^{MB} = V_{B\mathcal{R}}^{M}(k_M) + \sum_{M'B'} \int dk \frac{\chi^{M'B'MB}(k, k_M)V_{B'\mathcal{R}}^{M'}(k)}{\omega_k + E_{B'}(k) - W}. \quad (7)$$

Here $V_{B\mathcal{R}}^{M}(k)$ are the matrix elements of the quark-meson interaction between the baryon state B and the bare 3-quark state $\Phi_{\mathcal{R}}$, and $M_{\mathcal{R}}^{(0)}$ is the energy of the bare state. Solving the coupled system of equations (5) and (7) using a separable approximation [1] for the kernels (6), the resulting amplitudes take the form

$$\chi^{M'B'MB}(k, k_M) = -\sum_{\mathcal{R}} \widetilde{c}_{\mathcal{R}}^{MB} \widetilde{\mathcal{V}}_{B'\mathcal{R}}^{M'}(k) + \mathcal{D}^{M'B'MB}(k, k_M), \quad (8)$$

where the first term represents the contribution of various resonances while $\mathcal{D}^{M'B'MB}(k)$ originates in the non-resonant background processes. Here

$$\widetilde{c}_{\mathcal{R}}^{MB} = \frac{\widetilde{\mathcal{V}}_{B\mathcal{R}}^{M}}{Z_{\mathcal{R}}(W)(W - M_{\mathcal{R}})}, \quad (9)$$

$\widetilde{\mathcal{V}}_{B\mathcal{R}}^{M}$ is the dressed matrix element of the quark-meson interaction between the resonant state and the baryon state in the channel MB, and $Z_{\mathcal{R}}$ is the wave-function normalization. The physical resonant state $\mathcal{R}$ is a superposition of the dressed states built around the bare 3-quark states $\Phi_{\mathcal{R}'}$. The T matrix is finally obtained by solving the Heitler's equation

$$T = K + iTK. \quad (10)$$

In this work we concentrate on the negative parity partial waves S11 and D13; in both cases the amplitudes are dominated by two rather closely lying resonances, either the N(1535) S_{11} and N(1650) S_{11}, or the N(1520) D_{13} and N(1700) D_{13}. We have performed the calculation of the scattering amplitudes in the same model, the Cloudy Bag Model (CBM), with the same choice of model parameters as in the case of positive parity resonances. For the bag radius we use $R = 0.83$ fm and $f_{\pi} = 76$ MeV for the parameter determining the interaction strength, while the energies of the bare states are taken as free parameters.

3   The meson coupling to negative parity states in the CBM

We have used the bag model description for the resonances assuming that one of the three quarks is excited from the 1s state to the $1p_j$ state with the total angular momentum j either 1/2 or 3/2. The relevant quark bispinors in the $j\,m_j$ basis are

$$\psi_s(\mathbf{r}) = \frac{N_s}{\sqrt{4\pi}\,j_0(\omega_s)} \begin{pmatrix} -i\,j_0(\omega_s r/R) \\ \boldsymbol{\sigma}\cdot\hat{\mathbf{r}}\,j_1(\omega_s r/R) \end{pmatrix} \chi_{m_j}\,,$$

$$\psi_{p_{1/2}}(\mathbf{r}) = \frac{N_{p_{1/2}}}{\sqrt{4\pi}\,j_0(\omega_{p_{1/2}})} \begin{pmatrix} i\,j_1(\omega_{p_{1/2}} r/R)\boldsymbol{\sigma}\cdot\hat{\mathbf{r}} \\ j_0(\omega_{p_{1/2}} r/R) \end{pmatrix} \chi_{m_j}\,,$$

$$\psi_{p_{3/2}}(\mathbf{r}) = \frac{N_{p_{3/2}}}{\sqrt{6\pi}\,j_1(\omega_{p_{3/2}})} \begin{pmatrix} -i\,j_1(\omega_{p_{3/2}} r/R) \\ \boldsymbol{\sigma}\cdot\hat{\mathbf{r}}\,j_2(\omega_{p_{3/2}} r/R) \end{pmatrix} \sum_{m_s m} \chi_{m_s}\hat{r}_m C^{\frac{3}{2}m_j}_{\frac{1}{2}m_s 1m}\,.$$

Here χ_m is the spinor for spin $\frac{1}{2}$, R is the bag radius, $\omega_s = 2.043$, $\omega_{p_{1/2}} = 3.811$, $\omega_{p_{3/2}} = 3.204$, and

$$N_s^2 = \frac{\omega_s}{2R^2(\omega_s - 1)}\,,\quad N_{p_{1/2}}^2 = \frac{\omega_{p_{1/2}}}{2R^2(\omega_{p_{1/2}} + 1)}\,,\quad N_{p_{3/2}}^2 = \frac{9\omega_{p_{3/2}}}{4R^2(\omega_{p_{3/2}} - 2)}\,.$$

The wave function of the negative parity states in the j–j coupling scheme are taken from [5].

For the *quark pion coupling* we use the usual CBM form yielding

$$V^\pi_{l=0,t}(k) = \frac{1}{2f_\pi}\sqrt{\frac{\omega_{p_{1/2}}\omega_s}{(\omega_{p_{1/2}}+1)(\omega_s-1)}}\,\frac{1}{2\pi}\frac{k^2}{\sqrt{\omega_k}}\frac{j_0(kR)}{kR}\sum_{i=1}^{3}\tau_t(i)\,\mathcal{P}_{sp}(i)\,,$$

$$V^\pi_{1mt}(k) = \frac{1}{2f_\pi}\frac{\omega_s}{(\omega_s-1)}\frac{1}{2\pi}\frac{1}{\sqrt{3}}\frac{k^2}{\sqrt{\omega_k}}\frac{j_1(kR)}{kR}\sum_{i=1}^{3}\tau_t(i)$$
$$\times\left(\sigma_m(i) + r_{p_{1/2}}S^{[\frac{1}{2}]}_{1m}(i) + r_{p_{3/2}}S^{[\frac{3}{2}]}_{1m}(i)\right),$$

$$V^\pi_{2mt}(k) = \frac{1}{2f_\pi}\sqrt{\frac{\omega_{p_{3/2}}\omega_s}{(\omega_{p_{3/2}}-2)(\omega_s-1)}}\,\frac{\sqrt{2}}{2\pi}\frac{k^2}{\sqrt{\omega_k}}\frac{j_2(kR)}{kR}\sum_{i=1}^{3}\tau_t(i)\,\Sigma^{[\frac{1}{2}\frac{3}{2}]}_{2m}(i)\,.$$

Here

$$\mathcal{P}_{sp} = \sum_{m_j}|s m_j\rangle\langle p_{1/2} m_j|\,,\quad S^{[\frac{1}{2}]}_{1m} = \sqrt{3}\sum_{m_j m_j'}C^{\frac{1}{2}m_j}_{\frac{1}{2}m_j'1m}|p_{1/2}m_j\rangle\langle p_{1/2}m_j'|\,,$$

$$\Sigma^{[\frac{1}{2}\frac{3}{2}]}_{2m} = \sum_{m_s m_j}C^{\frac{1}{2}m_s}_{\frac{3}{2}m_j 2m}|s m_s\rangle\langle p_{3/2}m_j|\,,\quad S^{[\frac{3}{2}]}_{1m} = \frac{\sqrt{15}}{2}\sum_{m_j m_j'}C^{\frac{3}{2}m_j}_{\frac{3}{2}m_j'1m}|p_{3/2}m_j\rangle\langle p_{3/2}m_j'|\,,$$

and

$$r_{p_{1/2}} = \frac{\omega_{p_{1/2}}(\omega_s - 1)}{\omega_s(\omega_{p_{1/2}} + 1)}\,,\qquad r_{p_{3/2}} = \frac{2\omega_{p_{3/2}}(\omega_s - 1)}{5\omega_s(\omega_{p_{3/2}} - 2)}\,.$$

The ρ *meson coupling* to quarks is similar to the EM coupling. For the coupling of negative parity states to ρN, the dominant contribution is expected to

arise from the transverse ρ-mesons with the total $J = 1$ and the orbital angular momentum of the ρN system equal to either 0 or 2. In the spirit of the CBM model we assume that the ρ meson couples to the quarks only on the bag surface [6]. Assuming further a pure vector coupling $\gamma^{\mu}\rho_{\mu}$ we find (note that m in (1) and below refers to the total angular momentum rather than to the orbital one):

$$V^{\rho}_{l=0mt}(k) = \frac{1}{2f_{\rho}} \sqrt{\frac{\omega_s}{(\omega_s - 1)}} \frac{1}{2\pi} \frac{1}{\sqrt{\omega_k}} \frac{k^2}{kR} \frac{j_0(kR)}{kR} \sum_i \tau_t(i)$$
$$\times \left(\frac{\sqrt{8}}{3} \sqrt{\frac{\omega_{p_{1/2}}}{\omega_{p_{1/2}} + 1}} \Sigma^{[\frac{1}{2}]}_{1m} + 3 \sqrt{\frac{\omega_{p_{3/2}}}{\omega_{p_{3/2}} - 2}} \Sigma^{[\frac{1}{2}\frac{3}{2}]}_{1m}(i) \right) ,$$

$$V^{\rho}_{l=2mt}(k) = \frac{1}{2f_{\rho}} \sqrt{\frac{\omega_{p_{3/2}}\omega_s}{(\omega_{p_{3/2}} - 2)(\omega_s - 1)}} \frac{1}{2\pi} \frac{1}{3} \frac{k^2}{\sqrt{\omega_k}} \frac{j_2(kR)}{kR} \sum_{i=1}^{3} \tau_t(i)\Sigma^{[\frac{1}{2}\frac{3}{2}]}_{1m}(i) .$$

Here

$$\Sigma^{[\frac{1}{2}]}_{1m} = \sum_{m_s m_j} C^{\frac{1}{2} m_s}_{\frac{1}{2} m_j 1 m} |sm_s\rangle\langle p_{1/2} m_j| , \qquad \Sigma^{[\frac{1}{2}\frac{3}{2}]}_{1m} = \sum_{m_s m_j} C^{\frac{1}{2} m_s}_{\frac{3}{2} m_j 1 m} |sm_s\rangle\langle p_{3/2} m_j| ,$$

and f_{ρ} is the ρ-meson decay constant with the experimental value 208 MeV. For the coupling of the ρ meson to the nucleon we obtain a similar expression as for the coupling of the p-wave pions, with f_{π} replaced by f_{ρ}, yielding $g_{\pi NN}/g_{\rho NN} = f_{\rho}/f_{\pi}$ which is experimentally well fulfilled. The choice of the above form with $f_{\rho} \approx 200$ MeV is therefore not insensible.

For the *s-wave* η and K *mesons* we assume the SU(3) symmetry yielding

$$V^{\eta}(k) = \frac{1}{2f_{\pi}} \sqrt{\frac{\omega_{p_{1/2}}\omega_s}{(\omega_{p_{1/2}} + 1)(\omega_s - 1)}} \frac{1}{2\pi} \frac{k^2}{\sqrt{\omega_k}} \frac{j_0(kR)}{kR} \sum_{i=1}^{3} \lambda_8(i) \mathcal{P}_{sp}(i) ,$$

$$V^{K}_{t}(k) = \frac{1}{2f_{\pi}} \sqrt{\frac{\omega_{p_{1/2}}\omega_s}{(\omega_{p_{1/2}} + 1)(\omega_s - 1)}} \frac{1}{2\pi} \frac{k^2}{\sqrt{\omega_k}} \frac{j_0(kR)}{kR} \sum_{i=1}^{3} (V_t(i) + U_t(i)) \mathcal{P}_{sp}(i) ,$$

with $t = \pm\frac{1}{2}$, and $V_{\pm t} = (\lambda_4 \pm i\lambda_5)/\sqrt{2}$ and $U_{\pm t} = (\lambda_6 \pm i\lambda_7)/\sqrt{2}$.

The peculiar oscillating shape of the CBM form factor has little influence in the case of the p and d-wave pions but leads to the unphysical behaviour of the s-wave scattering amplitude since it crosses zero already at $W \sim 1950$ MeV. We have cured this problem by replacing $j_0(kR)$ by an exponential tail for $k > 1.6/R$ in such a way as not to alter the value of the self energy integral.

4   S11 resonances

For the S11 partial wave we have included the πN, πΔ, πN(1440), ρN and KΛ channels and the N(1535) and N(1650) resonances. We have used the quark-model wave-functions for the negative-parity states using the j–j coupling scheme [5]:

$$\Phi_{\mathcal{R}} = c^{\mathcal{R}}_A |(1s)^2(1p_{3/2})^1\rangle + c^{\mathcal{R}}_P |(1s)^2(1p_{1/2})^1\rangle_1 + c^{\mathcal{R}}_{P'} |(1s)^2(1p_{1/2})^1\rangle_2 ,$$

where the mixing coefficients $c_A^{\mathcal{R}}$, $c_P^{\mathcal{R}}$, and $c_{P'}^{\mathcal{R}}$ can be expressed in terms of the mixing angle ϑ_s between the spin-1/2 and spin-3/2 3-quark configurations. The mixing is a consequence of the gluon and the meson interaction; since the quark-gluon interaction is not included in the model, the mixing angle due to gluons is taken as a free parameter independent of W. In the energy region of the N(1535) and N(1650) resonances we obtain the best results using $\vartheta_s = -34°$ in agreement with the phenomenological analysis [7].

Resonance	Γ_{tot} [MeV]	Γ_i/Γ_{tot}					
		πN	ηN	$\pi\Delta$	$K\Lambda$	$\rho_1 N$	$\pi N(1440)$
N(1535)	165	0.29	0.69	0.01	-	0.01	0
PDG	125 – 175	0.35 – 0.55	0.53	0.01	-	0.02	0
N(1650)	188	0.59	0	0.19	0.13	0.04	0.04
N(1650)mod	156	0.72	0	0.08	0.10	0.05	0.04
PDG	150 – 180	0.60 – 0.95	0.02	0.02	0.03	0.01	0.03

Table 1. The total and the partial widths for the N(1535) and the N(1650) resonance at the K-matrix pole (1545 MeV and 1695 MeV, respectively) using the unmodified and the modified (*mod*) quark-model values for the quark-meson couplings. The PDG values are from [3].
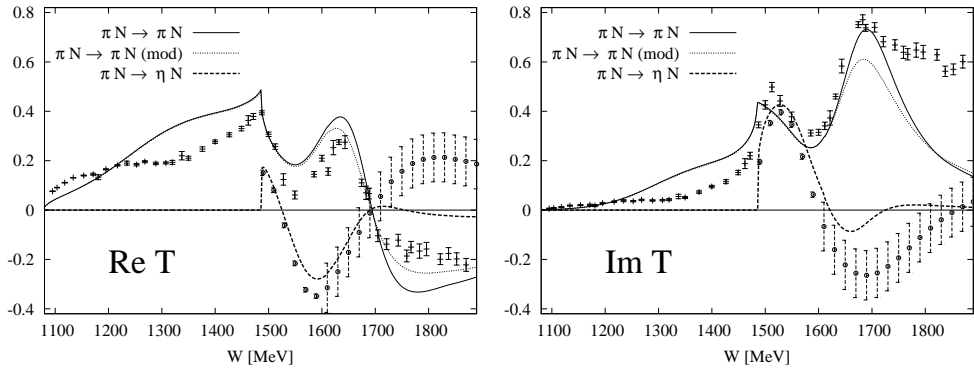
Fig. 1. The real and the imaginary part of the scattering amplitudes for the S11 wave. Dotted lines are for the elastic channel with unmodified quark-model verteces, full lines are those with the modified values, dashed lines correspond to the ηN channel. The data points for the elastic channel are from the SAID $\pi N \to \pi N$ partial-wave analysis [4], those for the inelastic one are taken from [9].

In the vicinity of the lower resonance, just above the η meson threshold, the elastic and inelastic amplitudes are dominated by the *s*-wave ηN channel. In the energy region of the upper resonance, additional channels open or become more important. We have considered the following additional channels: the $\pi\Delta(1232)$ channel with $l = 2$, the $K\Lambda(1116)$ channel with $l = 0$, two channels involving the ρ meson with $l = 0$ ($\rho_1 N$) and $l = 2$ ($\rho_3 N$), and the $\pi N^*(1440)$ channel with $l = 0$.
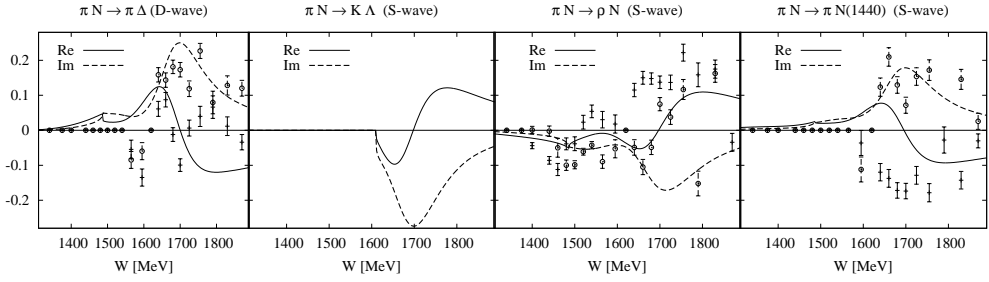
Fig. 2. The real and the imaginary part of the inelastic amplitudes for S11 partial wave. The experimental points are from [8].

Using the quark-model values for the quark-meson coupling as introduced in the previous section we obtain a good agreement between the model prediction and the experimental analysis for the lower resonance; for the upper resonance the agreement is worse. Though the extraction of the experimental data is less reliable and considerably differs between different authors, it clearly indicates that the strengths of the $\pi\Delta$ (d-wave) vertex is overestimated in our model; the same is probably true also for the $K\Lambda$ (s-wave) channel (Table 1). Multiplying the strength of the $\pi\Delta$ and the $K\Lambda$ vertex by 0.6 and 0.8, respectively, yields a better agreement in particular for the imaginary part of the T matrix (Figs. 1 and 2).

5   D13 resonances

In the D13 partial wave the model yields a consistent picture for the upper resonance but fails to reproduce the behaviour of the scattering amplitudes for the lower resonance. In the latter case, the quark-model values for the d-wave πN vertex and the s-wave $\pi\Delta$ vertex are of comparable strength and relatively weak. Dressing the verteces and introducing the mixing of the two (bare) resonances considerably enhances the verteces. However, the enhancement is stronger in the case of the $\pi\Delta$ channel and, as a consequence, the resonance disappears in the elastic channel. A reasonable agreement is obtained if the quark-model strength of the $\pi\Delta$ is multiplied by 0.3 (Table 2 and Fig. 3).

Resonance	Γ_{tot} [MeV]	Γ_i/Γ_{tot}			
		πN	$\pi\Delta$ (s-wave)	$\pi\Delta$ (d-wave)	ρN (s-wave)
N(1520)	64	0.56	0.40	0.00	0.03
PDG	100 – 125	0.55 – 0.65	0.15	0.11	0.09
N(1700)	55	0.02	0.10	0.70	0.18
PDG	50 – 150	0.05 – 0.15	0.11	0.79	0.07

Table 2. The total and the partial widths for the N(1520) and the N(1700) resonance at the K-matrix pole (1515 MeV and 1700 MeV, respectively) using the unmodified quark-model values for the quark-meson couplings except for the s-wave $\pi\Delta$ coupling which is taken with only 30 % of the model strength. The PDG values are from [3].
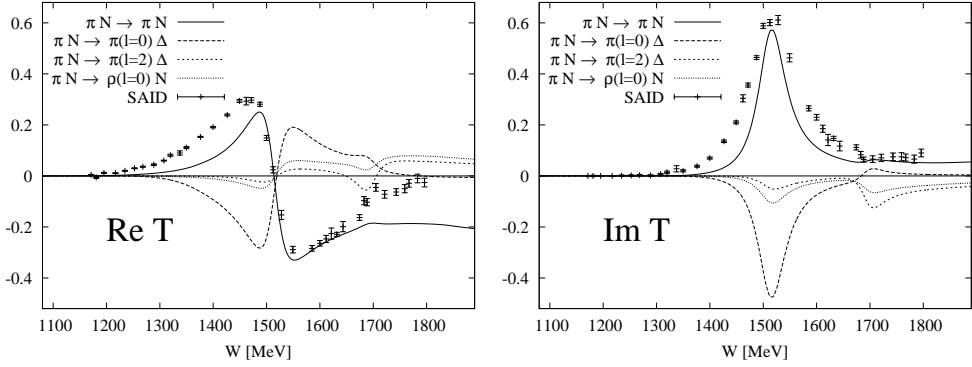
Fig. 3. The real and the imaginary part of the elastic and the dominant inelastic scattering amplitudes for the D13 wave. The data points for the elastic channel are from [4]

For the upper resonance (N(1700)), the model predicts the dominance of the d-wave $\pi\Delta$ channel in agreement with the phenomenological analysis.

6 Concluding remarks

The model reasonably well reproduces the behaviour of the amplitude in the S11 partial wave. The bare quark values for the meson verteces are generally too weak but are considerably enhanced through the meson cloud effects and the mixing of the bare quark resonances. At higher energies around and above N(1650), the model amplitudes are too small; here the contribution of higher resonances not included in our model becomes important as suggested by the phenomenological analysis [9]. The background contribution is in our model generated by the u-channel processes. We have not considered the Weinberg-Tomazawa term which would enhances the behaviour of the amplitudes near the pion threshold.

The situation is less favourable for the D13 partial wave. The model fails to reproduce a rather intriguing behaviour of the s and d-wave $\pi\Delta$ amplitudes in the energy region of the N(1520) resonance. Here the phenomenological analysis suggests that they are comparable in strength which is difficult to explain in a model calculation where at relatively low pion momenta the $l = 0$-wave coupling is strongly favoured over the $l = 2$ one.

References

1. B. Golli and S. Širca, Eur. Phys. J. A **38**, (2008) 271.
2. B. Golli, S. Širca, and M. Fiolhais, Eur. Phys. J. A **42**, 185 (2009)
3. C. Amsler et al. (Particle Data Group), Phys. Lett. B **667**, 1 (2008).
4. R. A. Arndt, W. J. Briscoe, I. I. Strakovsky, R. L. Workman, Phys. Rev. C **74** (2006) 045205.
5. F. Myhrer and J. Wroldsen, Z. Phys. C 25, 281 (1984).
6. R. F. Alvarez-Estrada and A. W. Thomas, J. Phys. G: Nucl. Phys. **9**, 161 (1983).
7. A. J. Hey et al. Nucl. Phys. **A362**, 317 (1981).
8. D. M. Manley, E. M. Saleski, Phys. Rev. D **45** (1992) 4002 and private communication.
9. A. Kiswandhi and S. Capstick, Phys. Rev. C **69** (2004) 025205

Are superheavy quark clusters viable candidates for the dark matter?[*]

Norma Mankoč Borštnik[a] and Mitja Rosina[a,b]

[a]Faculty of Mathematics and Physics, University of Ljubljana,
Jadranska 19, P.O. Box 2964, 1001 Ljubljana, Slovenia
[b]J. Stefan Institute, 1000 Ljubljana, Slovenia

Abstract. The ordinary matter, as we know it, is made mostly of the first family quarks and leptons, while the theory together with experiments has proven so far that there are (at least) three families. The explanation of the origin of families is one of the most promising ways to understand the assumptions of the *Standard Model*. The *Spin-Charge-Family* theory [1,2] does propose the mechanism for the appearance of families which bellow the energy of unification scale of the three known charges form two decoupled groups of four families. The lightest of the upper four families, is predicted [3] to have stable members and to be the candidate to constitute the dark matter. The clustering of quarks from the fifth family into baryons in the evolution of the universe is discussed.

In this contribution we study how much the electroweak interaction influences the properties of baryons of the fifth family.

1 Introduction

The *Standard Model* has no explanation for either the existence of families and their properties or for the appearance of the scalar field, which in the *Standard Model* determines the properties of the electroweak gauge fields. A theory which would explain the origin of families and the mechanism causing the observed properties of the quarks, leptons and gauge fields is needed. The *Spin-Charge-Family* theory [1,2] is very promising for this purpose.

The *Spin-Charge-Family* theory points out that there are two kinds of the γ^a operators, the Dirac ones and the ones observed by one of the authors (NMB) [1,2] and called $\tilde{\gamma}^a$, and it proposes that both should appear in an acceptable theory (or it should be proven that one of these two kinds has no application at the observable energy regime). Since the operators $\tilde{\gamma}^a$ and γ^b anticommute, while the corresponding generators of rotations in d-dimensional space commute ($[S^{ab}, \tilde{S}^{cd}] = 0$), both kinds form equivalent representations with respect to each other. If Dirac operators are used to describe spin and charges [1,2], then the other kind must be used to describe families, which obviously form an equivalent representations with respect to spin and charges.

---

[*] Delivered in two talks, by M. Rosina and by N. Mankoč Borštnik

The properties of the fifth family quarks and leptons, and corresponding baryons, have been evaluated in ref. [3], concluding that the fifth family neutron is very probably the most stable nucleon. In this paper, the formation of neutrons and anti-neutrons from the fifth family quarks and anti-quarks in the cooling plasma has been followed in the expanding universe. Their behaviour in the colour phase transition up to the present dark matter, as well as the scattering of the fifth family neutrons among themselves and on the ordinary matter has been evaluated.

The purpose of this contribution is to show an example how one can use standard hadronic calculations in order to examine possible higher families and candidates for dark matter. It is also a demonstration of how much the properties of clusters depend on the masses of the objects forming the clusters.

We shall use the promising unified *Spin-Charge-Family* theory [1] which has been developed by one of the authors (NMB) in the recent decade. The reader can find details about the theory in the references [1], while Sect. 2 is a short overview, needed for the purpose of this contribution.

Let us remind the reader about possible prejudices one might have at the first moment against accepting the particles which interact with the colour interaction, as candidates for dark matter. We discuss these prejudices in order to demonstrate that superheavy quark clusters are legitimate candidates worth exploring, provided they are stable.

1. *Superheavy quarks are too short-lived.* This is true for the fourth family predicted by the *Spin-Charge-Family* theory, or any other proposal if the mixing matrix elements to the lower mass families are not negligible. However, the *Spin-Charge-Family* theory [1,4] predicts eight families, with the upper four families (almost) decoupled from the lower four families. This makes one of the quarks of the fifth family, actually one of possible baryonic clusters, practically stable.

2. *Either the charged baryon $u_5u_5u_5$ or the charged baryon $d_5d_5d_5$ would be the lightest, depending on whether u_5 or d_5 is lighter.* Charged clusters cannot, of course, constitute dark matter. Forming the atoms with the first family electrons they would have far too large scattering amplitude to be consistent with the properties of dark matter. However, if one takes into account also the electro-weak interaction between quarks, then the neutral baryon $n_5 = u_5d_5d_5$ can very probably be the lightest, provided the u-d mass difference is not too large. The ref. [3] estimates the allowed differences, here we present the ratio between the weak and electromagnetic contributions for different fifth family baryons in more detail (Sect. 3).

3. *Strongly interacting particles have far too large cross section to be "dark".* The scattering cross section of any neutral cluster due to any interaction depends strongly also on the mass of the constituents. The fifth family baryons, interacting with the fifth family "nuclear force", have very small cross section if the masses are large enough. For $m_5 = 100$ TeV, for example, the size of the cluster is of the order 10^{-4} fm or less and the geometrical cross section as small as 10^{-10} fm^2.

4. *Did the fifth family quarks and/or their clusters form and survive after the big bang and during galaxy formation?* We kindly invite the reader to learn about the history of the fifth family clusters in the expanding universe from the paper [3]. In a hot plasma, when the temperature T is much higher than the mass of the fifth family members, $T \gg m_5$, the fifth family members behave as massless and are created out of plasma and annihilate back in the thermodynamically equilibrium in the same way as other fermions and fields, which are massless or have low enough masses. When due to the expansion of the universe the temperature lowers bellow the mass of the family members, $T < m_5$, they can be annihilated while the creation starts to be less and less probable. When the temperature falls bellow the binding energy of the clusters of the fifth family quarks they start to form clusters. Once the cluster is formed, it starts to interact with a very small "fifth family nuclear force" and survives also the colour phase transition up to now. In [3,5] the scattering of the fifth family neutrons in the experimental equipment of DAMA [6] and CDMS [7] is evaluated and discussed.

2   The Spin-Charge-Family theory

In this section a short introduction to the *Spin-Charge-Family* theory [1] is presented. Only the essential things are reviewed hoping to make the reader curious to start thinking about the differences in the hadronic properties of the very heavy fifth family hadrons as compared to the lowest three families.

The *Spin-Charge-Family* theory proposes in $d = (1 + (d − 1))$ dimensions a very simple starting action for spinors which carry both kinds of the spin generators (γ^a and $\tilde{\gamma}^a$ operators) and for the corresponding gauge fields. Multidimensional spinors unify the spin and electro-weak-colour charge degrees of freedom. A spinor couples in $d = 1 + 13$ to vielbeins and (through two kinds of the spin generators) to spin connection fields. Appropriate breaking of the starting symmetry leads to the left-handed quarks and leptons in $d = (1 + 3)$ dimensions, which carry the weak charge while the right handed ones carry no weak charge. The *Spin-Charge-Family* theory is offering the answers to the questions about the origin of families of quarks and leptons, about the explicit values of their masses and mixing matrices, predicting the fourth family to be possibly seen at the LHC or at somewhat higher energies [4], as well as about the masses of the scalar and the weak gauge fields, about the dark matter candidates [3], and about breaking the discrete symmetries.

The simple action in $d = (1+13)$-dimensional space of the *Spin-Charge-Family* theory [1]

$$S = \int d^d x \, E \, \mathcal{L}_f + \int d^d x \, E \, \mathcal{L}_g \tag{1}$$

contains the Lagrange density for two kinds of gauge fields linear in the curvature

$$\mathcal{L}_g = E \, (\alpha \, R + \tilde{\alpha} \tilde{R}),$$
$$R = f^{\alpha[a} f^{\beta b]} \, (\omega_{ab\alpha,\beta} − \omega_{ca\alpha} \omega^c{}_{b\beta}), \tilde{R} = f^{\alpha[a} f^{\beta b]} \, (\tilde{\omega}_{ab\alpha,\beta} − \tilde{\omega}_{ca\alpha} \tilde{\omega}^c{}_{b\beta}), \tag{2}$$

and for a spinor, which carries in $d = (1 + 13)$ dimensions two kinds of the spin represented by the two kinds of the Clifford algebra objects [1]

$$S^{ab} = \frac{i}{4}(\gamma^a\gamma^b - \gamma^b\gamma^a), \quad \tilde{S}^{ab} = \frac{i}{4}(\tilde{\gamma}^a\tilde{\gamma}^b - \tilde{\gamma}^b\tilde{\gamma}^a),$$

$$\{\gamma^a, \gamma^b\}_+ = 2\eta^{ab} = \{\tilde{\gamma}^a, \tilde{\gamma}^b\}_+, \quad \{\gamma^a, \tilde{\gamma}^b\}_+ = 0, \quad \{S^{ab}, \tilde{S}^{cd}\}_- = 0. \quad (3)$$

The interaction is only between the vielbeins and the two kinds of spin connection fields

$$\mathcal{L}_f = \frac{1}{2}(E\bar{\psi}\gamma^a p_{0a}\psi) + \text{h.c.}$$

$$p_{0a} = f^\alpha{}_a p_{0\alpha}, \quad p_{0\alpha} = p_\alpha - \frac{1}{2}S^{ab}\omega_{ab\alpha} - \frac{1}{2}\tilde{S}^{ab}\tilde{\omega}_{ab\alpha}. \quad (4)$$

This action offers a real possibility to explain the assumptions of the *standard model* [1].

The *Spin-Charge-Family* theory predicts an even number of families, among which is the fourth family, which might be seen at the LHC [1,4] or at somewhat higher energies and the fifth family with neutrinos and baryons with masses of several hundred TeV forming dark matter [4].

The action in Eq. (1) starts with the massless spinor which through two kinds of spins interacts with the two kinds of the spin connection fields. The Dirac kind of the Clifford algebra objects (γ^a) determines, when the group $SO(1, 13)$ is analysed with respect to the *Standard Model* groups in $d = (1+3)$ dimensions, the spin and all charges, manifesting the left handed quarks and leptons carrying the weak charge and the right handed weak-neutral quarks and leptons. Accordingly, the Lagrange density $\mathcal{L}_f$ manifests after the appropriate breaking of symmetries all the properties of one family of fermions as assumed by the *Standard Model*, with the three kinds of charges coupling fermions to the corresponding three gauge fields (first term of Eq.(5).

The second kind ($\tilde{\gamma}^a$) of the Clifford algebra objects (defining the equivalent representations with respect to the Dirac one) determines families. Accordingly, the spinor Lagrange density, after the spontaneous breaking of the starting symmetry ($SO(1, 13)$ into $SO(1, 7) \times U(1) \times SU(3)$ and further into $SO(1, 3) \times SU(2) \times SU(2) \times U(1) \times SU(3)$) generates the *Standard Model-like* Lagrange density for massless spinors of (four + four) families (defined by $2^{8/2-1} = 8$ spinor states for each member of one family). After the first symmetry breaking the upper four families decouple from the lower four families (in the Yukawa couplings). In the final symmetry breaking (leading to $SO(1, 3) \times U(1) \times SU(3)$) the upper four families obtain masses through the mass matrix (the second term of Eq.(5). The third term ("the rest") is unobservable at low energies

$$\mathcal{L}_f = \bar{\psi}\gamma^m(p_m - \sum_{A,i} g^A\tau^{Ai}A_m^{Ai})\psi + \sum_{s=7,8}\bar{\psi}\gamma^s p_{0s}\,\psi + \text{the rest}. \quad (5)$$

---

[1] This is the only theory in the literature to our knowledge, which does not explain the appearance of families by just postulating their numbers in one or another way, through the choice of a group, for example, but by offering the mechanism for generating families.

Here τ^{Ai} $(= \sum_{a,b} c^{Ai}{}_{ab} S^{ab})$ determine the hypercharge $(A = 1)$, the weak $(A = 2)$ and the colour $(A = 3)$ charge: $\{\tau^{Ai}, \tau^{Bj}\}_- = i\delta^{AB}f^{Aijk}\tau^{Ak}$, $f^{1ijk} = 0$, $f^{2ijk} = \varepsilon^{ijk}$, where f^{3ijk} is the $SU(3)$ structure tensor.

The evaluation of masses and mixing matrices of the lower four families [4] suggests that the fifth family masses should be above a few TeV, while evaluations of the breaks of symmetries from the starting one (Eq. 1) suggests that these masses should be far bellow 10^{10} TeV.

We have not yet evaluated a possible fermion number nonconservation in the dynamical history of the universe either for the first (the lower four) or for the fifth (the upper four) families. However, the evaluation of the history of the fifth family baryons up to today's dark matter does not depend much on the matter anti-matter asymmetry, as long as the masses are higher than a few 10 TeV. So our prediction that if DAMA [6] really measures the family neutrons, also other direct experiments like CDMS [7] should in a few years observe the dark matter clusters, does not depend on the baryon number nonconservation [3].

Following the history of the fifth family members in the expanding universe up to today and estimating also the scattering properties of this fifth family on the ordinary matter, the evaluated masses of the fifth family quarks, under the assumption that the lowest mass fifth family baryon is the fifth family neutron, are in the interval

$$200\,\text{TeV} < m_5 < 10^5\,\text{TeV}. \tag{6}$$

The fifth family neutrino mass $m_{\nu 5}$ is estimated to be in the interval between a few TeV and a few hundred TeV.

3   The superheavy neutron from the fifth family as a candidate for the dark matter

We want to put limits on u-d quark mass differences so that the neutral baryon n_5 appears as the lightest. First we calculate the dominant properties of a three-quark cluster [3], its binding energy and size. For this purpose we assume equal superheavy masses and we realize that in this regime the colour interaction is coulombic (one gluon exchange dominates at these energies). For three nonrelativistic particles with attractive coulombic interaction we solve the Hamiltonian

$$H = 3m + \sum_i \frac{\mathbf{p}_i^2}{2m} - \frac{(\sum_i \mathbf{p}_i)^2}{6m} - \sum_{i<j} \frac{2}{3}\frac{\alpha_s}{r_{ij}}. \tag{7}$$

The potential energy of the solution can be conveniently parametrized as

$$V_s = -\frac{2}{3}\alpha_s\epsilon, \quad \epsilon = \langle \sum_{i<j} \frac{1}{r_{ij}} \rangle = 3\eta\alpha_s m_5, \tag{8}$$

where m_5 is the average mass of quarks in the fifth family. The binding energy is then (according to the virial theorem)

$$E = \frac{1}{2} V_s = -E_{kin} = -\alpha_s^2\eta m_5. \tag{9}$$

The parameter η for a variational solution using Jacobi coordinates and exponential profiles was calculated in [3]: $\eta = 0.66$.

The splitting of baryons in the fifth family is caused by the u-d mass difference as well as by the potential energy of the electro-weak interaction. In the studied energy range, the electro-weak interaction has a coulombic form, determined by the exchange of one photon or one massless weak boson, and can be treated as a perturbation. Even if we are far above the electroweak phase transition, it is convenient to work in the basis using Weinberg mixing of γ and Z since this basis is more familiar to low energy hadron physicists.

We split the electro-weak interaction in five contributions, electric, Z-exchange Fermi (=vector), Z-exchange Gamow-Teller (=axial), W-exchange Fermi (=vector), W-exchange Gamow-Teller (=axial)

$$M = \sum_i m_i + E + \left(V_{EM} + V_Z^F + V_Z^{GT} + V_W^F + V_W^{GT} \right). \tag{10}$$

Separate terms are as follows

$$V_{EM} = \langle \sum_{i<j} Q_i Q_j \rangle \, \alpha_{EM} \epsilon,$$

$$V_Z^F = \langle \sum_{i<j} (\frac{t_i^0}{2} - \sin^2 \vartheta_W Q_i)(\frac{t_j^0}{2} - \sin^2 \vartheta_W Q_j) \rangle \, \alpha_Z \epsilon, \quad V_Z^{GT} = \langle \sum_{i<j} \frac{t_i^0 t_j^0}{4} \sigma_i \sigma_j \rangle \rangle \, \alpha_Z \epsilon,$$

$$V_W^F = \langle \sum_{i<j} \frac{t_i^- t_j^+ + t_i^+ t_j^-}{8} \rangle \, \alpha_W \epsilon, \quad V_W^{GT} = \langle \sum_{i<j} \frac{t_i^- t_j^+ + t_i^+ t_j^-}{8} \sigma_i \sigma_j \rangle \, \alpha_W \epsilon. \tag{11}$$

Here $t = \frac{1}{2}\tau$ are isospin operators, $t^+ = (t_x + t_y)$, and σ are Pauli spin matrices. Separate terms are evaluated in Table 1. Note that the vector contributions (also the electromagnetic) are the same for N and Δ baryons while the axial contributions differ dramatically. The lowest two lines give the sum of these contributions for the choice of the coupling constants given below. The unnecessary decimal places are there if you like to check the reproducibility of the results.

In the numerical example we choose the average quark mass $m_5 = 100$ TeV and the corresponding average momentum of each quark $p = \sqrt{2 m_5 E_{kin}/3} = 5.1$ TeV (see below). At this momentum scale, we read the running coupling constants from Particle Data Group diagram [8] as $\alpha_s = \alpha_3 = 1/13$, $\alpha_W = \alpha_2 = 1/32$ and $\alpha_1 = 1/56$. The latter gives $\sin^2 \vartheta_W = (1 + \frac{5}{3} \frac{\alpha_W}{\alpha_1})^{-1} = 0.255 \approx 1/4$, $\alpha_{EM} = \alpha_W \sin^2 \vartheta_W = 1/128$ and $\alpha_Z = \alpha_W / \cos^2 \vartheta_W = 1/24$.

In this example, the binding energy $E = -0.39$ TeV and the average reciprocal distance $\langle 1/r_{ij} \rangle = \epsilon/3 = \eta \alpha_s m_5 = 5.1$ TeV $= 2.6 \cdot 10^4$ fm^{-1}.

Finally, we come to our goal to make limits on u-d mass difference such that the neutral barion remains the lightest.

1. $m_{u5} - m_{d5} < (0.0273 - 0.0017)\epsilon = 0.0256\,\epsilon$ prevents udd→ddd.
2. $m_{u5} - m_{d5} > (-0.0273 + 0.0256)\epsilon = -0.0017\,\epsilon$ prevents udd→uuu.

For our value of $\epsilon = 15.24$ TeV this reads

$$-0.026\,\text{TeV} < m_{u5} - m_{d5} < 0.39\,\text{TeV}.$$

Table 1. Electro-weak contributions to superheavy baryon masses

	uuu	uud	udd	ddd
$V_{EM}/\epsilon\alpha_{EM}$	+4/3	0	−1/3	+1/3
$V_Z^F/\epsilon\alpha_Z$	+1/48	−1/48	0	+4/48
$V_Z^{GT}(N)/\epsilon\alpha_Z$		−15/48	−15/48	
$V_Z^{GT}(\Delta)/\epsilon\alpha_Z$	−9/48	+3/48	+3/48	−9/48
$V_W^F/\epsilon\alpha_W$	0	+1/4	+1/4	0
$V_W^{GT}(N)/\epsilon\alpha_W$		−30/48	−30/48	
$V_W^{GT}(\Delta)/\epsilon\alpha_W$	0	−1/4	−1/4	0
$V_{EW}(N)/\epsilon$		−0.0256	−0.0273	
$V_{EW}(\Delta)/\epsilon$	+0.0035	+0.0017	−0.0000	−0.0017

This limits are narrow compared to the mass scale $m_5 = 100$ TeV, but they are not so narrow if the mass generating mechanism is of order of 100 GeV.

4   Conclusion

In this contribution we put light on the hadronic properties of the very heavy stable fifth family as predicted by the *Spin-Charge-Family* theory, proposed by one of the authors [1]. The evaluations presented in Sect. 3 were already partially done in [3]. However, we try to convince the hadron physicists that if the *Spin-Charge-Family* theory is the right way to explain the assumptions of the *Standard Model* then the hadron physicists will have a pleasant time to study properties of the clusters forming dark matter with their knowledge form the lower three families.

References

1. N. S. Mankoč Borštnik, Phys. Lett. B **292** (1992) 25; J. Math. Phys. **34** (1993) 3731; Int. J. Theor. Phys. **40** (2001) 315; Modern Phys. Lett. **A 10** (1995) 587.
2. A. Borštnik, N. S. Mankoč Borštnik, in *Proceedings to the Euroconference on Symmetries Beyond the Standard Model*, Portorož, July 12-17, 2003, hep-ph/0401043, hep-ph/0401055, hep-ph/0301029; Phys. Rev. D **74** (2006) 073013, hep-ph/0512062.
3. G. Bregar and N. S. Mankoč Borštnik, Phys. Rev. D **80** (2009) 083534.
4. G. Bregar, M. Breskvar, D. Lukman, N.S. Mankoč Borštnik, New J. of Phys. **10** (2008) 093002.
5. N. S. Mankoč Borštnik, in "What comes beyond the standard models", Bled Workshops in Physics **11** (2010) No.2
6. R. Bernabei et al., Int. J. Mod. Phys. D **13** (2004) 2127-2160; Eur. Phys. J. C **56** (2008) 333-355.
7. Z. Ahmed et al., Phys. Rev. Lett. **102** (2009) 011301.
8. K. Nakamura et al. (Particle Data Group), J. Phys. G 37 (2010) 075021.

Lattice searches for tetraquarks: X,Y,Z states and light scalars

Saša Prelovšek

Faculty of Mathematics and Physics, University of Ljubljana
and J. Stefan Institute, 1000 Ljubljana, Slovenia

Abstract. Searches for tetraquarks and mesonic molecules in lattice QCD are briefly reviewed. In the light quark sector the most serious candidates are the lightest scalar resonances σ, κ, a_0 and f_0. In the hidden-charm sector I discuss lattice simulations of X(3872), Y(4140) and $Z^+(4430)$. The most serious challenge in all these lattice studies is the presence of scattering states in addition to possible tetraquark/molecular states. The topics covered in this talk are presented in [1], so only a brief outline is given below.

1 Introduction

Some of the observed resonances, i.e. light scalars and some hidden-charm resonances, are strong candidates for tetraquarks $[qq][\bar{q}\bar{q}]$ or mesonic molecules $(\bar{q}q)(\bar{q}q)$. Current lattice methods do not distinguish between both types, so a common name "tetraquarks" will be often used to denote both types of $\bar{q}\bar{q}qq$ Fock components below.

In order to extract the information about tetraquark states, lattice QCD simulations evaluate correlation functions on $L^3 \times T$ lattice with tetraquark interpolators $\mathcal{O} \sim \bar{q}\bar{q}qq$ at the source and the sink $C_{ij}(t) = \langle 0|\mathcal{O}_i(t)\mathcal{O}_j^\dagger(0)|0\rangle_{\mathbf{p}=0} = \sum_n Z_i^n Z_j^{n*} \, e^{-E_n \, t}$. If the correlation matrix is calculated for a number of interpolators $\mathcal{O}_{i=1,..,N}$ with given quantum numbers, the energies of the few lowest physical states E_n and the corresponding couplings $Z_i^n \equiv \langle 0|\mathcal{O}_i|n\rangle$ can be extracted from the eigenvalues $\lambda^n(t) = e^{-E_n(t-t_0)}$ and eigenvectors $\mathbf{u}^n(t)$ of the generalized eigenvalue problem $C(t)\mathbf{u}^n(t) = \lambda^n(t,t_0)C(t_0)\mathbf{u}^n(t)$.

In addition to possible tetraquarks, also the two-meson scattering states $M_1 M_2$ unavoidably contribute to the correlation function and this presents the main obstacle in extracting the information about tetraquarks. The scattering states $M_1(k)M_2(-k)$ at total momentum $\mathbf{p} = \mathbf{0}$ have discrete energy levels $E_{M_1 M_2} \simeq E_{M_1}(k) + E_{M_2}(-k)$ with $E_M(k) = \sqrt{m_M^2 + \mathbf{k}^2}$ and $\mathbf{k} = \frac{2\pi}{L}\mathbf{n}$ in the non-interacting approximation when periodic boundary conditions in space are employed.

The resonance manifests itself on the lattice as a state in addition to the discrete tower of scattering states and it is often above the lowest scattering state (at $E \simeq M_1 + M_2$ for S-wave decay). So the extraction of a few states in addition to

the ground state may be crucial. Once the physical states are obtained, one needs to determine whether a certain state corresponds to a one-particle (tetraquark) or a two-particle (scattering) state. The available methods to distinguish both are reviewed in [1] and all exploit the approximations employed on the lattice: the finite spatial or the finite temporal extent of the lattice.

2   Some results

The question whether the light scalar mesons σ and κ have a sizable tetraquark component has been addressed in simulation [2]. The energy spectrum has been determined using a number of $\bar{q}\bar{q}qq$ interpolators in a dynamical as well as quenched simulation. In $I = 0$ channel, an additional light state has been found on top of the expected scattering states $\pi(0)\pi(0)$ and $\pi(\frac{2\pi}{L})\pi(-\frac{2\pi}{L})$. This additional state may be related to the observed σ with the sizable tetraquark component. Similarly, an additional light state on top of $K(0)\pi(0)$ and $K(\frac{2\pi}{L})\pi(-\frac{2\pi}{L})$ scattering states has been found in the $I = 1/2$ channel; this state may be related to the observed κ with the sizable tetraquark component. Other lattice simulations aimed at the similar question are reviewed in [1].

The simulations [3–5] aimed at determining the nature of hidden-charm resonances X(3872), Y(4140) and Z^+(4430), extract only the ground state in the given J^{PC} channel using an exponential fit $C(t) \propto e^{-E_1 t}$. Then they try to determine whether the extracted state is a scattering state or a tetraquark/molecular state using the available criteria.

The $\bar{c}\bar{u}cu$ and $\bar{c}\bar{s}cs$ ground states with $J^{PC} = 1^{++}$ in the quenched simulation [3] seem to behave as one-particle states. They have been found at 3890 ± 30 MeV ($\bar{c}\bar{u}cu$) and at 4100 ± 50 MeV ($\bar{c}\bar{s}cs$), which is indeed close to the observed resonances X(3872) and Y(4140). Note however, that the lowest scattering states DD^* and $J/\psi\phi$ are extremely close and that they should be found in addition to the one-particle states before the indication for the tetraquarks/molecules can be fully trusted.

The dynamical simulation [4] studies the DD^* scattering, which is related to the resonance X(3872). The attractive interaction between D and D^* has been found, with a possible indication for a bound-state formation at small m_π.

The quenched simulation [5] searched for Z^+(4430) in $J^P = 0^-$, 1^-, 2^- channels using the molecular $D_1 D^*$ interpolators. The most reliable results are obtained for $J^P = 0^-$, where the attractive interaction between D_1 and D^* has been observed.

The only dynamical simulation that determined several energy levels using $\bar{c}\bar{q}cq$ and $\bar{c}c$ interpolators in the same variational basis was a pioneering simulation [6]. So far it found some candidates for $D\bar{D}$ scattering states and for charmonia, but no candidates for tetraquarks yet.

3   Conclusions

Proving a sizable tetraquark or molecular Fock component in a hadronic resonance using lattice QCD simulation is not an easy task. A resonance appears as a

state in addition to the discrete tower of scattering states. So the extraction of few states in addition to the ground state is expected to be crucial. Given the resulting physical eigenstates, one needs to determine whether a certain state corresponds to a one-particle (tetraquark/molecular) or a two-particle (scattering) state.

There are some indications for an additional state in $I = 0, 1/2$ light scalar channels, which might correspond to observed σ and κ with strong tetraquark components [2]. There have been surprisingly few lattice simulations of very interesting experimentally observed exotic XYZ resonances, and much more work on the lattice is needed to pin down their structure.

References

1. *Lattice searches for tetraquarks and mesonic molecules: light scalar mesons and XYZ states*, Sasa Prelovsek, proceedings for Excited QCD 2010, arXiv:1004.3636v1 [hep-lat].
2. S. Prelovsek, T. Draper, C.B. Lang, M. Limmer, K.-F. Liu, N. Mathur and D. Mohler, arXiv:1005.0948 [hep-lat].
3. T.W. Chiu and T.H. Hsieh, Phys. Rev. D73 (2006) 094510, Phys. Rev. D73 (2006) 111503(R), Phys. Lett. B646 (2007) 95;
4. L. Liu, PoS(LAT2009)099.
5. C.G. Meng *et al.*, Phys. Rev. D80 (2009) 034503.
6. C. Ehmann and G. Balli, PoS(LAT2009)113, arXiv:0911.1238.

π and ππ electro-production in the region of low-lying nucleon resonances

S. Širca[a,b]

[a]Faculty of Mathematics and Physics, University of Ljubljana, 1000 Ljubljana, Slovenia
[b]J. Stefan Institute, 1000 Ljubljana, Slovenia

Abstract. Highlights of experiments devoted to low-lying nucleon resonances at MAMI and Jefferson Laboratory were reported in this talk. The structure of the nucleon-to-Δ transition and the electro-excitation and electro-production amplitudes of the P11(1440) Roper resonance, as well as its neighbors S11(1535), S11(1650), and D13(1520) were discussed. In this written contribution, only our work on the recent Roper experiment at MAMI is briefly presented.

The $P_{11}(1440)$ (Roper) resonance [1] is the lowest positive-parity N* state. The study of its properties remains one of the major theoretical challenges (quark models and Lattice QCD) as well as one of the cornerstones of nucleon resonance experimental programmes at MAMI and Jefferson Lab.

The most fruitful way to study the structure of the Roper appears to lead through measurements of double-polarization observables in pion electro-production off protons. This strategy benefits substantially from the experience gained in the well-studied N $\to$ Δ transition, the showcase of which were given in the landmark JLab [2] and MAMI [3] experiments In the JLab experiment, measurements in the $p(e, e'p)\pi^0$ channel were performed at relatively high momentum transfer of $Q^2 = (1.0 \pm 0.2)\,(\text{GeV/c})^2$ and $W = (1.23 \pm 0.02)\,\text{GeV}$, where two Rosenbluth combinations and 14 structure functions were separated [4].

A similar experiment, but much more restricted in scope, has been designed for the MAMI/A1 experimental setup, partly motivated by the proposal [5]. Instrumental constraints at Mainz prevent us from measuring in parallel or anti-parallel kinematics for the proton and at the same time achieve complete coverage in terms of the proton azimuthal angle. Our measurement was therefore performed at $Q^2 = 0.1\,\text{GeV}^2$ with the invariant mass of $W \approx 1440\,\text{MeV}$, and at a single value of the center-of-mass angle, $\theta_{\text{cms}} = 90°$. The proton kinetic energy in the center of the carbon secondary scatterer was $T_{cc} \approx 200\,\text{MeV}$, which allows for optimal figures-of-merit of the focal-plane polarimeter. The low value of Q^2 is not favourable only because of the kinematics reach of the setup; according to state-of-the-art calculations in the MAID [6,7] and DMT [8–10] models, the sensitivities of the multipole amplitudes to the Roper couplings appear to be larger at smaller Q^2.

Data was taken with a beam current of $\approx 10\,\mu A$ impinging on a 5 cm LH2 target in a beamtime lasting approximately two weeks. We have collected enough data to allow us to determine the three components of the proton recoil polarization to within a few percent statistical accuracy, i.e. $\Delta P_x' \approx 0.03$, $\Delta P_y \approx 0.03$, and $\Delta P_z' \approx 0.051$. The analysis of this data is work in progress. Gain-matching and time-calibration of the scintillation detectors has been done. Odd-even parameters for the horizontal drift chambers have been adjusted. Figure 1 shows preliminary azimuthal distributions in the focal-plane polarimeter.
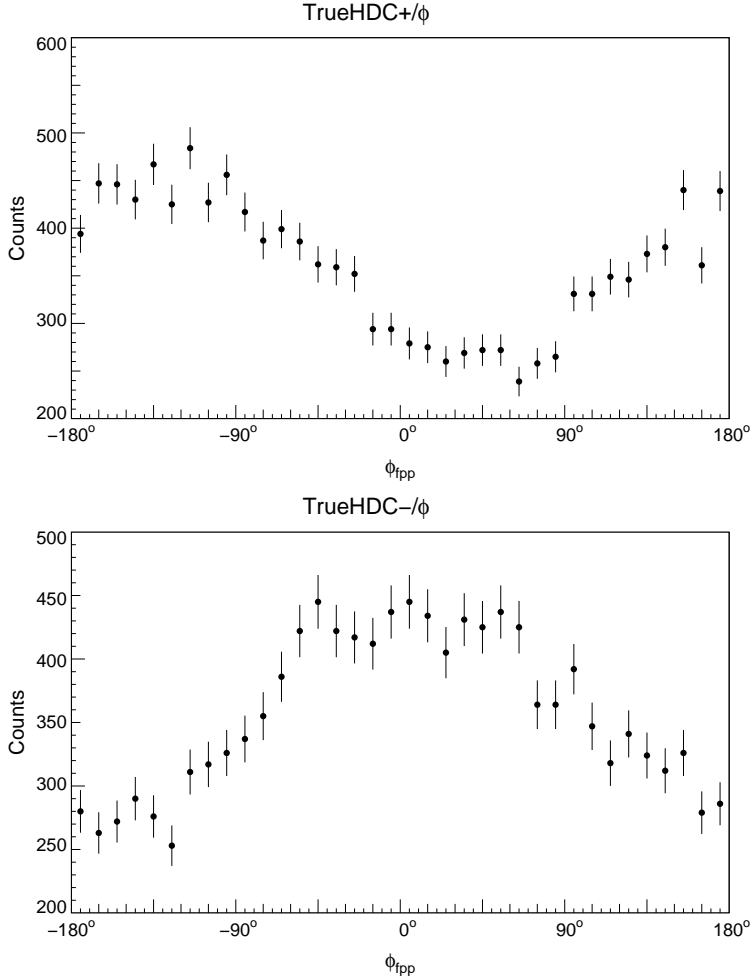
Fig. 1. The distributions of events in terms of the azimuthal angle in the focal-plane polarimeter (secondary scattering) for two helicity states of the electron beam. Top: helicity sum $N_+ + N_-$. Apart from acceptance corrections and possible false asymmetries, this distribution should be flat. Bottom: helicity difference $N_+ - N_-$. By taking into account the spin transport properties of the spectrometers, this asymmetry directly maps into proton polarization components at the target.

References

1. L. D. Roper, Phys. Rev. Lett. **12** (1964) 340.
2. J. J. Kelly, A. Sarty, S. Frullani (co-spokespersons), JLab Experiment E91-011.
3. Th. Pospischil et al. (A1 Collaboration), Phys. Rev. Lett. **86** (2001) 2959.
4. J. J. Kelly et al. (Hall A Collaboration), Phys. Rev. Lett. **95** (2005) 102001; see also J. J. Kelly et al. (Hall A Collaboration), Phys. Rev. C **75** (2007) 025201.
5. O. Gayou, S. Gilad, S. Širca, A. Sarty (co-spokespersons), JLab Proposal PR05-010.
6. D. Drechsel, O. Hanstein, S.S. Kamalov, L. Tiator, Nucl. Phys. **A** 645 (1999) 145.
7. http://www.kph.uni-mainz.de/MAID/maid2003/maid2003.html
8. S. S. Kamalov, S. N. Yang, Phys. Rev. Lett. **83** (1999) 4494.
9. S. S. Kamalov et al., Phys. Rev. C **64** (2001) 032201(R).
10. http://www.kph.uni-mainz.de/MAID/dmt/dmt2001.html